การวัดอัตราปริมาณรังสีแกมมา ณ พื้นที่จากต้นกำเนิดแบบแผ่นโดยใช้หัววัดรังสีเจอร์มาเนียม
บริสุทธิ์สูง
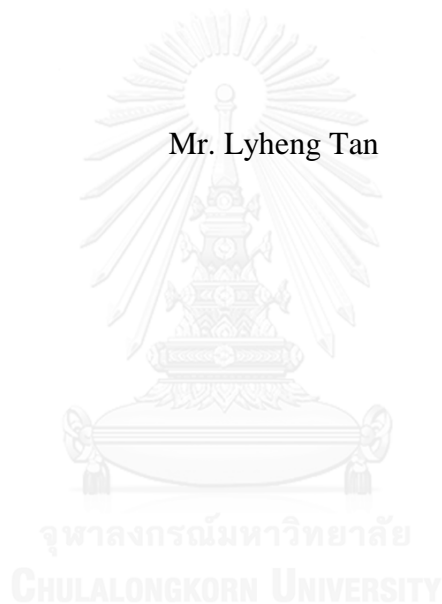
นายลีเฮง ตัน

วิทยานิพนธ์นี้เป็นส่วนหนึ่งของการศึกษาตามหลักสูตรปริญญาวิทยาศาสตรมหาบัณฑิต
สาขาวิชาเทคโนโลยีนิวเคลียร์ ภาควิชาวิศวกรรมนิวเคลียร์
คณะวิศวกรรมศาสตร์ จุฬาลงกรณ์มหาวิทยาลัย
ปีการศึกษา 2558
ลิขสิทธิ์ของจุฬาลงกรณ์มหาวิทยาลัย

IN SITU GAMMA-RAY DOSE RATE MEASUREMENT FROM PLANAR
SOURCE USING HIGH PURITY GERMANIUM DETECT0R

Mr. Lyheng Tan

A Thesis Submitted in Partial Fulfillment of the Requirements

for the Degree of Master of Science Program in Nuclear Technology

Department of Nuclear Engineering

Faculty of Engineering

Chulalongkorn University

Academic Year 2015

Thesis Title	IN SITU GAMMA-RAY DOSE RATE MEASUREMENT FROM PLANAR SOURCE USING HIGH PURITY GERMANIUM DETECT0R
By	Mr. Lyheng Tan
Field of Study	Nuclear Technology
Thesis Advisor	Associate Professor Nares Chankow
Thesis Co-Advisor	Associate Professor Somyot Srisatit

Accepted by the Faculty of Engineering, Chulalongkorn University in Partial Fulfillment of the Requirements for the Master's Degree

....Dean of the Faculty of Engineering
(Professor Bundhit Eua-arporn, Ph.D.)

THESIS COMMITTEE

....Chairman
(Associate Professor Sunchai Nilsuwankosit, Ph.D.)

....Thesis Advisor
(Associate Professor Nares Chankow)

....Thesis Co-Advisor
(Associate Professor Somyot Srisatit)

....Examiner
(Somboon Rassame, Ph.D.)

....External Examiner
(Assistant Professor Attaporn Pattarasumunt)

ลีเฮง ตัน : การวัดอัตราปริมาณรังสีแกมมา ณ พื้นที่จากต้นกำเนิดแบบแผ่นโดยใช้หัววัดรังสีเจอร์มา
เนียมบริสุทธิ์สูง (IN SITU GAMMA-RAY DOSE RATE MEASUREMENT FROM PLANAR
SOURCE USING HIGH PURITY GERMANIUM DETECT0R) อ.ที่ปรึกษาวิทยานิพนธ์หลัก:
รศ. นเรศร์ จันทน์ขาว, อ.ที่ปรึกษาวิทยานิพนธ์ร่วม: รศ. สมยศ ศรีสถิตย์, 99 หน้า.

งานวิจัยนี้ได้นำเสนอวิธีง่าย ๆ สำหรับการวัดอัตราปริมาณรังสีจากต้นกำเนิดรังสีแบบแผ่นโดยใช้
หัววัดรังสีเจอร์มาเนียมบริสุทธิ์สูงในการวัดสเปกตรัมรังสีแกมมา ค่าความเข้มรังสีสุทธิของพีคพลังงานต่าง ๆ จาก
สเปกตรัมที่ได้จะถูกใช้ในการคำนวณหาอัตราปริมาณรังสีรวม โดยเริ่มจากการซื้อสีทาฝ้าเพดานที่มียูเรเนียมและ
ทอเรียมมาจำนวน 4 ตัวอย่างและทำการหาปริมาณยูเรเนียมและทอเรียมด้วยวิธีแกมมาเรย์สเปกโทรเมตรีที่ใช้
หัววัดรังสีชนิดเจอร์มาเนียมบริสุทธิ์สูงซึ่งมีประสิทธิภาพสัมพัทธ์ 30% โดยพบว่ามีนิวไคลด์ลูกของยูเรเนียม เช่น
ตะกั่ว-214, บิสมัท-214 และนิวไคลด์ลูกของทอเรียม เช่น ทัลเลียม-208 (^{208}Tl), แอกทิเนียม-228 (^{228}Ac) ใน
ตัวอย่างทั้งหมด คือมี ^{238}U อยู่ในช่วง 144.61±3.28 ถึง 299.76±4.87 Bq/kg และ ^{232}Th อยู่ในช่วง
1773.59±23.66 ถึง 2121±26.52 Bq/kg ตามลำดับ จากนั้นได้เตรียมตัวอย่างทดสอบจำนวน 8 ชิ้นจากสีทาฝ้า
เพดาน 4 ตัวอย่างดังกล่าว โดยนำไปทาบนแผ่นไม้อัดขนาด 30 ซม. X 30 ซม. ตัวอย่างละ 2 แผ่น ทำให้ได้แผ่น
ไม้ที่มีความแรงรังสีจำเพาะของ ^{238}U และ ^{232}Th อยู่ในช่วง 0.018 – 0.071 Bq/cm^2 และ 0.22 – 0.49 Bq/cm^2
ตามลำดับ อีกสองตัวอย่างทดสอบได้เตรียมจากการผสมสีที่ไม่มีกัมมันตภาพรังสีกับสารมาตรฐานแร่ยูเรเนียม
และทอเรียมในสัดส่วนต่างกันแล้วนำไปทาบนแผ่นไม้อัดขนาดเดียวกันทำให้ได้ความแรงรังสีจำเพาะของ ^{238}U
และ ^{232}Th เท่ากับ 0.027 กับ 0.030 Bq/cm^2 และ 0.043 กับ 0.056 Bq/cm^2 ตามลำดับ จากนั้นจึงใช้หัววัดรังสี
ชนิดเจอร์มาเนียมบริสุทธิ์สูงที่มีประสิทธิภาพสัมพัทธ์ 10% วัดรังสีจากตัวอย่างแผ่นไม้อัดแต่ละแผ่น โดยวาง
หัววัดรังสีห่างจากกึ่งกลางของแผ่นไม้อัด 2 ซม. บริเวณด้านข้างของหัววัดรังสีมีก้อนตะกั่ววางอยู่โดยรอบเพื่อ
จำกัดพื้นที่สำหรับการวัดให้เหลือเพียง 10 ซม. X 10 ซม. ผลการวัดพบว่านิวไคลด์กัมมันตรังสีหลัง ^{222}Rn ใน
อนุกรม ^{238}U และหลัง ^{220}Rn ในอนุกรม ^{232}Th ไม่อยู่ในสมดุลทางกัมมันตรังสีกับนิวไคลด์แม่ จึงทำให้ค่าที่วัดได้
ต่ำกว่าค่าที่ได้จากการคำนวณ อย่างไรก็ตามมีเพียง ^{228}Ac เท่านั้นที่ค่าที่ได้จากการวัดใกล้เคียงกับที่ได้จากการ
คำนวณเพราะเป็นตัวเดียวที่อยู่ในสมดุลทางกัมมันตรังสีกับ ^{232}Th ซึ่งเป็นนิวไคลด์แม่ จึงได้ใช้วิธีใหม่เพื่อ
แก้ปัญหานี้โดยทำการปรับเทียบด้วยต้นกำเนิดรังสีแกมมาแบบจุด ซึ่งวางไว้ที่ตำแหน่งต่าง ๆ กัน แล้วคำนวณหา
ค่าปรับแก้ทางเรขาคณิต และพบว่ามีค่าเท่ากับ 0.74 สำหรับทุกพลังงาน จากการวัดด้วยวิธีนี้พบว่าอัตราปริมาณ
รังสีที่วัดจากตัวอย่างทดสอบทั้ง 10 ตัวอย่างได้ผลเป็นที่น่าพอใจมาก นอกจากนี้ยังได้เตรียมสูตรที่ใช้ในการ
ปรับเทียบและการคำนวณอัตราปริมาณรังสีบนเวอร์คชีตเพื่อความสะดวกในการทำงาน

5670575021 : MAJOR NUCLEAR TECHNOLOGY

KEYWORDS: GAMMA-RAY SPECTRUM / CEILING PAINT / RADIOACTIVE ISOTOPES

LYHENG TAN: IN SITU GAMMA-RAY DOSE RATE MEASUREMENT FROM PLANAR SOURCE USING HIGH PURITY GERMANIUM DETECT0R. ADVISOR: ASSOC. PROF. NARES CHANKOW, CO-ADVISOR: ASSOC. PROF. SOMYOT SRISATIT, 99 pp.

This research proposes a simple method for dose rate measurement from planar source using a high purity germanium (HPGe) detector by measurement of gamma-ray spectrum. Net peak intensities of all energies from the measured spectrum were then used to obtain the total dose rate. First of all, 4 ceiling paint samples containing uranium and thorium were purchased and determined uranium and thorium contents by using high resolution gamma-ray spectrometry equipped with an HPGe detector of 30% relative efficiency. Radioactive isotopes including uranium daughter radionuclides such as ^{214}Pb and ^{214}Bi as well as thorium daughter radionuclides such as ^{208}Tl and ^{228}Ac were found in all samples. The specific activities of ^{238}U in the range of 144.61±3.28 to 299.76±4.87 Bq/kg and ^{232}Th in the range of 1773.59±23.66 to 2121±26.52 Bq/kg respectively. After that 8 test specimens were prepared from the four paint samples by painting on 30 cm x 30 cm plywood, two pieces per paint sample. The specific activities of ^{238}U and ^{232}Th on the plywood samples were in the range of 0.018 – 0.071 Bq/cm^2 and 0.22 – 0.49 Bq/cm^2 respectively. The other two radioactive paint samples were prepared by mixing non-radioactive paint sample with standard uranium and standard thorium ores of different proportions to make the specific activities of ^{238}U and ^{232}Th on the plywood of 0.027 and 0.030 Bq/cm^2 and 0.043 and 0.056 Bq/cm^2 respectively. A portable gamma-ray spectrometer equipped with 10% relative efficiency HPGe was then used to measure radioactivity from the prepared ten plywood samples at 2 cm distance at right angle from the middle of the samples. To limit the detector detecting area to 10 cm x 10 cm, the detector sides were surrounded by lead blocks. Unfortunately, the radionuclides after ^{222}Rn in ^{238}U series and after ^{220}Rn in ^{232}Th series were not in radioactive equilibrium with the parent radionuclides which made the measured dose rates lower than the calculated values. However, the dose rate of ^{228}Ac was in good agreement with the calculated value because it was the only radioisotope that was in radioactive equilibrium with the parents ^{232}Th. To overcome the problem, a new technique was then introduced by calibrating the detector with point gamma-ray standard sources at different position to obtain geometrical correction factors. The correction factor was found to be 0.74 for all energies. The results of dose rate measurements from the ten test specimens using the proposed technique were very satisfactory. In addition, a worksheet with necessary formulae was prepared for convenience in calibration and calculation of the dose rate.

Department:	Nuclear Engineering	Student's Signature _____
Field of Study:	Nuclear Technology	Advisor's Signature _____
Academic Year:	2015	Co-Advisor's Signature _____

ACKNOWLEDGEMENTS

CONTENTS

LIST OF TABLES

LIST OF FIGURES

Chapter 1

Introduction

Radionuclides in Naturally Occurring Radioactive Materials (NORMs) consist primarily of material containing ^{40}K and the isotopes which belong to the primordial series such as the long-lived isotopes of ^{238}U in uranium series and ^{232}Th in thorium series. These radionuclides present since the creation of the earth (4.5 billion years). Human beings can be exposed to ionizing radiation through the external sources such as terrestrial radiation and cosmic radiation. They irradiate the body with the gamma photon. However, the internal hazard requires the incorporation of the radioactive materials into our body by ingestion or inhalation. Radon-222 (^{222}Rn) is a daughter product of radium-226 (^{226}Ra), which is derived from uranium-238 (^{238}U). Thoron (^{220}Rn) is the daughter of thorium-232 (^{232}Th). ^{222}Rn and ^{220}Rn are naturally occurring radioactive gas which can cause lung cancer.

Nowadays ceiling paint may contain these radionuclides which can cause harmful to people and animals. According to the United State Environmental Protection Agency as well as the Scientific and Medical Communities, they have recognized Radon as a class A carcinogen (Schmidt, 2011, p. 3). Furthermore, the Environmental Protection Agency estimated that 14,000 American die every year from radon-related lung cancer, but this number could range from 7,000 to 30,000 deaths per year (EPA, 1993, p. 3). The data regarding the specific activity of ^{238}U, ^{232}Th, and ^{40}K in ceiling paint belonging to Thailand is not available in literature. Moreover, Knowledge of radioactivity in ceiling paint samples enables one to assess any possible radiological risk to human health (Kumar et al, 2003, p 465). Therefore, the specific activity of these radionuclides were firstly determined in our low background HPGe gamma-ray spectrometer with a CANBERRA lead shield (coated inside by the thin layer of copper). This semiconductor detector is the best choice for this research because of its superior energy resolution. Furthermore, the gamma-ray spectrometry of this detector is a power method which can identify and quantify the radionuclides for determining the specific

activity of gamma emitting isotopes in a variety of matrices. According to the rule that all exposure to radiation should be kept "as low as reasonably achievable" (ALARA), and the results obtained in the present study are compared with the relevant results available in some other countries of the world.

In this research, the ceiling paint samples have been primarily analyzed in our low background HPGe gamma-ray spectrometer with a CANBERRA lead shield (coated inside by the thin layer of copper). This analysis was used to determine the specific activity and the present of those radionuclides in the samples. The dose rate of the samples were also estimated. Moreover, these samples were simulated as the sources which were painted on the plywood with the surface area of 30 cm × 30 cm for the in situ measurements. It is based on the in situ gamma-rays measurement of a high purity germanium (HPGe) detector. This in situ measurement of the gamma-ray dose rate from planar sources based a collimator of a lead shielding with the distance of 2 cm. The dose rate of these samples were determined. The results obtained from this measurement will be compared with the results obtained from the calibrated gamma-ray survey meters, the dose rate calculated from the known activity of ^{238}U and ^{232}Th content, and the ISOC software.

1.1   Background information

In the last century, man-made activities have begun to contribute significantly to the radiation level in the environment due to the release of the anthropogenic radionuclides. This release is primarily from two different sources:

1. The releases from the nuclear reactors caused by the accident

2. The releases from the atmospheric testing of the nuclear explosive devices

The radionuclides were found in the radioactive fallout such as ^{131}I, ^{133}I, ^{134}Cs, ^{137}Cs, ^{95}Zr, ^{141}Ce, ^{95}Nb, and ^{132}Te (Brune, 2001). For example, in the Chernobyl fallout, the radionuclides which have contributed the most to the human radiation exposure are ^{131}I and ^{137}Cs (Brune, 2001). The average contribution to the human exposure for the

worldwide scale from the anthropogenic sources is about one order of magnitude lower than that from radioactivity (Brune, 2001). However, dose rate can be very high locally. Therefore, the accurate methods for assessing the activity levels in the environment, both for emergency preparedness purpose and on longer timescale for the radioecological surveys are essential because the radioactivity in the environment can have the severe implications on the human health.

In general, the immediate estimated result of dose rate measurement is obtained by using the hand-held instruments. However, this measurement cannot be used for identification or quantification of the individual radionuclides. It means that the dose rate of the temporal change cannot be predicted. Therefore, the in situ gamma-ray spectrometry is a powerful method that can identify and potentially quantify the radionuclides directly at the measurement site. It can be performed as the mobile measurements such as on foot, car, or airborne. Nowadays, the high purity germanium (HPGe) detectors are often the choice for the in situ measurements because of their superior energy resolution.

An example of an HPGe spectrum from an air filter exposed for 24 hours on March 23-24, 2011 at the LBF facility at LBNL containing both natural and fission radionuclides (counted for 1250 minutes) (Smith. R. A. 2014)
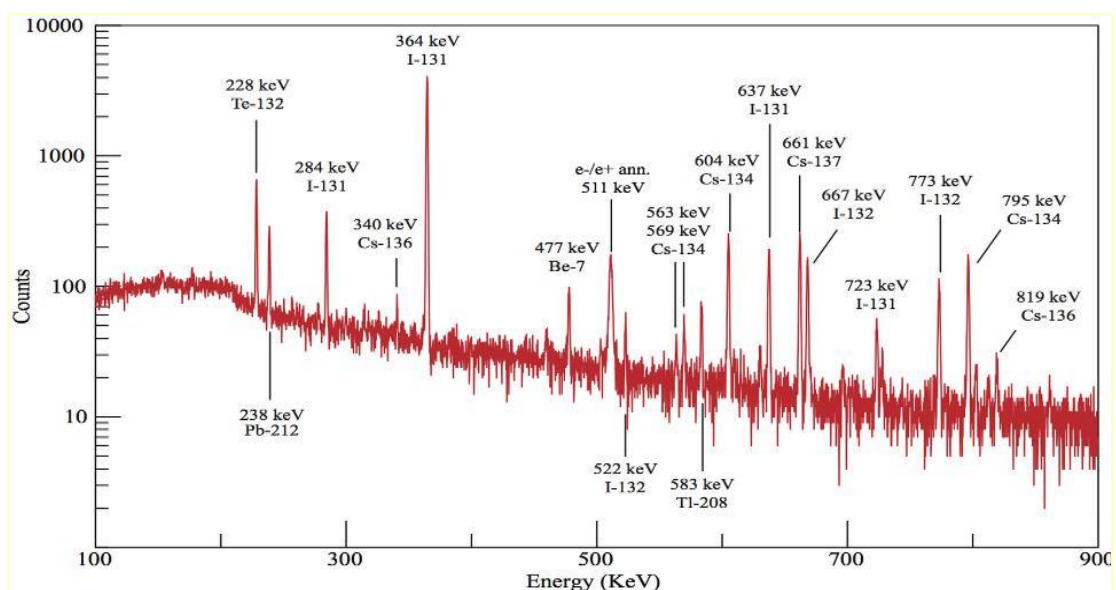
Figure 1.1: HPGe spectrum from an air filter exposed for 24 hours

1.1.1 Sources of radiation exposure

There are two main sources of radiation exposure such as natural and manmade radiation sources. The NORMs are the Naturally Occurring Radioactive Materials such as ^{40}K (potassium-40), ^{238}U (uranium-238), and ^{232}Th (thorium-232). All of these radionuclides exist since the creation of the earth. Human and animals can be exposed to ionizing radiation by the terrestrial radiation and cosmic radiation which irradiate into the body with the gamma photon, but the internal hazard requires the incorporation of radioactive materials into the body by ingestion or inhalation. ^{222}Rn (radon-222) is a daughter product of ^{226}Ra (radium-226). Thoron (^{220}Rn) is the daughter of thorium-232 (^{232}Th). ^{222}Rn and ^{220}Rn are naturally occurring radioactive gas which can cause lung cancer. Although some harmful effects can be produced by exposure to natural background radiation, those effects are relatively minor and, in most cases, not even can be measurable. It is a fact that human activities have added to normal background radiation. For example, when the nuclear weapons were exploded, they released radioactive isotopes into the atmosphere.

A pie chart in the Figure 1.2 below shows the various sources of radiation from both natural and manmade sources. The main source for radiation exposure with 55 % which comes from the radon sources (NCRP, 1987).
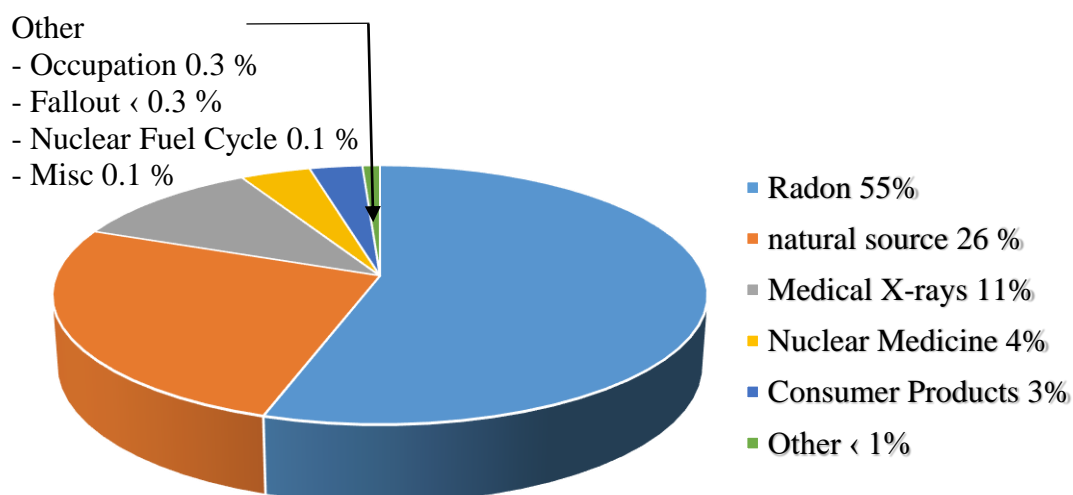
Figure 1.2: A pie chart of the natural and manmade resources

1.2   Objectives

There are two main objectives:

1. To develop a simple technique for in situ measurement of the gamma-ray dose rate from planar sources

2. To prepare the worksheet for calibration and calculation of the gamma-ray dose rate

1.3   Scopes

This study is focused on:

1. Development of a simple technique for in situ measurement of the gamma-ray dose rate from planar sources using an HPGe detector for the desired coverage areas based on a collimator and the detector-to-source distance.

2. Preparation of the worksheet to calibrate the energy and efficiency based on linear relations and to calculate the gamma-ray dose rate based on generally accepted formulas.

3. Measurement of the dose rate from planar sources having area of $\leq$ $1m^2$ using the the developed method in comparison with those obtained from **ISOC** software and a calibrated gamma-ray survey meter.

1.4   Benefits

The developed method and worksheet can be used to identify radionuclides and accurately measure the gamma-ray dose rate using an HPGe detector from planar sources both in normal situations and after incident such as spillage, dirty bomb explosion, etc.

Chapter 2

Theory and Literature Review

2.1   Natural and manmade radiation sources

Throughout history, mankind has been exposed to radiation from the environment which comes from two main sources such as:

1. Cosmic rays (highly energetic radiation bombarding the earth from outer space),

2. Terrestrial radiation, originating in radionuclides found in the earth and in our own bodies.

Nowadays, these natural radiation sources are augmented by medical x-rays, nuclear weapons, nuclear reactors, television, and numerous other radiation producing devices. It is very important to know the magnitude of the doses that the public receives from these sources. Then the standards of the radiation exposure were established by the various regulatory bodies.

2.1.1   Cosmic rays

The primary cosmic radiation incident on the earth primarily consisted of a mixture of protons ($\sim$87%), alpha particles ($\sim$11%), a trace of heavier nuclei ($\sim$1%), and electrons ($\sim$1%). The range of the energies of these particles was between 10^8 and 10^{11} eV. There was no known mechanism for the production of such highly energetic radiation. In short, the origin of cosmic rays was not understood. The primary cosmic rays were almost entirely attenuated as they interact in the first few hundred g/cm^2 of the atmosphere such as neutron, additional protons, and charged pions (short-lived subnuclear particles). The subsequent decay of the pions resulted in the production of electrons, muons (other subnuclear particles), and a few photons. The resulting particles fluxed depended on somewhat on the geomagnetic latitude.

The annual cosmic ray dose rate was between 26 and 27 mrems at sea level. The dose rate increased with the altitude. For instance, persons living in Denver received approximately twice the annual dose from cosmic rays as people living at sea level. The average annual dose due to cosmic rays in the United States was about 31 mrems. Because some of this radiation was shielded by buildings, this dose were reduced to 28 mrems.

2.1.2   Terrestrial radiation

There were approximately 340 naturally occurring nuclides which were found on earth, and 70 of them were radioactive. There was radioactivity everywhere, and there was no one can escape from radiation exposure due to natural radioactivity in the environment or in human body. The natural radionuclides were divided into two groups depending on their origin, such as:

1. Primordial radionuclides, those that have been here since the creation of the earth
2. Cosmogenic radionuclides, those that were produced by the action of cosmic rays

The primordial nuclides were very long lived. Since the earth was formed approximately 4.5×10^9 years, so a nuclide with a half-life even as long as 10 million years would have passed through 450 half-lives. The most common primordial nuclides were ^{238}U with the half-life of 4.5×10^9 years, ^{235}U with the half-life of 7.1×10^8 years, ^{232}Th with the half-life of 1.4×10^{10} years, ^{87}Rb with the half-life of 4.8×10^{10} years, and ^{40}K with the half-life of 1.3×10^9 years.

The presence on earth of naturally occurring short-lived radionuclides (^{14}C with the half-life of 5730 years) was because of their production by cosmic rays. If ^{14}C was not continually replenished, it would disappear billions years ago. There were about 25 other cosmogenic radionuclides that they have been identified, but only ^{14}C leaded to the significant radiation doses. This nuclide was primarily formed in the interaction of

the thermalized cosmic-ray neutrons with nitrogen in the atmosphere via the exothermic reaction ^{14}N (n, p) ^{14}C.

External exposure to terrestrial radioactivity originated with the gamma-ray which was emitted following by the decay of uranium, thorium, and their daughter products. The Colorado Plateau was a top geological formations rich in uranium and radium. As a result, this region tended to have a much higher radiation level than other parts of the country. In Brazil and India, the present thorium bearing monazite sands leaded to radiation levels that were especially high (up to 3 mR/hr). The annual external terrestrial dose of the average population in the United States was 26 mrems.

The principal source of the internal terrestrial exposure was from primordial ^{40}K. This nuclide decays both by negative beta decay to ^{40}Ca and by positive beta decay or electron capture to ^{40}Ar. Its isotopic abundance was 0.0118 %. Thus there was about 0.0157 g of ^{40}K from a total of 130 g of potassium in an average person weighing 70 kg. The total activity of the ^{40}K in the body was approximately 0.11 μci.

The heavy primordial nuclides and their daughters will enter the body by ingestion of drinking water or foodstuffs in which they were distributed in various trace amounts. Heavy radionuclides also entered the body as the results of inhalation of ^{222}Rn with the half-life of 3.8 days and its daughter products such as ^{210}Pb with the half-life of 21 years. ^{222}Rn was the immediate daughter of the decay of ^{226}Ra. Therefore, it was in radium bearing rocks, soil, and construction materials. Since ^{222}Rn is the noble gas, it diffused into the atmosphere, and it may travel large distances before it decayed via several short-lived species to ^{210}Pb. The half-life of ^{222}Rn is long if it was compared with the residence time of air in the lungs. The more important of chemical inertness of radon prevented its long-term retention within the body. Therefore, ^{222}Rn itself contributed very little to the internal body dose. However, ^{210}Pb may also entered the body through ingestion or by the decay of ingested parents. In any event, if these were not already complicated enough, the ^{210}Pb did not itself lead to significant internal doses because it was only a weak beta ray emitter. Rather, it was ^{210}P with the half-life of 138 days, the decay product of ^{210}Pb, which will emit a powerful 5.3 MeV alpha particle

that provided the ultimate dose. Therefore, the ^{222}Rn and ^{210}Pb can be viewed as different sorts of the carriers for ^{210}Po, the actual source of radiation damage.

The heavy radionuclides will provide local doses out of proportion to their concentration. This was because many of these nuclides such as ^{210}Po decay by emitting alpha particle were more energetic than the beta rays or gamma rays emitted by other species. In an addition, alpha particles were more harmful biologically because of their higher quality factors. Both ^{226}Ra and ^{228}Ra were chemically similar to calcium which tended to concentrate in the bone. The dose to the structural bone tissue was considerably higher than the dose to the marrow. Fortunately, these tissues were not radiosensitive. The bulk of the heavy element dose to the gonads and marrow was due to ^{210}Po although some studies suggested that radon and its progeny were the second leading cause of lung cancer behind smoking.

^{14}C was the only cosmogenic nuclide to make a significant contribution to internal human exposure. The concentration of ^{14}C in natural carbon has been found to be the same in all living species, 7.5 picocuries per total body burden of an average 70 kg man is approximately 0.1 μCi. This gave an estimated dose of 0.7 mrem/year.

2.1.3 Manmade sources

Medical exposures: The largest nontrivial-localized dose which was received by the public at large from man-made sources was in connection with the healing arts. This dose included contributions from medical and dental diagnostic radiology, clinical nuclear medicine (the use of radionuclides for various purposes), radiation therapy, and occupational exposure of medical and dental personnel.

Fallout: It was from a nuclear weapon. It consisted of fission fragments and neutron activation products in weapon debris which became attached to dust and water particles in the atmosphere. The larger of these particles soon came to earth near the

site of detonation, but the smaller particles may remain aloft in the upper uniformly around the world. Furthermore, it contributed to the general level of environmental radiation, and the long-term exposure from fallout was mostly internal, from fission.

Nuclear power: The dose was due not only to radiation released from power plants themselves, but also from uranium mines, mills and fabrication plant, and fuel reprocessing facilities. In general, the population averaged dose in the United States was less than 1 mrem per year in 1980.

Building materials: Many building materials such as granite, cement, and concrete contained a few parts per million of uranium and thorium, together with their radioactive daughters, and ^{40}K. The annual dose of the radiation emanating directly from the walls of brick or masonry structures was 7 mrem per year.

Building materials were also a source of ^{22}Rn, especially those with poor ventilation, may receive substantial lung doses from the subsequent decay of the ^{210}Po. Radon also entered buildings from other natural sources through basement openings, window, and other openings. It was also from the burning of natural gas, which frequently contained large amounts of radon. The average radon related dose to an individual was estimated to be 200 mrem per year.

Air Travel: The radiation dose from air travel stemmed from modern jet aircraft fly at high altitudes, from 9 to 15 km, where cosmic ray dose rate was much greater than it was on the ground. For example, at 43^0 north latitude (just north of Chicago) and at an altitude of 12 km, the dose rate was 0.5 mrem per hour. Moreover, a 10 hour round trip flight across the United States can result in a total dose of as much as 5 mrems.

Television: Radiation was released in the form of x-rays. Because of increasing numbers of television viewers exposed to this radiation, the US congress in 1968 passed standards requiring that the exposure rate averaged over 10 cm^2 at any readily accessible point 5 cm from the surface of a television received not exceed 5 mR/hr.

Moreover, with the adoption of this averaged annual dose to the gonads of viewers is now between 0.2 to 1.5 mrems.

Tobacco: As noted earlier, ^{222}Rn diffused from the earth to the atmosphere and then decays into ^{210}Pb, which subsequently fallen to the earth attached to dust or moisture particles. If these particles fall onto leafy vegetables or pasture grasses, the ^{210}Pb may enter directly into the food chain. It is the fact that if the particles fall onto broadleaf tobacco plants, the ^{210}Pb and its daughter ^{210}Po may be incorporated into commercial smoking materials. As a result, measurement showed that there was on the order of 10 to 20 pCi of both ^{210}Pb and ^{210}Po in an average pack of cigarettes. The inhalation of the cigarette smoke deposited these radionuclides on the tracheobronchial tree, where the ^{210}Po irradiated the radiosensitive basal cells of the bronchial tissue. The annual local dose to this tissue for an average cigarette smoker (1.5 packs per day) was estimated to be as high as 8 rems (8000 mrems) and proportionately higher for heavy smokers.

Other manmade sources: Segments of the public were exposed to several other, often unsuspected, sources of radiation. For example, clocks and wristwatches with luminous dials, eyeglasses or porcelain dentures containing uranium or thorium, smoke detectors with alpha emitting sources, fossil fueled power plants emitted radioactive ash. Moreover, many other manmade devices resulted in generally small whole body doses, but occasionally high local doses. For instance, porcelain teeth and crowns in the United States contained approximately 0.02 % uranium by weight. This was estimated to give an annual local tissue dose of about 30 rem per year, mostly from alpha particles.

2.2   Nuclear weapons fallout

2.2.1 Vertical migration studies of ^{137}Cs from nuclear weapons fallout and the Chernobyl accident (Almgren. S, 2006)

33 sampling sites were studied from the vertical migration of ^{137}Cs which originated from the nuclear weapons fallout and the Chernobyl accident in western

Sweden. This study was used the field gamma in situ measurement to compare traditional soil sampling technique for determining the activity of ^{137}Cs. For in situ gamma-rays measurement, an HPGe detector was placed 1 m above the ground looking downwards with the counting time of 15 and 30 minutes. The activities of ^{137}Cs were given as the equivalent surface deposition and then corrected for the actual depth distribution. For the traditional soil sampling technique, it was performed at each reference site by using a specially design metal corer. This sampling device delivered soil cores from the acquired depth with a diameter of 80 mm. At each site, three cores placed in the corners of a triangle with 60 cm side were taken and cut into slices at 0-2 cm, 2-4 cm, 4-6 cm, 9-12 cm, and 12-15 cm depth. The vertical transport of ^{137}Cs was found to be very slow, and mostly was still present in the upper most part of the soil with an average depth of the maximum activity of 5.4±2.2 (1SD) cm. The apparent diffusion coefficient (D) and the apparent convection velocity (v) were in the same ranges as the values found in other studies.

2.3   Radiological monitoring

2.3.1 Radiological monitoring of terrestrial natural radionuclides in Kinta District, Perak, Malaysia (Lee. S. K, 2009)

From 2003 to 2005 in Kinta District, Perak, Malaysia, Natural background gamma radiation and radioactivity concentrations were investigated. Sample locations were distant from any 'among' processing plants. In various rocks and soils external, the gamma dose contributions were mainly from the presence of ^{40}K, ^{232}Th and ^{238}U and their progeny. Dose measurements were made at approximately every 1 km (more frequently if the significant change in radiation level was detected) for using a portable survey meter. The position of the locations was determined by using the global positioning system, GPS Garmin Model 12X with accuracy ±50. The HPGe detector was used for the measurement of gamma-energy spectrum. For lab measurement, soil samples were collected from areas of different soil types at 128 locations. About 2 to 3 kg of soils samples were collected from the top 10 cm of the soil. The dose rate ranged from 39 nGy h^{-1} to 1039 nGy h^{-1} are over the world average.

2.4 Validation of in situ object counting system (ISOCS)

2.4.1 Validation of in situ object counting system (ISOCS) mathematical efficiency calibration software (Venkataraman. R, 1999)

The ISOCS calibration method was used for calibrating the detector efficiency as a function of energy for a wide variety of source geometries and activity distributions. The ISOCS software consisted of a Canberra characterization of the detector. Source geometry data was input, and the efficiency calibration was produced. Firstly, an MCNP model of the detector was developed. The model was independently validated using measurements with a NIST traceable source. It contained a series of mathematical models that can simulate a wide variety of sample shapes. Each source region into a number of voxels was divided by the ISOCS software. At a given energy, the detector efficiency was calculated for each voxel, taking into account the attenuation due to absorbers both inside and outside the source. At the given energy, the efficiencies for all the voxels were summed up. About 109 samples were tested to determine the accuracy of this calibration method. With the same geometry, a reference efficiency calibration was compared to an ISOCS efficiency calibration for each test. The tests were categorized into three different counting geometries, namely, Field, Laboratory, and Collimated geometry. The mean ratio of ISOCS/True efficiencies was (I) 1.09 ± 0.014 for the Collimated geometries (II) 0.97 ± 0.007 for the Laboratory geometries, and (III) 1.01 ± 0.007 for the Field geometries.

2.5   In situ and air borne of gamma-ray spectrometry

(Andrew N. Tyler, 2008)

In situ and air borne of gamma-spectrometry were commonly used for the measurement of environmental radioactivity. The ability of these two methods can make rapid real time measurements of environmental radioactivity to bring immediate benefits to surveys for the purposes of prospecting, baseline monitoring, contamination

mapping, and site characterization. In addition, a detector based at 1 m for in situ gamma spectrometry (IGS) and 100 m for airborne gamma spectrometry, AGS). The obtained results showed that AGS clearly has an important role to play in nuclear emergency response. Influences of the vertical activity distribution generally had a greater impact on IGS measurements than AGS measurements because of the larger solid angle between the IGS detector and source, unless the detector was collimated.

2.6 Decay series of ^{232}Th and ^{238}U

In nuclear science, the decay chain referred to the radioactive decay of the different discrete radioactive decay products such as the chained series of transformation. This transformation takes place over a defined period of time (known as a half-life) as a result of electron capture, fission or the emission of alpha particles, beta particles, or photons (gamma radiation or x-rays) from the nucleus of an unstable atom. Moreover, a parent isotope was one that undergoes decay to form a daughter isotope. For example, Uranium, atomic number 92, decayed into thorium, atomic number 90. The daughter isotope may be stable, or it may decay to form a daughter isotope of its own. The figure below were the ^{232}Th and ^{232}U series respectively.
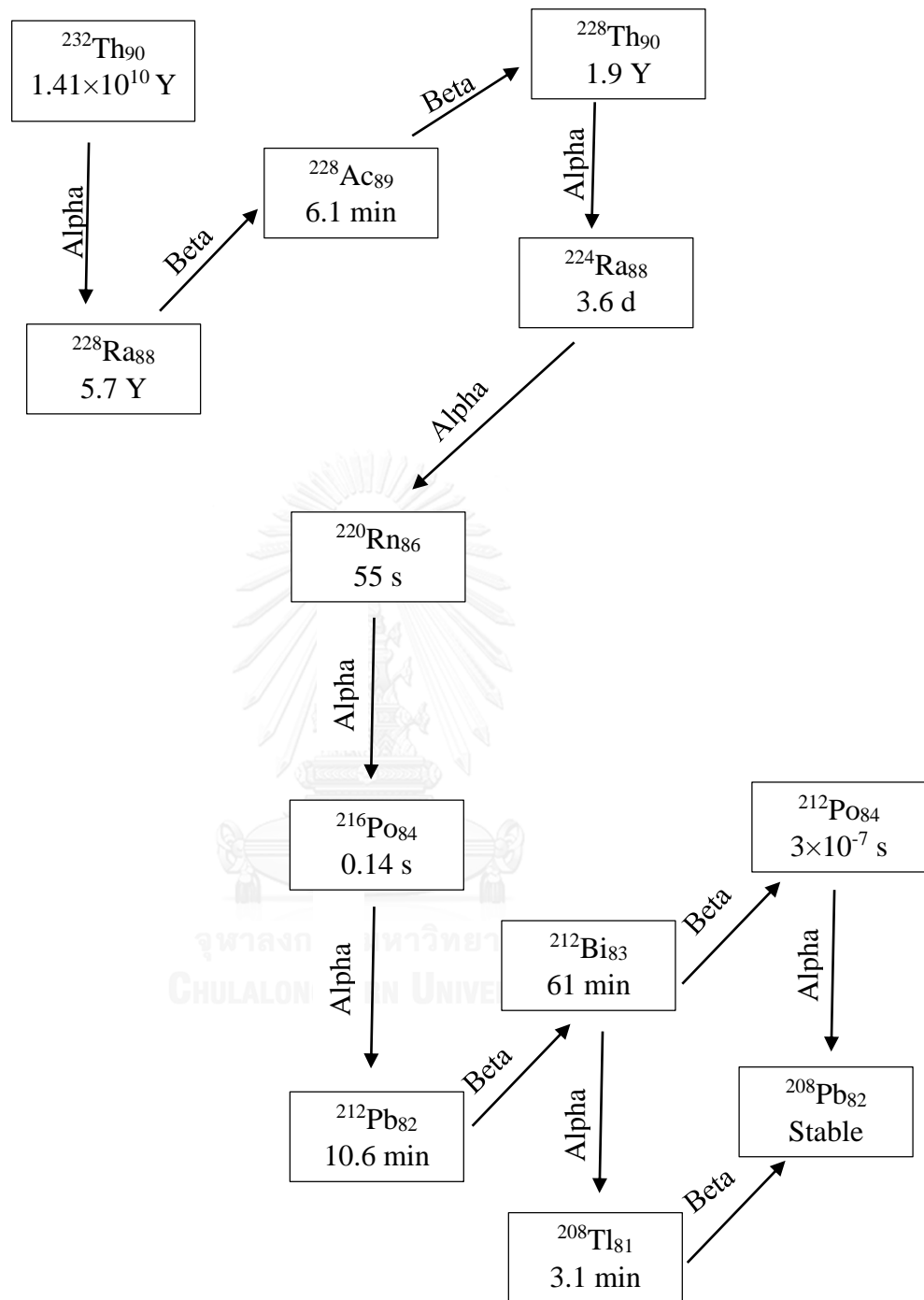
Figure 2. 1: ^{232}Th decay series
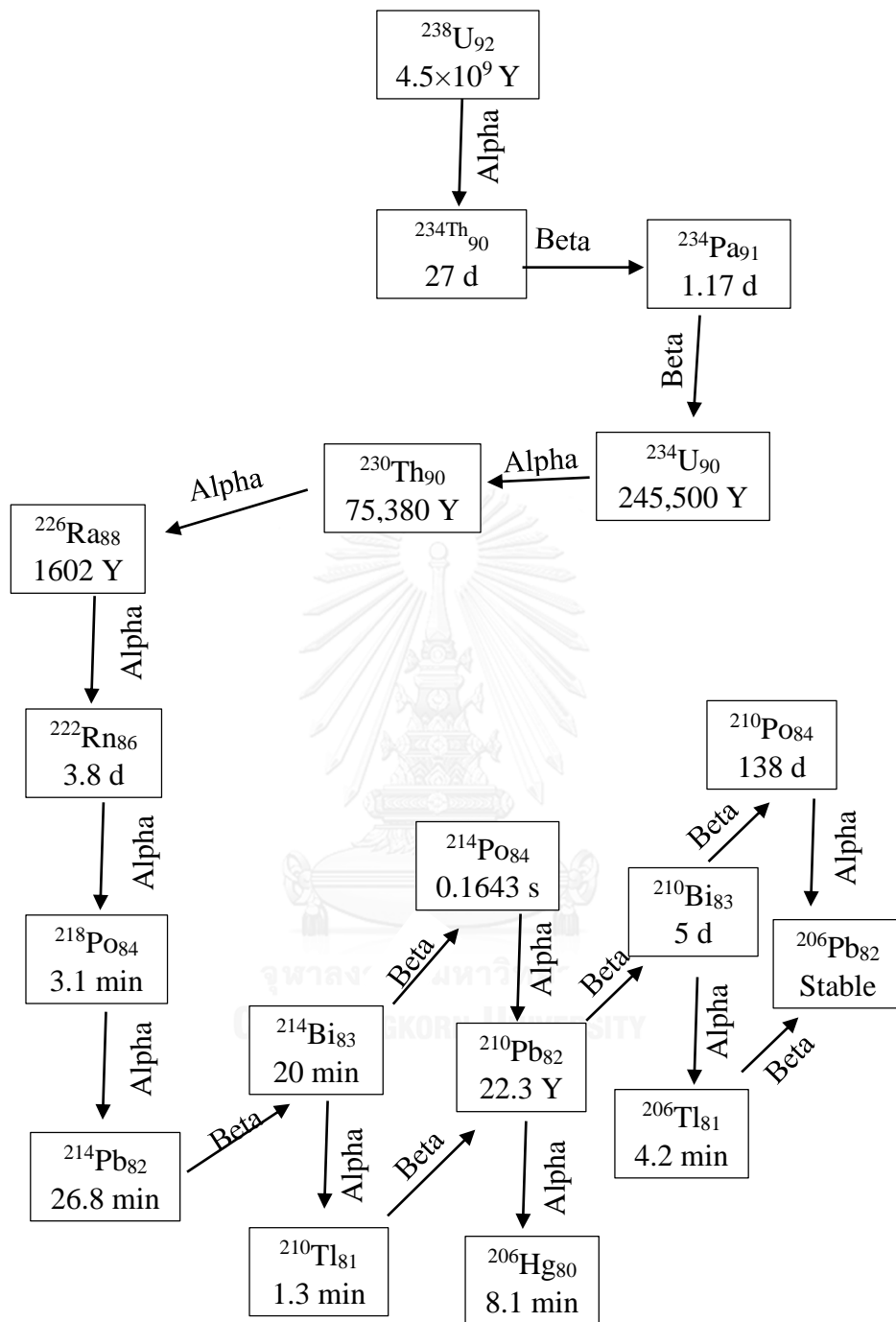
Figure 2. 2: ^{238}U decay series

2.7   Interaction of gamma-rays with matters

There are three major interaction processes of gamma photon with matter:

1. Photoelectric Effect (E < 0.5MeV): A photon interacted with an orbital electron bound in an inner shell (K or L), and then it gave the full energy (hv). The electron liberated from the orbit, called photo electron, and it had kinetic energy of E_e= hv-b, where b was binding energy of orbit. Another orbital electron filled the vacancy, and a characteristic X-ray or an Auger electron was emitted, of which energy was equal to the difference of each binding energy. Cross section for K-electron was proportional to $Z^5(hv)^{-3.5}$.

Photo electron
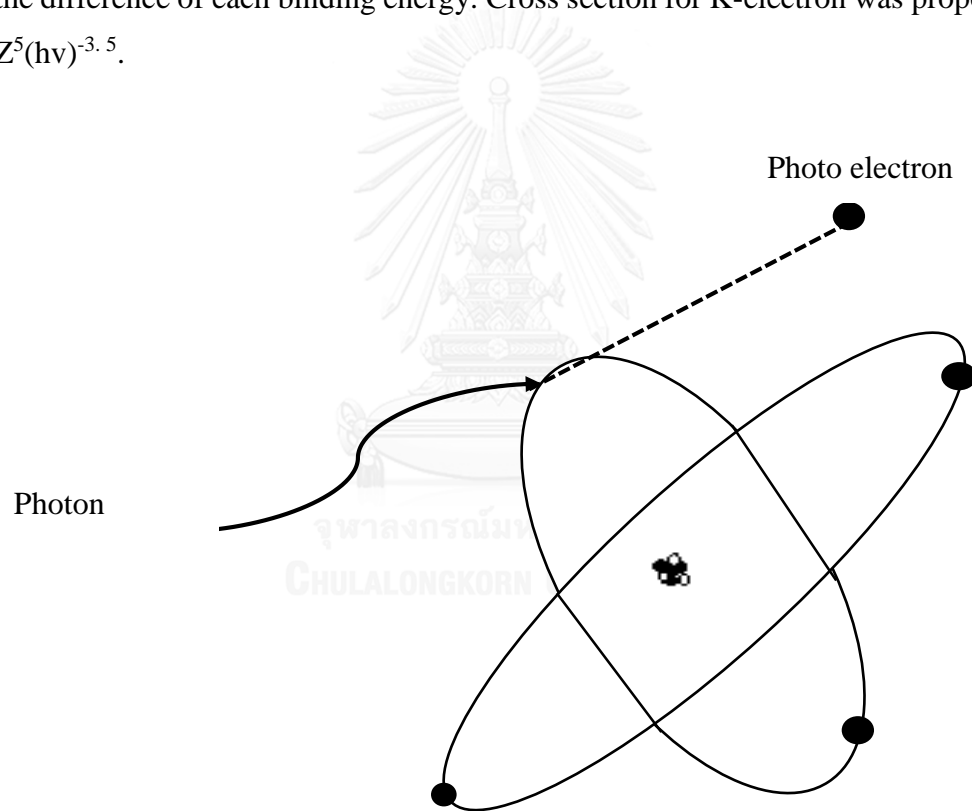
Photon

Figure 2. 3: Photoelectric effect

2. Compton Scattering (E > 0.5MeV): A photon interacted with an electron, and it gave a partial energy. Then it scattered for different direction. Energies of the scattered photon and the secondary electron are calculated by:

Scattered photon: $h\nu' = \frac{h\nu}{\{1+\alpha(1-cos\theta)\}}$ $\qquad$ *when* $\alpha = {h\nu}/{m_0 v^2}$

Secondary electron $\quad E_e = h\nu - h\nu'$
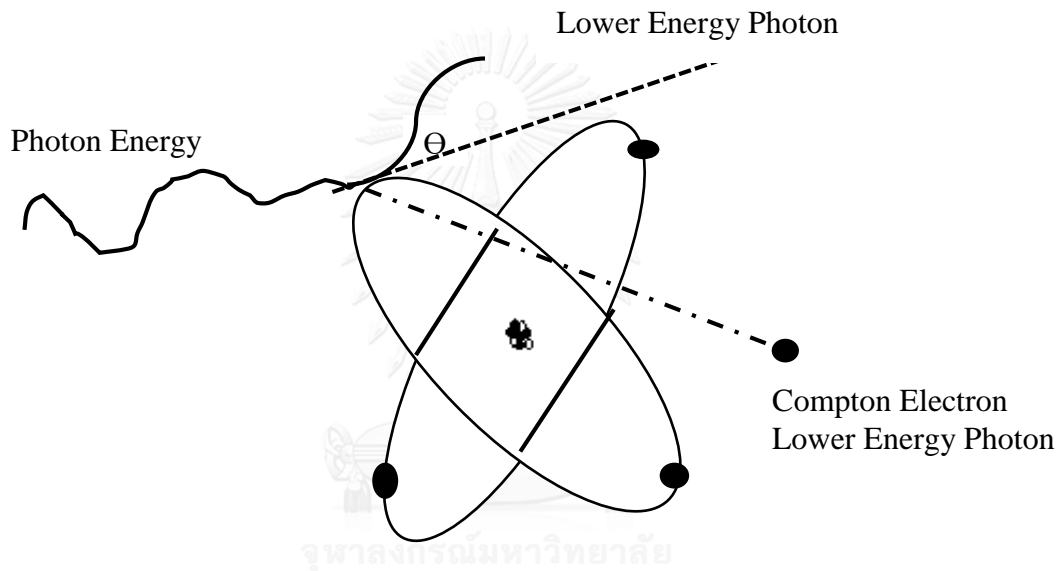
Figure 2. 4: Compton Scattering

3. Pair production (E ~ 1.022 MeV): A photon produces an electron (e⁻) and a positron (e+) near the nucleus, and the total kinetic energy of both electron is:

$E_{e^-} + E_{e^+} = h\nu - 2m_0 c^2$

Positron combined with an electron nearby after losing kinetic energy, then the electron and positron pair annihilated and emitted two photons (annihilation photon: $m_0 c^2 = 511$ keV). This process is called positron annihilation.
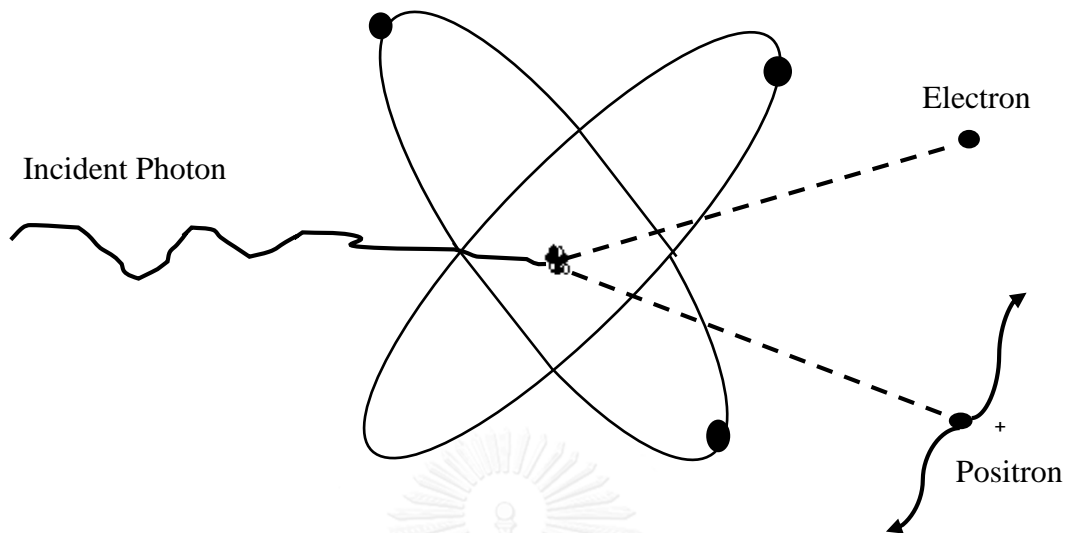
Figure 2. 5: Pair production

2.8   Gamma-rays detectors

Many different detectors was used to register the gamma-rays and its energy. In Non-Destructive Analysis (NDA), it was necessary to measure not only the amount of radiation emanating from a sample but also its energy spectrum. Therefore, the detectors of most use in NDA applications were those whose signal outputs were proportional to the energy deposited by the gamma-rays in the sensitive volume of the detector.

1. Semiconductor detectors: There are several types of semiconductor detectors such as Surface Barrier, Diffused Junction, Silicon Lithium-Drifted Si (Li), Silicon Lithium-Drifted Si (Li), CdTe, HgI_2, and High Purity Germanium (HPGe) detectors.

- The Surface Barrier detectors: Silicon of high purity, normally n-type, is cut, ground, polished, and etched until a thin wafer with a high grade surface is obtained. Then the silicon is left exposed to air or to another oxidizing agent for several days. As a result, the surface energy states are produced that induce a high density of holes and form,

especially a p-type layer on the surface. A very thin layer of gold evaporated on the surface serves as the electrical contact, and it will lead the signal to the preamplifier.

- The Diffused-Junction detectors: Silicon of high purity, usually p-type, is the basic material for this detector. The silicon piece has the shape of a thin wafer with the surface barrier detectors. A thin layer of n-type silicon is formed on the front face of the wafer by applying a phosphorus compound to the surface and then heating the assembly to temperatures as high as 800 to 1000 ^{0}C for less than an hour. The phosphorus diffuses into the silicon and "dopes" it with donors. The n-type silicon in front and the p-type behind it form the p-n junction.

- The Silicon Lithium-Drifted Si (Li) detectors: The sensitive region has an upper limit of about 2000 μm for both surface barrier and diffused junction detectors. This limitation has affected the maximum energy of a charged particle that can be measured. For electrons in Si, the range of 2000 μm corresponds to an energy of about 1.2 MeV, and for protons the corresponding energy is about 17 MeV. Moreover, for alpha, it is about 90 MeV. The length of the sensitive region can be increased if lithium ions are left to diffuse from the surface of the detector towards the other side. This process has been used successfully with Si and Ge, and it has produced the so called Si (Li) and Ge (Li) semiconductor detectors. Moreover, Lithium drift detectors have been produced with depth up to 5 mm in the case of Si (Li) detectors and up to 12 mm in the case of Ge(Li) detectors.

The lithium drifting process consists of two major steps such as formation of an n-p conjunction by lithium diffusion and increase of the depletion depth by ion drifting. Lithium diffuses into a p-type silicon for forming the n-p conjunction. The simplest method consists of painting a lithium in oil suspension onto the surface. This method drifting is to begin, and other methods are lithium deposition under vacuum or electrodepositing. Moreover, lithium is an n-type impurity (donor atom) with high mobility in silicon. N_p is always constant throughout the silicon crystal, while the donor concentration (N_n) is high on the surface and zero everywhere else. The donor

concentration has changed with depth as the diffusion has proceeded. Drifting is accomplished by heating the junction from 120 to 150 ^{0}C while applying a reverse bias that may range from 25 V up to about 1000 V. Therefore, higher the temperature and the voltage are the faster the drifting proceeds.

- The High Purity Germanium (HPGe) detectors: As the production of high purity germanium (HPGe) with an impurity concentration of 10^{16} atoms/m^3, it has made possible the construction of detectors without lithium drifting. By applying a reverse bias across a piece of germanium, the detector is simply formed. The sensitive depth of the detector (depletion layer) depends on the impurity concentration and the applied voltage. The fabrication of HPGe detectors follows the same procedure as with Ge (Li) detectors, except the lithium-drifting process is not needed. The construction of the ohmic contacts is very important step of fabrication of the HPGe detectors. The n side contact (on the front surface) has been formed by letting lithium diffuse into the crystal or by depositing gold or palladium on it. According to a recent breakthrough reported by one of the manufacturers, it makes possible to eliminate the front metal contact. The good contact on the back side has been made by using metals or by implanting boron.

The HPGe detectors are made in planar or coaxial geometry which do not have undrafted central core of Ge (Li) detectors. Therefore, the central part along the axis of the crystal is removed, and a contact is made on the inside of this central hole. It can be made with either n- or p-type germanium. Moreover, it blocks up to 60 mm in diameter which have been produced, making feasible the construction of coaxial detectors with a volume up to 2×10^5 mm^3. Planar detectors with a thickness up to 20 mm and coaxial ones with a volume up to 5×10^4 mm^3 have been constructed. The major advantage of this detector is that they can be stored at room temperature because of the absence of lithium drifting. At room-temperature storage is particularly helpful when here is a need to ship the detector.

- CdTe, HgI$_2$, and other detectors: The major disadvantage of lithium drifted detectors is the requirement for continuous cooling. For HPGe detectors, it needs to cool down during operation, and cooling requires a cryostat. There is a great incentive to develop

semiconductor detectors that can be stored and operated at room temperature. CdTe or HgI_2 semiconductor detectors have been constructed with thickness up to 0.7 mm to $100 \, mm^2$. It requires a small detector volume such as monitoring in space, measurement of facility in nuclear power plants, medical portable scanning, or medical imaging devices. Although the detector volume is small, the efficiency is considerable because the high atomic number of the elements is involved. The energy which is needed for the production of an electron hole pair is larger for CdTe and HgI_2 detectors. They are used in measurement where their energy resolution is adequate while, at the same time, their small volume and room temperature operation offer a distinct advantage over Si (Li) and Ge (Li).

2. The Scintillation detectors: Luminescent material (a solid, liquid, or gas) is the sensitive volume of a scintillation detector. It is viewed by a device that detects the gamma-rays induced light emissions (usually a photomultiplier tube). There are three main types of scintillators such as inorganic scintillators, organic scintillators, and gaseous scintillators.

- The Inorganic scintillators (Crystal scintillators): Most of the inorganic scintillators are crystal of the alkali metals. In alkali iodides, they contain a small concentration of an impurity such as NaI (Tl), CsI (Tl), LiI (Tl), and CaF_2 (Eu). The element which is showed in the brackets is the impurity or activator. This activator is the agent which is responsible for the luminescence of the crystal. Although the activator has relatively small concentration, thallium in NaI (Tl) is 10^{-3} on a per mole basis. Inorganic scintillator of NaI (Tl) is the most commonly used for gamma-rays. It has been produced in the singled crystals of up to 0.75 m in diameter and considerable thickness of 0.25 m with relative high density is $3.67 \times 10^3 \, kg/m^3$. Moreover, its high atomic number combines with the large volume which makes it a gamma-rays detector with very high efficiency. They cannot replace the NaI (Tl) in experiments where the large detector volumes are needed although semiconductor detectors have better energy resolution. The emission spectrum of NaI (Tl) peaks at 410 nm, and the light-conversion efficiency is the highest of all inorganic scintillators. Furthermore, it is brittle and

sensitive to temperature gradients and thermal shocks. It is also so hygroscopic that it should be kept encapsulated at all times. It always contains a small amount of potassium, which creates a certain background because of the radioactive ^{40}K.

-The Organic scintillators: The materials which are efficient organic scintillators belong to the class of aromatic compounds. They consist of the planar molecules which are made up of the benzenoid rings. For example, toluene and anthracene are the class of aromatic compounds. Organic scintillators are formed when the appropriate compounds are combined. They are classified as unitary, binary, ternary, and so on, depending on the number of compounds in the mixture. The substance with the highest concentration is called the solvent, and the others are called solutes. For instance, a binary scintillator consists of a solvent and a solute, while a ternary scintillator is made of a solvent, a primary solute, and a secondary solute. There are two types of the organic scintillators.

Firstly, the organic crystal scintillator, activator is not needed to enhance the luminescence of organic crystals. In fact, any impurities are undesirable because their presence reduces the light output and makes the crystal pure. The most common crystal scintillators are Anthracene and trans-stilbene. Anthracene has a density of 1.25×10^3 kg/m^3, and it has the highest light conversion efficiency of all organic scintillators. It is still only about one third of the light conversion efficiency of NaI (Tl). Its decay time ($\sim$ 30 ns) is much shorter than that of inorganic crystals. It can be obtained in different shapes and sizes. Trans-Stilbene has a density of 1.15×10^3 kg/m^3 and a short decay time (4-8 ns). It conversion efficiency is about half of that for anthracene. Moreover, it can be obtained as a clear, colorless and single crystal with a size up to several millimeters. Stilbene crystals are sensitive to the thermal and the mechanical shock.

Secondly, the organic liquid scintillators, it consists of a mixture of a solvent with one or more solutes. Xylene, toluene, and hexamethylbenzene are the compounds that have been used successfully as solvents. In a binary scintillator, the incident radiation deposits almost all of its energy in the solvent, but the luminescence is due almost entirely to the solute. Thus, in the case of inorganic scintillators, an efficiency energy

transfer is taking place from the bulk of the phosphor to the material with the small concentration (activator in inorganic scintillators, solute in organic ones). It acts as the wavelength shifter if a second solute is added. It increases the wavelength of the light which is emitted by the first solute. As a result, the emitted radiation is better matched with the characteristics of the cathode of the photomultiplier tube. This scintillator is very useful for measurements where a detector with large volume is needed to increase efficiency.

- The gaseous scintillators: They are mixtures of the noble gases, and the scintillations are produced as a result of the atomic transitions. Other gases, such as nitrogen, are added to the main gas to act as the wavelength shifters because the light which is emitted by noble gases belongs to the ultraviolet region. Thin layer of fluorescent materials uses for coating the inner walls of the gas container to achieve the same effect. The gaseous scintillators exhibit such as very short decay time, light output per MeV deposited in the gas depending very little on the charge and mass of the particle being detected, and very low efficiency for gamma detection.

3. The gas-filled detectors: they operate by utilizing the ionization which are produced by radiation as it passes through a gas. Counter consists of two electrodes, and it is filled with a gas. Ionizing radiation which passes through the space between the electrodes dissipates part or all of its energy by generating electron-ion pairs. Both electron and ions are the charge carriers which move under the influence of the electric field. Their motion induces a current on the electrodes that may be measured.

The ionization chambers: No charge multiplication will take place. The output signal is proportional to the particle energy which is dissipated in the detector. Therefore, the measurement of particle energy is possible. Since the signal from an ionization chamber is not large, only strongly ionizing particles such as alpha, photons, fission fragments, and other heavy ions are detected by such counters. Furthermore, the voltage applied is less than 1000 V.

The proportional counters: Charge multiplication will take place, but the output signal is still proportional to the energy which is deposited in the counter. The measurement of the particle energy is possible. An alpha particle and an electron having the same energy and entering either of the counters will give the different signal. The alpha particle signal will be bigger than the electron signal, and the range of the applied voltage for the proportional counter is between 800 and 2000 V.

The Geiger-Muller (GM) counters: They are very useful because their operation is simple, and they provide a very strong signal, so strong that a preamplifier is not necessary. They can be used with any kind of ionizing radiation, with different level of the efficiency. The disadvantage of GM counters is that their signal is independent of the particle type and its energy. Therefore, a GM counter provides information only about the number of particles. Another minor disadvantage is their relatively long dead time (200 to 300 µs). The range of applied voltage for GM counters is from 1000 to 3000 V.

There are two main widely used detectors for gamma-rays measurement such as HPGe and NaI detector.

Table 2.1: The purpose and comments of HPGe and NaI detector

Detectors	Purpose of use	Comments
HPGe	- Gamma-rays measurement and spectrometry	- Used for dose measurement and gamma spectrometry (Good energy resolution)
NaI	- Gamma-rays measurement and spectrometry	- Used for dose measurement and gamma spectrometry (Poor energy resolution)

An Example of Energy Spectrum of ^{238}U using a HPGe and a NaI detector (Luca. C. 2006)
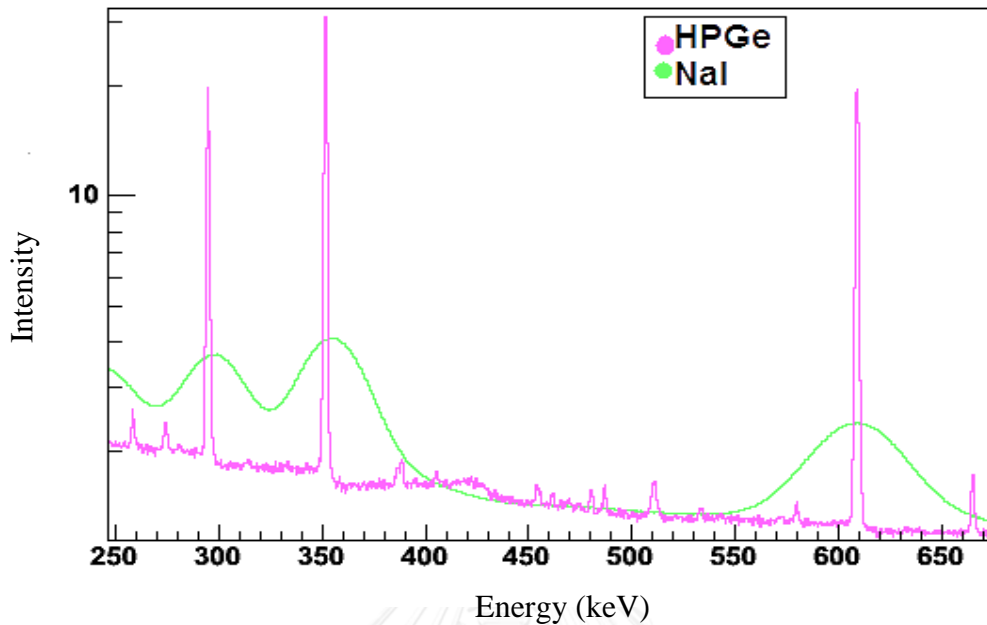
Figure 2. 6: The spectrum of HPGe Vs NaI

2.9   Characteristics of gamma-rays detector

Require high Z and large volume particularly for high energy photons

No restriction for specimen size and thickness

Low energy photon may require self-absorption factor

Need proper shielding

In Situ measurement is possible

Measurement of complex gamma-rays spectrum is most practical for identifying unknown radionuclides

2.10   Calculation of efficiency

The efficiency is calculated by using the formula as the following:

$$Absolute\ efficiency = \frac{Cps}{f \times A} \qquad (1)$$

Where,

- Cps is the net peak area per second

- f is the gamma-ray fraction

- A is the point source activity now expressed in Bq

$$A = A_0 \times e^{-\lambda t} \qquad (2)$$

- A_0 is the original point source activity expressed in Bq

- t is the time of the source decay until now expressed in s

- λ is the decay constant expressed in s⁻

$$\lambda = \frac{ln2}{t_{1/2}} \qquad (3)$$

- $t_{1/2}$ is the half-life of the source

2.11   Calculation of activity

This quantity tells us how many atoms in a sample of a radioactive material are disintegrating per unit time. In other word, the activity of a radioactive source is the number of nuclei decaying in one second. For example, at the end of the first second, ten million atoms have decayed, so ninety million will be left. 10 % or 9 million will decay. In this way, the activity of the source will decrease every second. After a certain time, it will have only half of its original activity. This period of time is called the half-life of the source. The decay of a radionuclides is statistical in nature and it is impossible to predict when any particular atom will disintegrate. The result of this uncertainty regarding the behavior of any particular atom is that the radioactive decay law is exponential in nature, and is expressed mathematically as the follow:

$$N = N_0 \times e^{-\lambda t} \qquad (4)$$

Where,

- N_0 is the number of nuclei present initially

- N is the number of nuclei present at time t

- λ is the radioactive decay constant

The half-life ($T_{1/2}$) of a radioactive species is the time required for one half of the nuclei in a sample to decay. It is obtained by putting $N = N_0/2$ in the above equation.

$$\frac{N_0}{2} = N_0 \times e^{-\lambda t} \qquad (5)$$

Then dividing across by N_0 and taking natural logarithm

$$\ln\left(\frac{1}{2}\right) = -\lambda \times T_{\frac{1}{2}} \qquad (6)$$

$$T_{1/2} = \frac{\ln 2}{\lambda} \qquad (7)$$

Because of the disintegration rate or activity of the sample is proportional to the number of unstable nuclei, this varies exponentially with time.

$$A = A_0 e^{-\lambda t} \qquad (8)$$

Where,

- A is the activity of nuclei present at time t

- A_0 is the activity of nuclei present initially

- λ is the radioactive decay constant

Each radionuclides has its own particular half-life which never changes, regardless of the quantity, past history, or form of the materials such as liquid, solid, gas, element or compound. The half-lives range from microsecond for some radionuclides to millions of years for others.

The activity of nuclei can be also calculated by:

$$A = \lambda \times N \qquad (9)$$

Where,

- A is the activity of nuclei

- λ is the decay constant

$$\lambda = \frac{ln2}{T_{1/2}}$$, $T_{1/2}$ is the half life of the nuclei   (10)

- N is the number of atoms

$$N = \frac{N_A \times W}{A}$$ (11)

Where,

- N_A is the Avogadro's number (6.022×10^{23} atoms/mole)

- A is the atomic weight

- W is the weight of the nuclei

From the measurement, the amount of uranium and thorium could be obtained from the following relationships in equation.

Sample Act= (Std Act × Sample Area × Mass Std)/ (Std Area × Mass Sample)   (12)

Where,

- Std and Sample Area are the net peak area per second of the standard and sample respectively expressed in (cps)

- Mass Std and Sample are the mass in gram of the standard and sample respectively expressed in (kg)

- Std and Sample Act are the specific activity of standard and sample respectively expressed in (Bq/kg).

2.12   Calculation of dose rate (John R. Lamarsh, 2001)

The energy deposition rate per unit mass is given by $I\,E\,(\mu_a/\rho)^{air}$ and 1R $= 5.47 \times 10^7 MeV/g$ then it follows that the exposure rate X is given by:

$$X = \frac{IE(\mu_a/\rho)^{air}}{5.47 \times 10^7} \qquad (13)$$

$$= 1.83 \times 10^{-8} IE(^{\mu_a}/_\rho)^{air} \; {^R}/_{sec} \qquad (14)$$

Where,

- **I (photons/cm²-sec)** is the gamma-ray intensity

- **E (MeV)** is the gamma-ray energy

- $(^{\mu_a}/_\rho)^{air}$ **(cm²/g)** is the mass absorption coefficient of air at the energy E

For many practical problems, it is more appropriate to express X in mR/hr, rather than in R/sec.

$$1{^R}/_{sec} = 3.6 \times 10^6 \frac{mR}{hr} \qquad (15)$$

Then exposure rate can be written as:

$$X = 0.0659 IE(^{\mu_a}/_\rho)^{air} \; {^{mR}}/_{hr} \qquad (16)$$

Where, X is the exposure rate expressed in (mR/h), I is the gamma ray intensity expressed in (photon/cm²-sec), E is the gamma ray energy expressed in (MeV), and $(\mu_a/\rho)^{air}$ is the mass absorption coefficient of air at the energy E expressed in (cm²/g) (Larmarsh and Baratta, 2001, pp. 511-539). The mass absorption coefficient of air (cm²/g)^{air} at the energy E can be calculated by interpolation between two energy in the figure below.

THE MASS ABSORPTION COEFFICIENT (μ_A/ρ) FOR SEVERAL MATERIALS, IN CM²/G*

Material	Gamma-ray energy, MeV																	
	0.1	0.15	0.2	0.3	0.4	0.5	0.6	0.8	1.0	1.25	1.50	2	3	4	5	6	8	10
H	.0411	.0487	.0531	.0575	.0589	.0591	.0590	.0575	.0557	.0533	.0509	.0467	.0401	.0354	.0318	.0291	.0252	.0255
Be	.0183	.0217	.0237	.0256	.0263	.0264	.0263	.0256	.0248	.0237	.0227	.0210	.0203	.0164	.0151	.0141	.0127	.0118
C	.0215	.0246	.0267	.0288	.0296	.0297	.0296	.0289	.0280	.0268	.0256	.0237	.0209	.0190	.0177	.0166	.0153	.0145
N	.0224	.0249	.0267	.0288	.0296	.0297	.0296	.0289	.0280	.0268	.0256	.0236	.0211	.0193	.0180	.0171	.0158	.0151
O	.0233	.0252	.0271	.0289	.0296	.0297	.0296	.0289	.0280	.0268	.0257	.0238	.0212	.0195	.0183	.0175	.0163	.0157
Na	.0289	.0258	.0266	.0279	.0283	.0284	.0284	.0276	.0268	.0257	.0246	.0229	.0207	.0194	.0185	.0179	.0171	.0168
Mg	.0335	.0276	.0278	.0290	.0294	.0293	.0292	.0285	.0276	.0265	.0254	.0237	.0215	.0203	.0194	.0188	.0182	.0180
Al	.0373	.0283	.0275	.0283	.0287	.0286	.0286	.0278	.0270	.0259	.0248	.0232	.0212	.0200	.0192	.0188	.0183	.0182
Si	.0435	.0300	.0286	.0291	.0293	.0290	.0290	.0282	.0274	.0263	.0252	.0236	.0217	.0206	.0198	.0194	.0190	.0189
P	.0501	.0315	.0292	.0289	.0290	.0290	.0287	.0280	.0271	.0260	.0250	.0234	.0216	.0206	.0200	.0197	.0194	.0195
S	.0601	.0351	.0310	.0301	.0301	.0300	.0298	.0288	.0279	.0268	.0258	.0242	.0224	.0215	.0209	.0206	.0206	.0206
Ar	.0729	.0368	.0302	.0278	.0274	.0272	.0270	.0260	.0252	.0242	.0233	.0220	.0206	.0199	.0195	.0195	.0194	.0197
K	.0909	.0433	.0340	.0304	.0298	.0295	.0291	.0282	.0272	.0261	.0251	.0237	.0222	.0217	.0214	.0212	.0215	.0219
Ca	.111	.0489	.0367	.0318	.0309	.0304	.0300	.0290	.0279	.0268	.0258	.0244	.0230	.0225	.0222	.0223	.0225	.0231
Fe	.225	.0810	.0489	.0340	.0307	.0294	.0287	.0274	.0261	.0250	.0242	.0231	.0224	.0224	.0227	.0231	.0239	.0250
Cu	.310	.107	.0594	.0368	.0316	.0296	.0286	.0271	.0261	.0247	.0237	.0229	.0223	.0227	.0231	.0237	.0248	.0261
Mo	.922	.294	.141	.0617	.0422	.0348	.0315	.0281	.0263	.0248	.0239	.0233	.0237	.0250	.0262	.0274	.0296	.0316
Sn	1.469	.471	.222	.0873	.0534	.0403	.0346	.0294	.0268	.0248	.0239	.0233	.0243	.0259	.0276	.0291	.0316	.0339
I	1.726	.557	.260	.100	.0589	.0433	.0366	.0303	.0274	.0252	.0241	.0236	.0247	.0265	.0283	.0299	.0327	.0353
W	4.112	1.356	.631	.230	.1219	.0786	.0599	.0426	.0353	.0302	.0281	.0271	.0287	.0311	.0335	.0355	.0390	.0426
Pt	4.645	1.556	.719	.262	.138	.0892	.0666	.0465	.0375	.0315	.0293	.0280	.0296	.0320	.0343	.0365	.0400	.0438
Tl	5.057	1.717	.791	.285	.152	.0972	.0718	.0491	.0393	.0326	.0301	.0288	.0304	.0326	.0349	.0354	.0406	.0446
Pb	5.193	1.753	.821	.294	.156	.0994	.0738	.0505	.0402	.0332	.0306	.0293	.0305	.0330	.0352	.0373	.0412	.0450
U	9.63	2.337	1.096	.392	.208	.132	.0968	.0628	.0482	.0383	.0346	.0324	.0332	.0352	.0374	.0394	.0443	.0474
Air	.0233	.0251	.0268	.0288	.0296	.0297	.0296	.0289	.0280	.0268	.0256	.0238	.0211	.0194	.0181	.0172	.0160	.0153
NaI	1.466	.476	.224	.0889	.0542	.0410	.0354	.0299	.0273	.0253	.0242	.0235	.0241	.0254	.0268	.0281	.0303	.0325
H_2O	.0253	.0278	.0300	.0321	.0328	.0330	.0329	.0321	.0311	.0298	.0285	.0264	.0233	.0213	.0198	.0188	.0173	.0165
Concrete	.0416	.0300	.0289	.0284	.0297	.0296	.0295	.0287	.0278	.0272	.0256	.0239	.0216	.0203	.0194	.0188	.0180	.0177
Tissue	.0271	.0282	.0293	.0312	.0317	.0320	.0319	.0311	.0300	.0288	.0276	.0256	.0220	.0206	.0192	.0182	.0168	.0160

Figure 2. 7: The mass absorption coefficient for several materials in cm²/g

Exposure rate (mR/h) can be converted to dose rate (Sv/hr or μSv/hr) in air by the following factors:

1rad   =   100ergs/g

1R   =   87.5 ergs/g

1R   =   0.875rad

1Gy   =   100rad

1R   =   0.00875Gy

For gamma-ray, the quality factor (Q) = 1

Therefore, 1R =   0.00875 Sv   = 0.00875×10^6 μSv

The gamma ray intensity was calculated using the flux or gamma ray intensity from a planar disc source.

$$I = (S/4) \times \ln[1 + (R^2/X^2)] \qquad (17)$$

Where, S is the activity expressed in gamma-ray isotropically per cm^2-sec, R is the radius of the ceiling expressed in (m) and X is the distance between source and people or the center of the detector expressed in (m). The exposure rate (mR/hr) can be converted to the dose rate (μSv/hr).

Chapter 3

Methodology

3.1   Equipment

3.1.1 Equipment for analysis of uranium-238 and thorium-232 contents

- Four cans of ceiling paint samples (Two cans are white ceiling paint, and other two are grey ceiling paint)

- One can of non-radioactive paint which is used as the a blank

- Two Standard Reference Materials IAEA RGU-1 and RGTh-1

- The portable HPGe detector with relative efficiency 30%

- The Canberra Genie 2000 Gamma Analysis Software

- The Canberra low level background lead shield surrounding

- The Digital Spectrum Analyzer (DSA)

- Five plastic containers of 3" diameter-2" height

- The cryotank with liquid nitrogen

- The Desktop

3.1.2 Equipment for in situ dose rate measurement

- Four cans of ceiling paint samples (Two cans are white ceiling paint, and other two are grey ceiling paint)

- One can of non-radioactive paint which is used as the a blank

- Two Standard Reference Materials IAEA RGU-1 and RGTh-1

- Three point standard sources of ^{137}Cs, ^{60}Co, and ^{152}Eu

- Two calibrated gamma survey meters of HDS-101 GN and GM energy compensated

- The ISOC software

- The portable HPGe detectors with relative efficiency 10%

- The Canberra Genie 2000 Gamma Analysis Software

- The Multi-Channel Analyzer (MCA), Amplifier, and High Voltage

- Eight pieces of lead shield

- Eleven pieces of plywood (30 cm × 30 cm in each piece)

- The cryotank with liquid nitrogen

- The Desktop

3.2   Experiment procedures

3.2.1   Samples collection

Samples collection for both laboratory and in situ measurement

From our preliminary survey used a simple GM pancake survey meter to measure radiation outside the paint cans, and it was found that two kinds of paint samples are radioactive. They were ceiling paints of the same brand having different colours i.e. ash grey and white. The first two samples were then bought, one for each colour weighing approximately 3.8 kg. The other two samples were later bought from another shop to obtain samples from different lots.

3.2.2   Samples preparation
Samples preparation for laboratory measurement

Four samples weighing 312, 314, 313, 336, and 276 g namely W1, W2, G1, G2, and a non-radioactive paint sample respectively were taken from the cans to fill in a 3"diameter-2" height plastic container. Then they were sealed to prevent the escape of radioactive radon gas and left for at least 30 days to obtain the radioactive equilibrium between uranium-238 (238U) and its daughters as well as thorium-232 (232Th) and its daughters (Abudlkarim et al, 2013, p. 867).

Figure 3. 1: Showing a sample in the container for laboratory analysis

Samples preparation for in situ measurement

The samples were taken from the can to paint on the 30 cm × 30 cm of the planar plywood and then kept about 3 days until they were dry. There were four cans of the ceiling paint which were W1, W2, G1, and G2. Each can was taken for two samples. The samples W1a and W1b from the sample W1 and the samples W2a and W2b from the sample W2 were the white ceiling paints. Moreover, the samples G1a and G1b from the sample G1 and G2a and G2b from the sample G2 were the grey ceiling paints. Therefore, there were eight samples. A non-radioactive paint sample was also bought to be used as our blank. In addition, the IAEA RGU-1 and RGTh-1 with the weight of 5.538 g and 7.538 g respectively were also used to mix with the blank to paint on the plywood for the measurements, and this standard represents sample M. Another IAEA RGU-1 and RGTh-1 with the weight of 10.35 g and 11.86 g respectively were later used for the measurement, and this standard represents sample N.

Sample (30 cm × 30 cm)

Figure 3. 2: A photo of painted plywood sample for in situ measurement

3.3   Laboratory analysis for uranium-238 and thorium-232 contents

A gamma spectrometer equipped with a high purity germanium (HPGe) semiconductor detector Canberra model GC3021 was used for the measurements. It had a relative efficiency of 30%. To reduce the natural gamma-ray background level, the detector was installed inside a low background lead shield with 10 cm thickness as illustrated in Figures 3.3 & 3.4. The detector was connected to a digital spectrum analyzer (DSA) which was connected with a desktop computer. Canberra Genie-2000 Gamma Analysis Software run on the desktop computer was used to control the measurement and to perform data acquisition and spectrum analysis. The Standard Reference Materials including RGU-1 (uranium ore standard) and RGTh-1 (thorium ore standard) obtained from the International Atomic Energy Agency (IAEA) were used in this research. The specific activities of RGU-1 and RGTh-1 were 4903.47 Bq/kg with the weight of 324.15 g and 3257.89 Bq/kg with the weight of 313 g respectively. These Standard Reference Materials were filled in a 3"diameter-2" height plastic container and then were kept as the same samples. Two Standard Reference Materials, four samples, and a blank (a non-radioactive paint sample) were used for the measurements, and they were placed on top of the HPGe detector for measurement one after the other for 7,200 seconds. All spectra were then analyzed to identify radioactive isotopes from

their energy peaks and to calculate the specific activity of uranium-238 and thorium-232 from the net peak intensities by using the method of the direct comparison.

Figure 3. 3: Lead shield to lower gamma background level
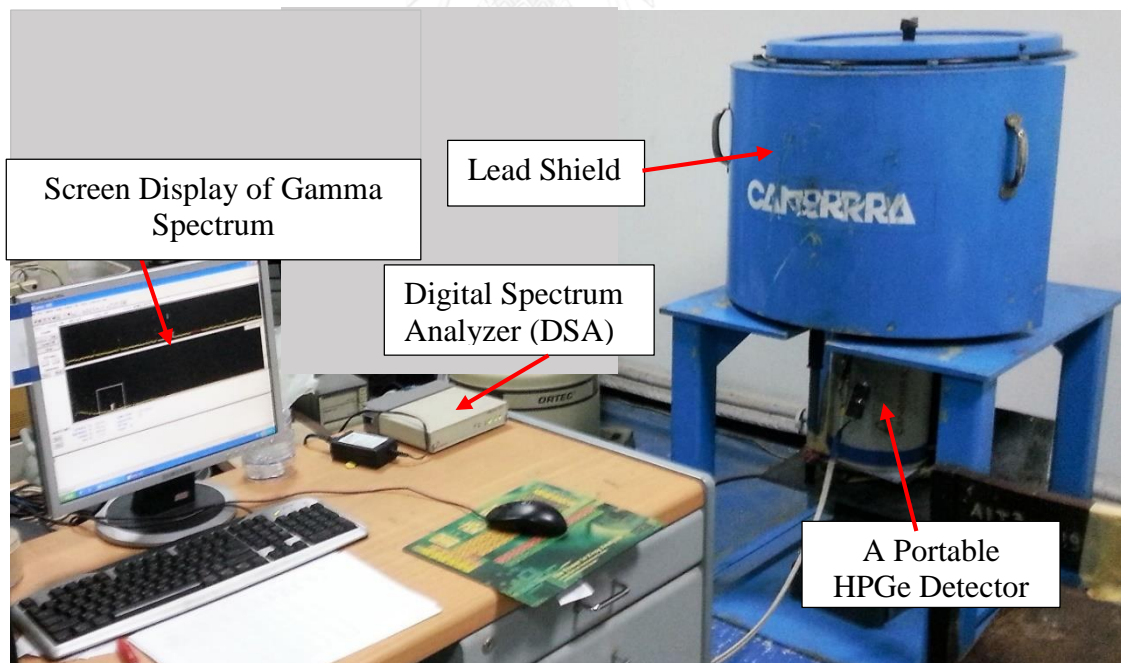
Figure 3. 4: The laboratory analysis using a High Purity Germanium (HPGe) detector

3.3.1 Energy Calibration for laboratory analysis

Table 3.1: The energy and channels using the standard sources of uranium-ore and thorium-ore

Sources	Energy (keV)	Channels
^{226}Ra	186	346
^{214}Pb	242	451
	295	549
	352	655
^{214}Bi	609	1133
^{228}Ac	911	1693
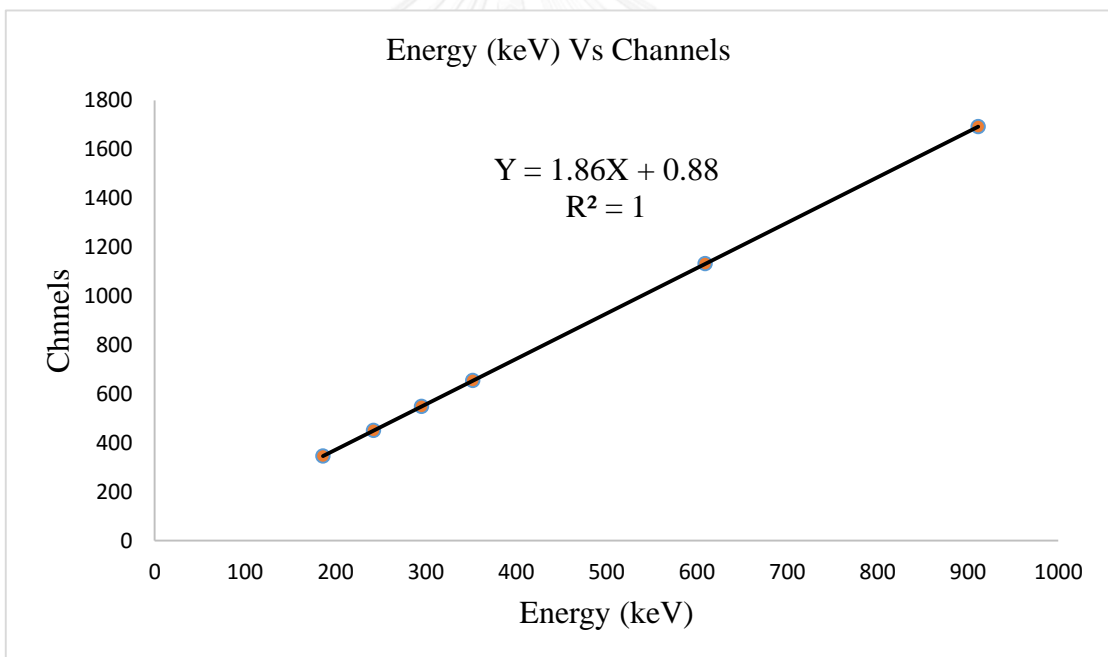
Figure 3. 5: The linear line of energy calibration

3.3.2   Calculation of the specific activity

The specific activity of ^{238}U and ^{232}Th in the ceiling paint samples was determined in our laboratory with the low level background lead shield. These specific activities were determined using the method of the direct comparison in equation (12).

3.4   In situ gamma measurement using a High Purity Germanium (HPGe)

A gamma spectrometer equipped with the High Purity Germanium (HPGe) semiconductor detector Canberra model GC1020 was used for the measurements. It has the relative efficiency 10%. To reduce the natural gamma-rays background level, the detector was installed inside the lead shield with 5 cm thickness as illustrated in Fig. 3.6. The detector was connected to a Multi-Channel Analyzer (MCA) and a notebook computer. The Canberra Genie 2000 Gamma Analysis Software ran on the notebook computer was used to control the measurement and to perform the data acquisition and the spectrum analysis.

The point sources of ^{152}Eu, ^{60}Co, and ^{137}Cs were used for the energy calibration. Moreover, the point sources of ^{152}Eu and ^{137}Cs were used for the standard efficiency calibration curve. The standard materials including RGU-1 (uranium standard) and RGTh-1 (thorium standard) obtained from the International Atomic Energy Agency (IAEA) were also used in this research for the dose measurement. The low intensity of RGU-1 and RGTh-1 with the weight of 5.54 and 7.54 g respectively were mixed with the blank, a non-radioactive paint sample, and then were painted on the plywood for the measurements. Moreover, the high intensity of RGU-1 and RGTh-1 with the weight of 10.35 and 11.86 g respectively were also mixed with the blank, a non-radioactive paint sample, and then were painted on the plywood for the measurements. Each point source, reference material, sample, and blank was placed 2 cm away from the center of the HPGe detector for the measurement one after the other for 7,200 seconds. All

spectra were then analyzed to identify the radioactive isotopes from their energy peaks and to calculate the dose rate from these samples.
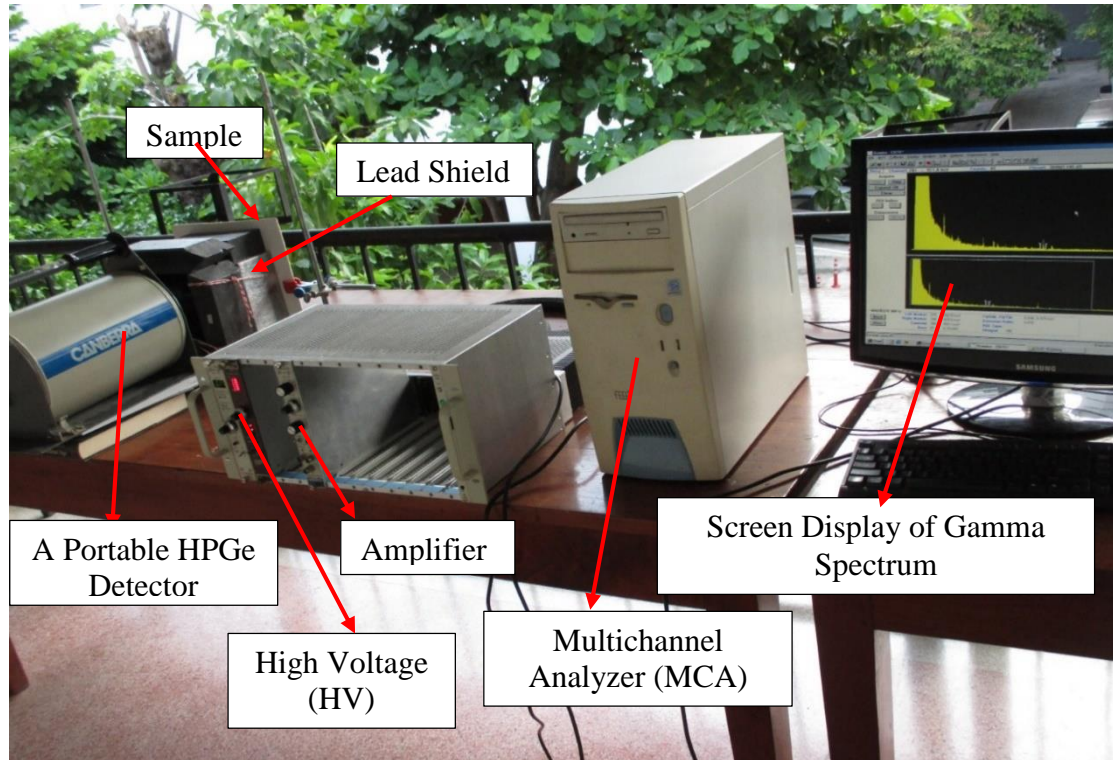
Figure 3. 6: The in situ measurement using the HPGe detector

The ceiling paint sample with the areas of 30 cm × 30 cm at 2 cm from the center of the detector using the lead shield of 5 cm thickness with 10 cm ×10 cm detectable areas
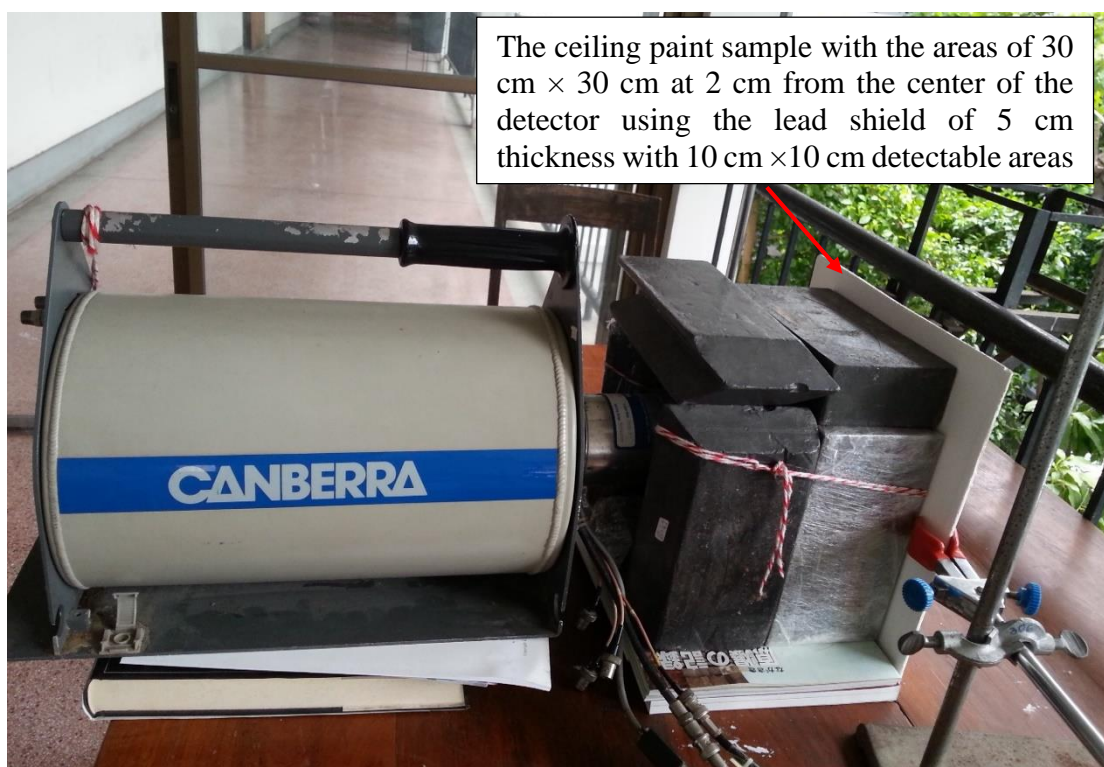
Figure 3. 7: The HPGe detector with the sample and the lead shield

3.4.1 Energy Calibration for in situ measurement

Table 3.2: The energy and channels of the standard sources

Sources	Energy (keV)	Channels
^{152}Eu	121.78	37
	244.7	77
	344.28	110
^{137}Cs	662	213
^{152}Eu	778.9	251
	964.08	311
	1089.5	351
	1112.07	360
^{60}Co	1172	380
	1132	431
^{152}Eu	1408	456
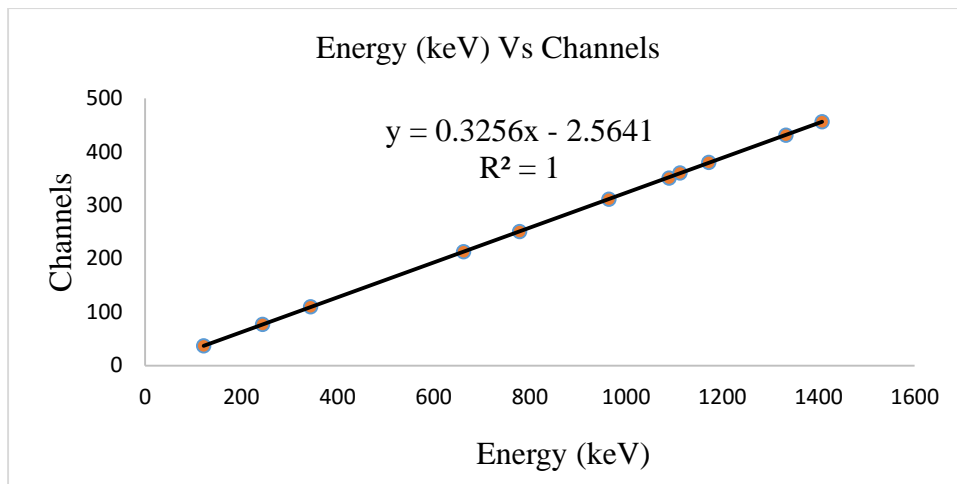
Figure 3. 8: The linear equation of energy calibration using standard sources of ^{152}Eu, ^{137}Cs, and ^{60}Co

3.4.2 Efficiency

The efficiency of this measurement is calculated based on the point sources of ^{152}Eu and ^{137}Cs which are placed on the center of the detector with the distance of 2 cm. Then these point sources are moved from the center of the detector to the right side at 1 cm, 2 cm, and 3cm until the end of the detectable side in the same line. Moreover, these sources were also moved to the left the same as the right. The sources were moved to the right and left in order to find the correction factor for the accurate efficiency.

3.4.3 In situ dose rate calculated from known activity and from measurement

In this research the dose rate of planar plywood can be calculate by:

Dose rate calculated from the activity of known ^{238}U and ^{232}Th contents.

- The activity (in Bq/g) of the paint samples and the standard reference materials (RGU-1 and RGTh-1) were known, so it can be converted to Bq/cm^2. Therefore, with the radius of our samples and the distances from the center of the detector, the dose rate and the flux were calculated in equation (16) and (17) respectively.

Dose rate calculated from the measurement

- The efficiency of the planar plywood with the surface of 10 cm × 10 cm of each energy was calculated by the equation in the standard efficiency curve of the point sources with the correction factor. Then the activity (Bq/100cm^2) was calculated by the equation

$$Activity\ (Bq/100cm^2) = \frac{Net\ area}{(Efficiency\ \times decay fraction)} \quad (18)$$

- Net area is the net peak area at each energy expressed in cps
- Efficiency it the absolute efficiency at each energy
- decay fraction the gamma-ray fraction at each energy

The activity (Bq/cm^2) can be converted from this activity. As the result, the dose rate and the flux were calculated in equation (16) and (17) respectively.

3.5   In situ object counting software (ISOCS)

Canberra designed the ISOCS product to be a complete In Situ Object Counting System or Software. It is now practical to use the in situ gamma spectroscopy in a wide variety of applications with this product. It can be used accurately to access the contamination levels in or on soil, building surfaces, pipes, ducts, tanks, boxes, bags, drums, and other objects with the different shapes and the activity distributions. The ISOCS measurements can be performed more quickly and at lower cost than other assessment method.

A complete ISOCS package which is integrated by Canberra typically includes an MCNP-characterized germanium detector, a Canberra MCA, a personal computer, appropriate shielding, the Basic Spectroscopy and Gamma Analysis packages for genie 2000, and the ISOC software. The Genie 2000 Efficiency CAM file must be created using ISOC software on the PC and then moved to the VMS system.

The steps of the ISOCS measurement process are to:

- Characterize the detector at the factory

- Acquire spectral data from the sample

- Specify the dimensions and physical composition of the measured object

- Generate an efficiency calibration file appropriate for the specified counting configuration

- Use these efficiency results to analyze the acquired spectra

The ISOCS calibration software is used to enter all necessary measurement parameters and to generate the efficiency calibration file. Moreover, the Canberra's Genie 2000 software is used to acquired and analyze the spectral data.

3.6   In situ gamma measurement using the survey meter of HDS-101 GN and GM energy compensated

3.6.1   Survey meter of HDS-101 GN

Power on:

- Press the On/Off push button, and the device will go into a Power Up Sequence

- Check the profile choice and the alarm level choice

- The HDS will go to a self-test procedure, a radiation background update phase

(**Attention!** No radiation source should be located close to the HDS-101 during the power up sequence)

- At the end of the count down, it switches to Detection mode with the default user profile.

Notice for routine checks:

- No fault message

- Background level is displayed

- Goes from "Calib. ID" to "ID Ready in less than two minutes.

For this measurement, the mode number 3 which is the integration mode was used because:

- Making a measurement with a high precision

- Acquiring a cumulated spectrum

- Identifying a radioactive source

- The integration screen shows the following information:

- Instant gamma counts per second

- Indication about the position of the HDS-101:

1. Source OK: means that the HDS-101 is positioned at a distance which give an acceptable count rate.

2. Source too far: means that the HDS-101 is too far from the source which results in a too low counts rate which will lead to a long measurement time.

3. Source to close: means to that the HDS-101 is too close from the source which results in a too high counts rate which will lead to a saturated spectrum and may give a wrong identification.

The screen display of the survey meter during the measurement as be shown in the Fig. 3.9 below is "source too far". Then the button **"Acq"** was pressed for the measurement. When integration is completed, three screens are available. The first screen is the identification result, which gives the list of isotopes identified (isotope category, name and confidence index). The gain error is indicated and should be less than 3%. The second screen gives the spectrum. The last screen gives the mean values, dose rate, during the integration period.
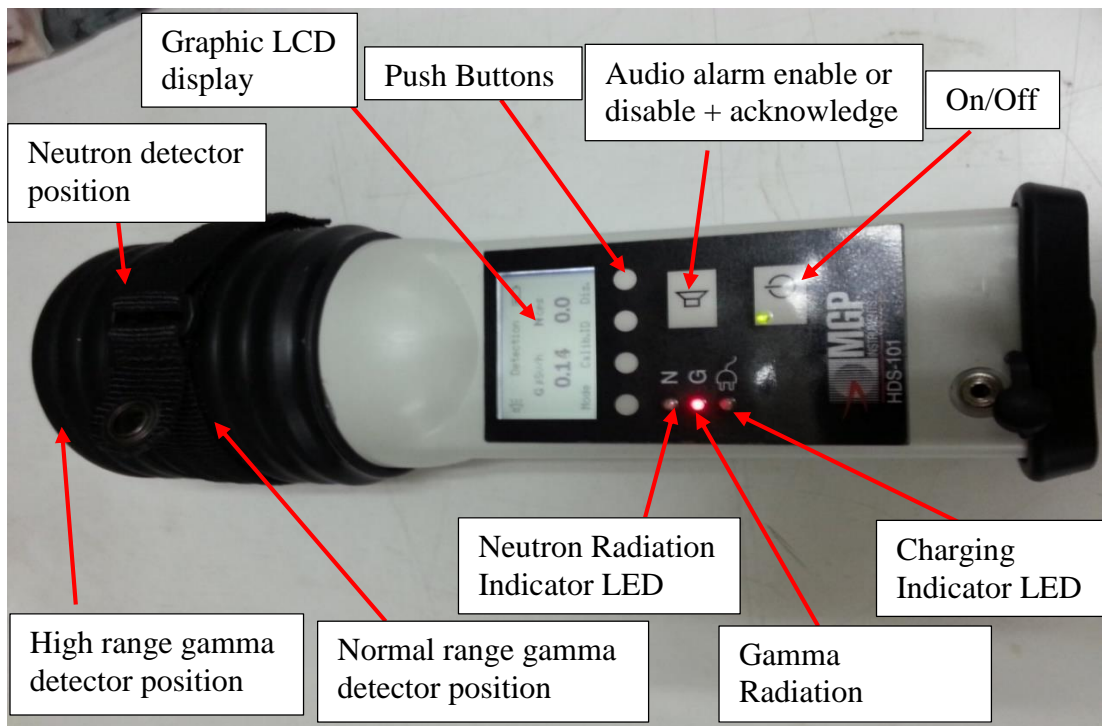
Figure 3. 9: The picture of survey meter, HDS-101 GN

Figure 3. 10: The in situ measurement using the survey meter of the HDS-101 GN

3.6.2 Survey meter of GM energy compensated

Another survey meter which is called gamma neutron survey meter, GM energy compensated was also used for this measurement. This survey meter displayed the dose rate in μSv/hr.
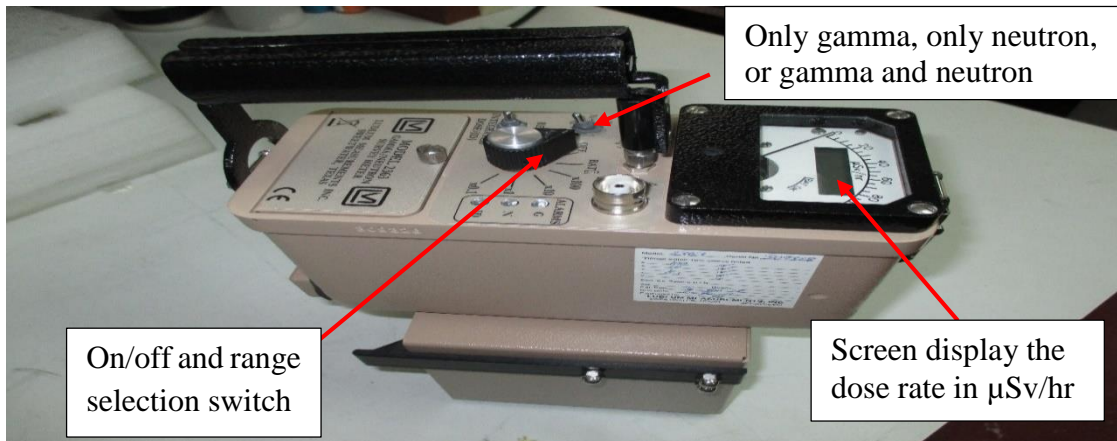
Figure 3. 11: The gamma neutron survey meter, GM energy compensated
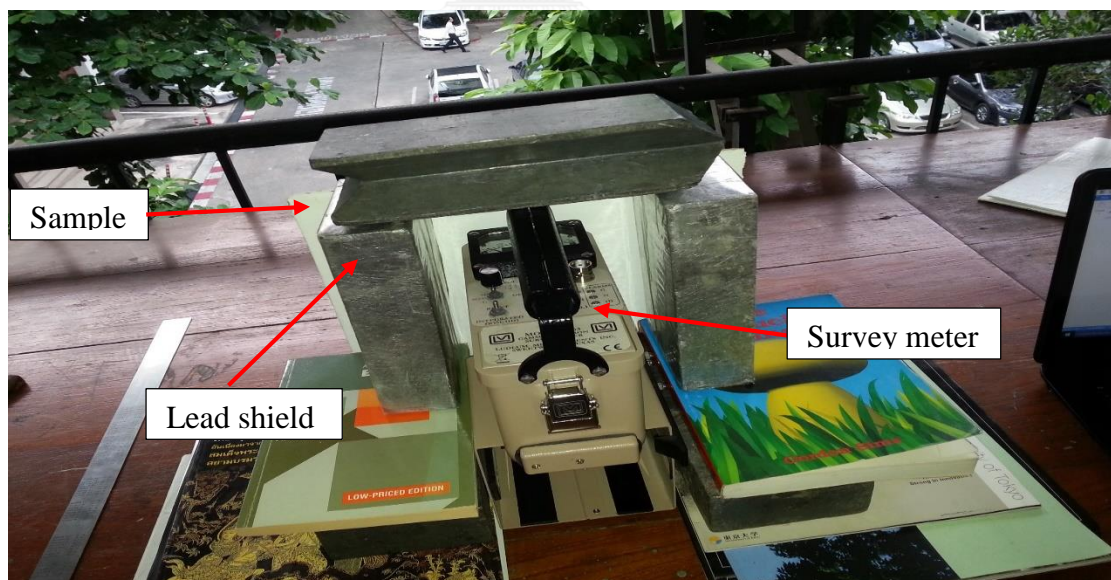
Figure 3. 12: The GM energy compensated in side lead shield for the measurement

Chapter 4

Data Analysis and Results

4.1 Data analysis and results for laboratory measurement

4.1.1 Energy calibration for samples by using the standard sources

By using the linear equation of Y = 1.86X +0.88 in the energy calibration curve of standard sources of RGU-1 and RGTh-1, the channels of each energy can be calculated.

Where,

Y is the channel number, and X is the energy in keV.

Table 4.1: The energy and channels of the radionuclides

Radionuclides	Energy (keV)	Channels
Pb-214	352.2	656
Bi-214	609.3	1134
Ac-228	209.4	390
Pb-212	238.7	445
Ac-228	270.5	504
Tl-208	277.6	517
Ac-228	337.9	629
Ac-228	462.5	861
Tl-208	510.9	951
Tl-208	583.1	1085
Bi-212	726.7	1353
Ac-228	794.2	1478
Tl-208	860.1	1601
Ac-228	910.8	1695
Ac-228	969.0	1803
Tl-208	2612.9	4861
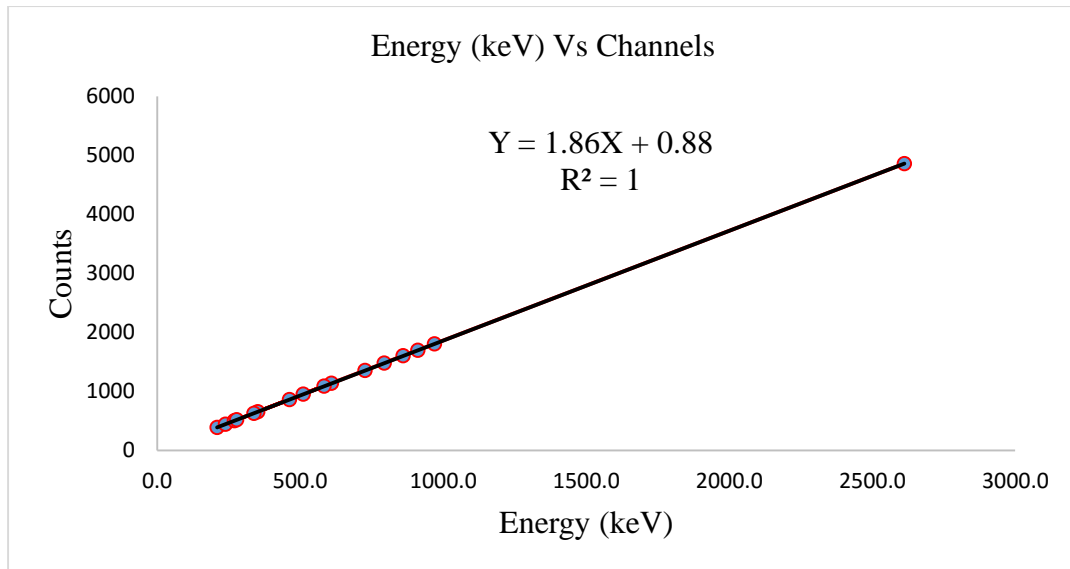
Figure 4. 1: The energy calibration curve

4.1.2 Calculation of the specific activity of ^{238}U and ^{232}Th

The obtained spectra of all four ceiling paint samples showed the peaks of uranium daughters such as lead-214 (^{214}Pb) and bisbmuth-214 (^{214}Bi) and thorium daughters such as actinium-228(^{228}Ac) and thallium-208 (^{208}Tl). The spectra indicated that there were uranium and thorium in the ceiling paint samples. Uranium and thorium mainly present in soil and rock. Products having raw materials from soil and rock always contain uranium and thorium such as construction materials, ceramic tiles, fertilizers, coals, etc. Normally paint samples should not contain uranium and thorium at a detectable level except they are intentionally added.

From our measurement, the amount of uranium and thorium could be obtained by using the method of direct comparison in equation (12). The uncertainties of these specific activities were determined by using the error propagation formula (Ahmad. 1997, p. 13; Knoll. G. F., 2000. p. 89). The specific activities of the radionuclides ranged from 149.22±3.58 to 2124.55±26.30 Bq/kg for all samples as be shown in Table 4.2 below.

Table 4.2: The specific activity (Bq/kg±1σ) of some natural radionuclides with counting time of 2 hours

Samples (Activity)	^{214}Bi (E=609.3 keV)	^{228}Ac (E=910.8 keV)
W1	176.87±3.86	2124.55±26.30
W2	171.88±3.82	2018.70±25.50
G1	149.22±3.58	1792.45±23.61
G2	306.07±5.30	2116.97±27.64

The highest specific activity of these radionuclides was found in the sample W1 (2124.55±26.30 Bq/kg) in ^{232}Th series of ^{228}Ac (E=911 keV), but the lowest specific activity was found in the sample G1 (149.22±3.58 Bq/kg) in ^{238}U series of ^{214}Bi (E=609.3 keV). Moreover, in ^{238}U series, the specific activity of ^{214}Bi (609 keV) in all samples ranged from 149.22±3.58 to 306.07±5.30 Bq/kg. Furthermore, in ^{232}Th series, the specific activity of ^{228}Ac (911 keV) ranged from 1792.45±23.61 to 2124.55±26.30 Bq/kg.

The gamma-rays spectra of the standard reference materials of RGU-1 and RGTh-1 were be shown below. For RGU-1 and RGTh-1, there were several peak intensities emitting from the several radionuclides. The specific activity of ^{238}U was calculated based on the radionuclide of ^{214}Bi (E=609 keV), and the specific activity of ^{232}Th was calculated based on the radionuclide of ^{228}Ac (E=911 keV). Their peak intensities represented the emitted radiation from the radionuclides with their energy in keV.
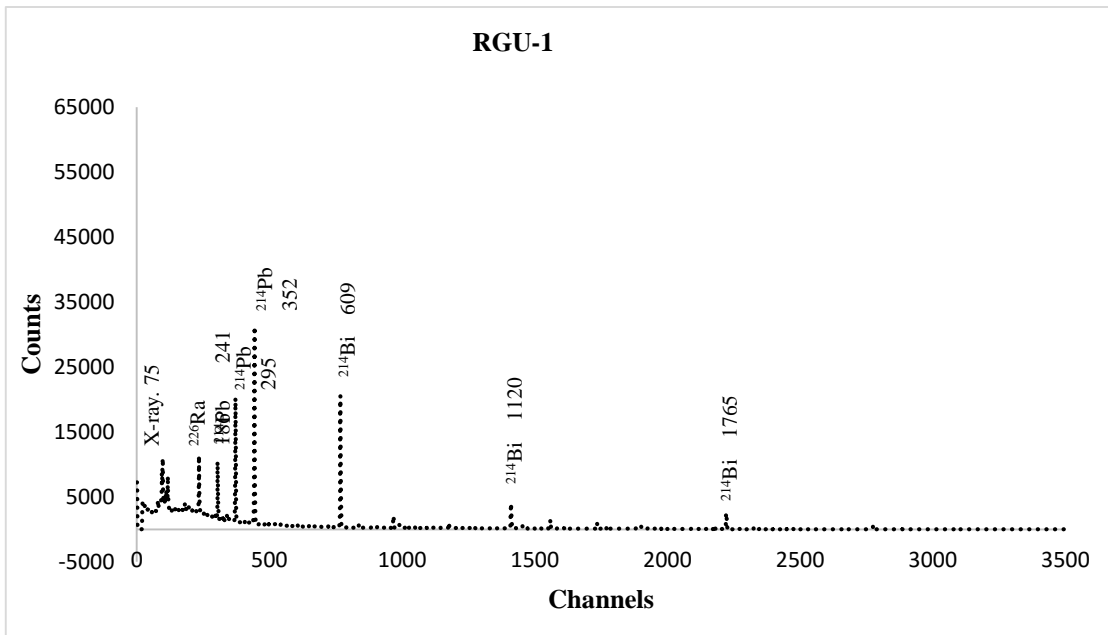
Figure 4. 2: Characteristic Gamma Spectrum of RGU-1 with Counting Time 7,200
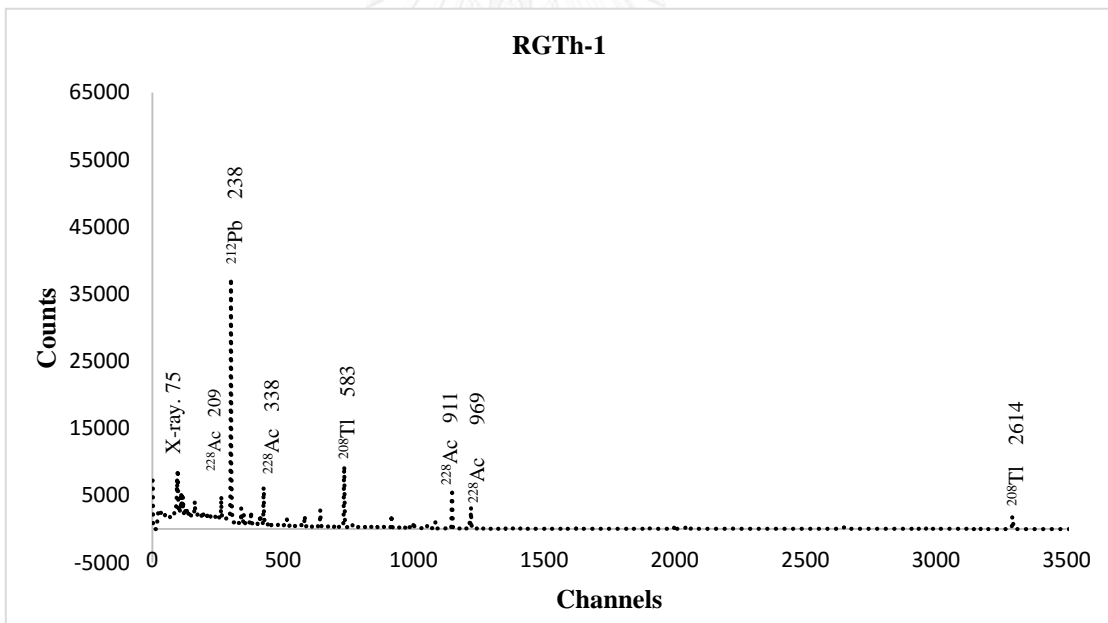
*F*igure 4. 3: Characteristic Gamma Spectrum of RGTh-1 with Counting Time 7,200 s

The gamma spectra of four samples and a blank were shown below. The gamma spectrum of the blank showed very low peak intensities of radionuclides while the spectra of four samples showed several energy peaks with high peak intensities. Their peak intensities represented the emitted radiation from the radionuclides with their energy in keV.
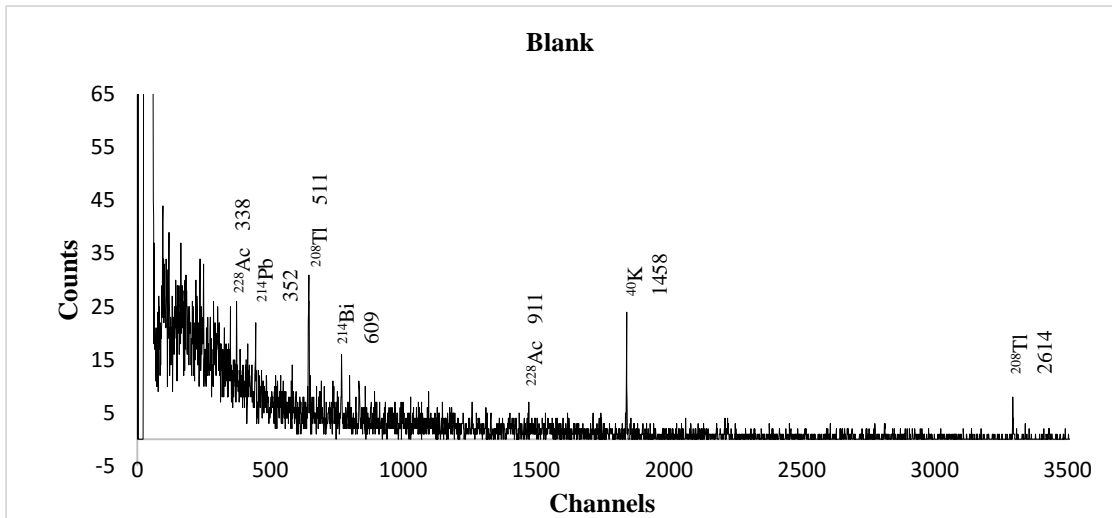
Figure 4. 4: Characteristic Gamma Spectrum of blank (interior paint sample) with Counting Time 7,200 s
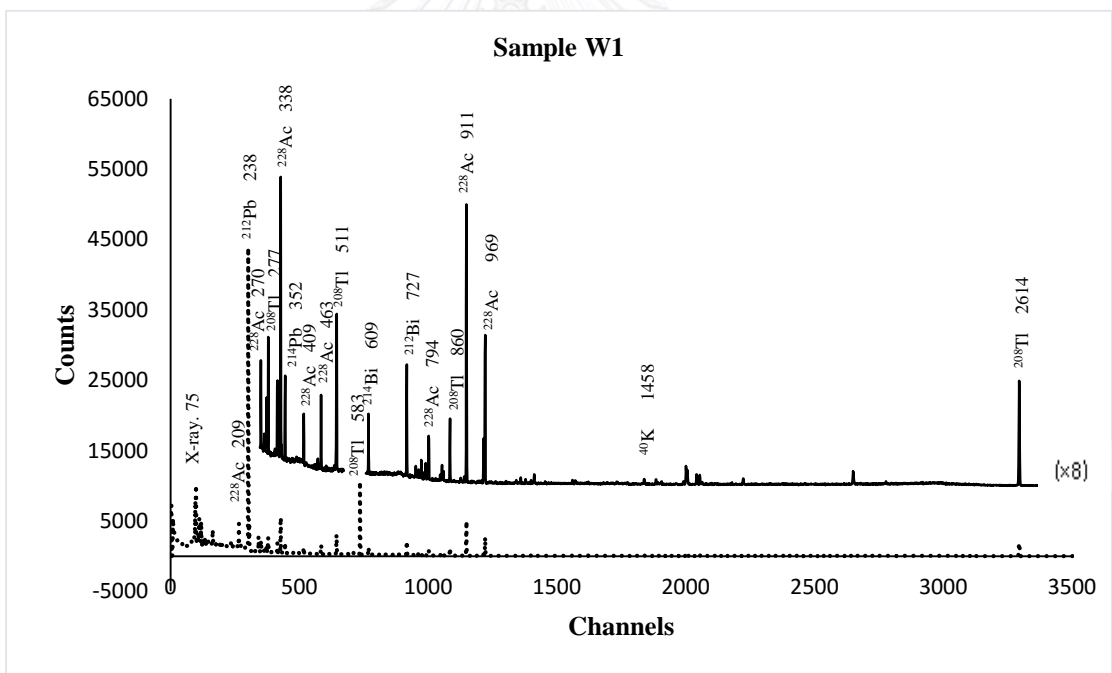
Figure 4. 5: Characteristic Gamma Spectrum of Ceiling Paint Sample W1 with Counting Time 7,200 s
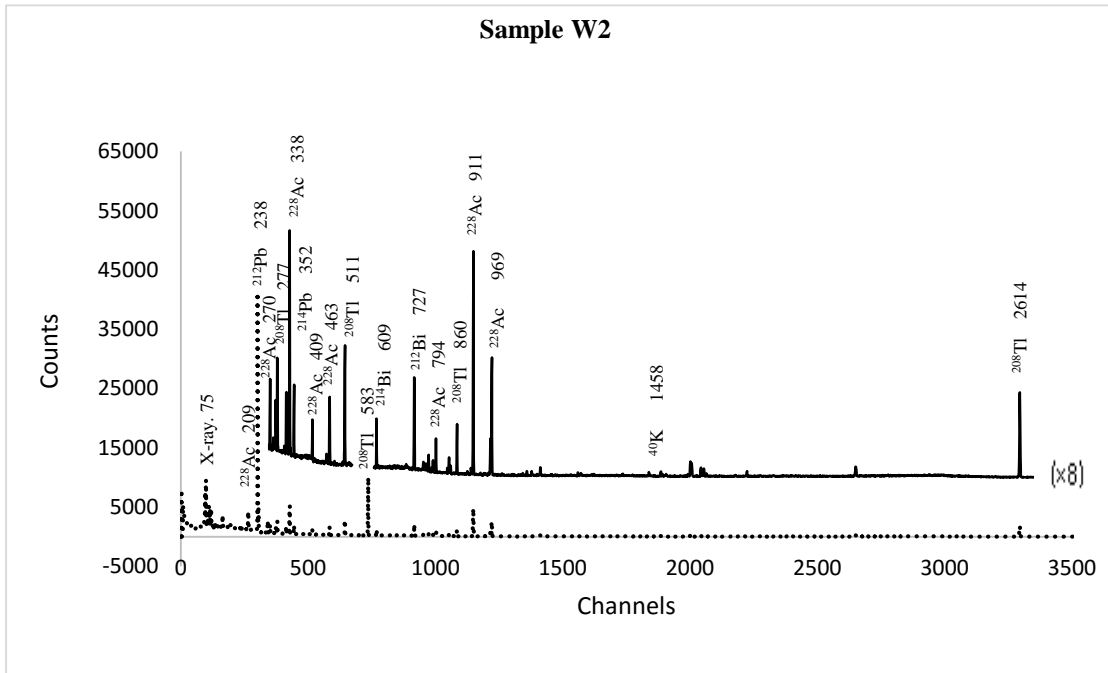
Figure 4. 6: Characteristic Gamma Spectrum of Ceiling Paint Sample W2 with Counting Time 7,200 s
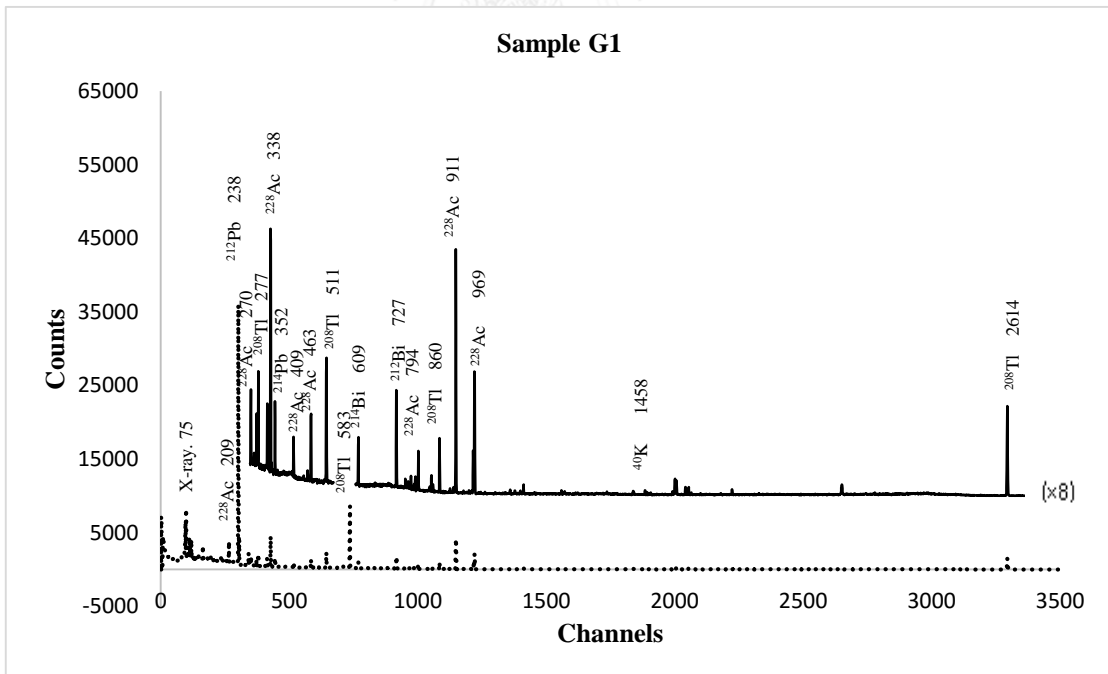
Figure 4. 7: Characteristic Gamma Spectrum of Ceiling Paint Sample G1 with Counting Time 7,200 s
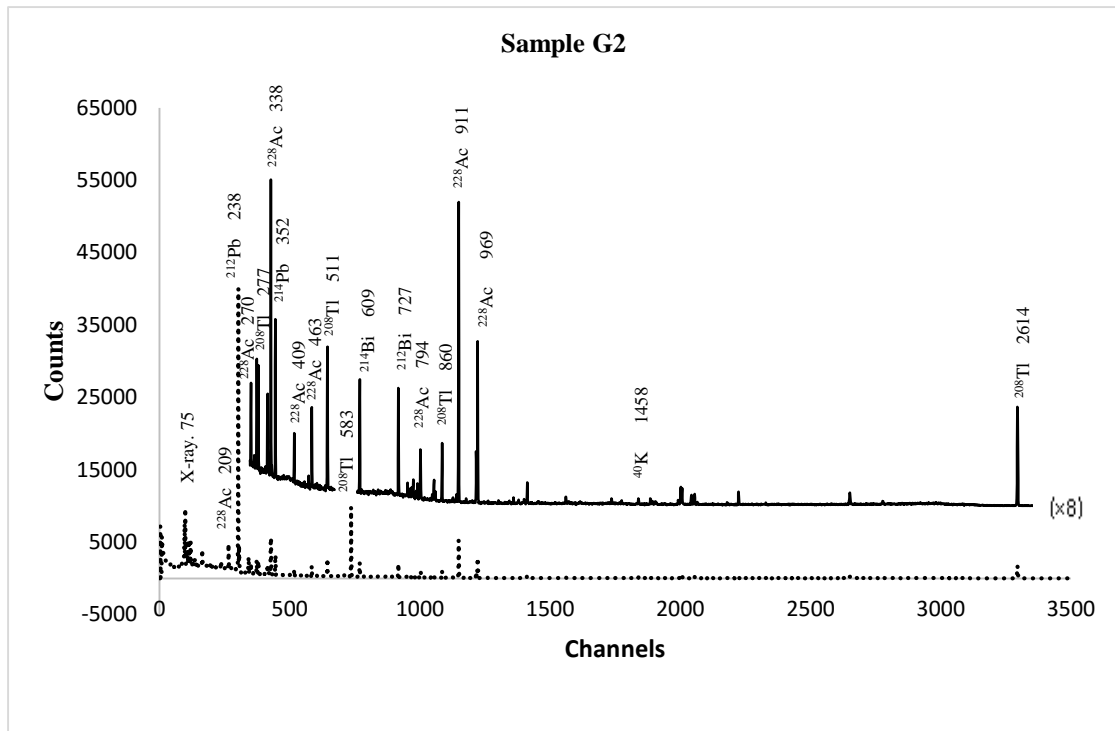
Figure 4. 8: Characteristic Gamma Spectrum of Ceiling Paint Sample G2 with Counting Time 7,200 s

The peak intensity of ^{214}Bi (E=609 keV) in the uranium ore standard were higher than the speak intensity of ^{214}Bi (E=609 keV) in all samples. Moreover, the peak intensity of ^{228}Ac (911 keV) in the thorium ore standard were slightly higher than the peak intensities of ^{228}Ac (911 keV) in all samples.

The gamma spectrum of the blank in Fig. 4.4 showed that the background was very low. This means that this blank was not radioactive. However, the spectra of four samples such as W1, W2, G1, and G2 were shown that there were the several peak intensities emitting from the different radionuclides with their individual energy in keV. The peak intensities of those radionuclides were found out that they were the daughters of ^{238}U, and ^{232}Th series because the energy peaks of them were the same as the energy peaks of the uranium and thorium standards.

The specific activity of ^{238}U was calculated as ^{226}Ra (The parent of ^{222}Rn) activity based on its decay products ^{214}Bi (E=609.3 keV) in the radioactive equilibrium

with their parent. In the ^{238}U decay series, ^{214}Bi is considered as ^{226}Ra indicators corresponding with the radium mobility in geological times because of the geochemical reasons (Corte et al., 2005, p. 590). In the secular equilibrium, the specific activity of ^{220}Rn was equal to the specific activity of its parent, ^{232}Th. The uncertainties of these specific activities were determined using the error propagation formula.

Table 4.3: The specific activity (Bq/kg±1σ) of ^{238}U and ^{232}Th

Samples Activity	^{238}U	^{232}Th
W1	176.87±3.86	2124.55±26.30
W2	171.88±3.82	2018.70±25.50
G1	149.22±3.58	1792.45±23.61
G2	306.07±5.30	2116.97±27.64

In secular equilibrium, the specific activity of ^{238}U and ^{232}Th is equal to the specific activity of their daughters. The highest specific activities of ^{232}Th was found in sample W1 (2121.11±26.52 Bq/kg), and the highest specific activity of ^{238}U was found in sample G2 (299.76±4.87 Bq/kg). The lowest specific activities of ^{238}U and ^{232}Th were found in sample G1 (144.61±3.28 and 1773.59±23.66 Bq/kg) respectively. The specific activities of ^{238}U and ^{232}Th of these four samples were higher than the corresponding world mean values for the building materials (50 and 50 Bq/kg respectively) (UNSCEAR, 1993, p. 41).

4.2. Data analysis and results for in situ measurement

4.2.1 Energy calibration for samples by using standard point sources

By using the linear equation of Y = 0.33X – 2.56 in the energy calibration curve of standard sources of ^{152}Eu, ^{60}Co, and ^{137}Cs, the channels of each energy can be calculated.

Where,

Y is the channel number, and X is the energy in keV.

Table 4.4: The energy and cannels of the radionuclides

Radionuclides	Energy (keV)	Channels
Pb-212	238.7	76
Ac-228	337.9	109
Pb-214	352.2	114
Ac-228	462.5	150
Tl-208	510.9	166
Tl-208	583.1	190
Bi-214	609.3	199
Bi-212	726.7	237
Ac-228	910.8	298
Ac-228	969	317
Tl-208	2612.9	860
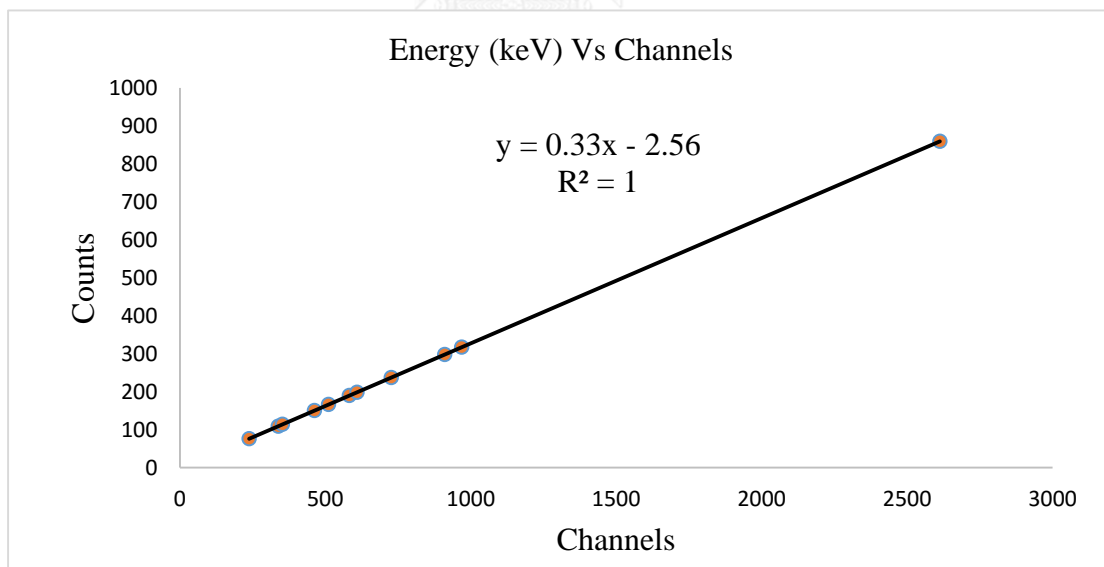
Figure 4. 9: The linear line of energy Vs Channels

4.2.2 Efficiency

Table 4.5: The efficiency at the center and right side of the detector

Sources with energy (keV)	Efficiency at center	Efficiency move 1 cm to right	Efficiency move 2 cm to right	Efficiency move 3 cm to right
^{152}Eu at 121.78	0.0473	0.0445	0.348	0.0242
^{152}Eu at 242.7	0.0208	0.0205	0.0170	0.0131
^{152}Eu at 344.28	0.0141	0.0135	0.0114	0.0086
^{137}Cs at 662	0.0061	0.0059	0.0051	0.0039
^{152}Eu at 778.9	0.0061	0.0056	0.0048	0.0037
^{152}Eu at 964.08	0.0049	0.0049	0.0040	0.0032
^{152}Eu at 1085.9	0.0055	0.0051	0.0040	0.0028
^{152}Eu at 1408	0.0036	0.0034	0.0029	0.0022

Table 4.6: The efficiency at the left side of the detector

Sources with energy (keV)	Efficiency move 1 cm to left	Efficiency move 2 cm to left	Efficiency move 3 cm to left
^{152}Eu at 121.78	0.0434	0.0350	0.0263
^{152}Eu at 242.7	0.0204	0.0164	0.0127
^{152}Eu at 344.28	0.0137	0.0113	0.0089
^{137}Cs at 662	0.0057	0.0048	0.0039
^{152}Eu at 778.9	0.0054	0.0047	0.0039
^{152}Eu at 964.08	0.0045	0.0041	0.0033
^{152}Eu at 1085.9	0.0035	0.0035	0.0024
^{152}Eu at 1408	0.0033	0.0027	0.0022

By taking the average of the efficiency from the left and right at the same position then divide by the efficiency at center. The center also needs to divide by itself.

The result of the taking average and dividing the center represents the counting rate related to position 0. As a result, the correction factor is determined.

- Efficiency at center/center represents position 0 cm

- The average efficiency of left and right at 1cm from the center and then divide the efficiency at the center represents position 1 cm

- The average efficiency of left and right at 2 cm from the center and then divide the efficiency at the center represents position 2 cm

- The average efficiency of left and right at 3 cm from the center and then divide the efficiency at the center represents position 3 cm

Table 4.7: The ratio efficiency of different position with different energy

Energy (keV)	Position (cm)	Counting rate related to position 0
^{152}Eu at 121.78	0	1
^{152}Eu at 242.7	0	1
^{152}Eu at 344.28	0	1
^{137}Cs at 662	0	1
^{152}Eu at 778.9	0	1
^{152}Eu at 964.08	0	1
^{152}Eu at 1085.9	0	1
^{152}Eu at 1408	0	1
^{152}Eu at 121.78	1	0.93
^{152}Eu at 242.7	1	0.98
^{152}Eu at 344.28	1	0.96
^{137}Cs at 662	1	0.95
^{152}Eu at 778.9	1	0.9
^{152}Eu at 964.08	1	0.96
^{152}Eu at 1085.9	1	0.78
^{152}Eu at 1408	1	0.93
^{152}Eu at 121.78	2	0.74

Energy (keV) (cont.)	Position (cm) (cont.)	Counting rate related to position 0 (cont.)
[152]Eu at 242.7	2	0.8
[152]Eu at 344.28	2	0.8
[137]Cs at 662	2	0.81
[152]Eu at 778.9	2	0.78
[152]Eu at 964.08	2	0.83
[152]Eu at 1085.9	2	0.68
[152]Eu at 1408	2	0.78
[152]Eu at 121.78	3	0.53
[152]Eu at 242.7	3	0.62
[152]Eu at 344.28	3	0.62
[137]Cs at 662	3	0.64
[152]Eu at 778.9	3	0.62
[152]Eu at 964.08	3	0.66
[152]Eu at 1085.9	3	0.47
[152]Eu at 1408	3	0.61

The curve of ratio efficiency of different position for different energy and the fitting of ratio efficiency of different position for different energy were plotted in order to find the correction factor for the accurate efficiency were shown in the figures below.
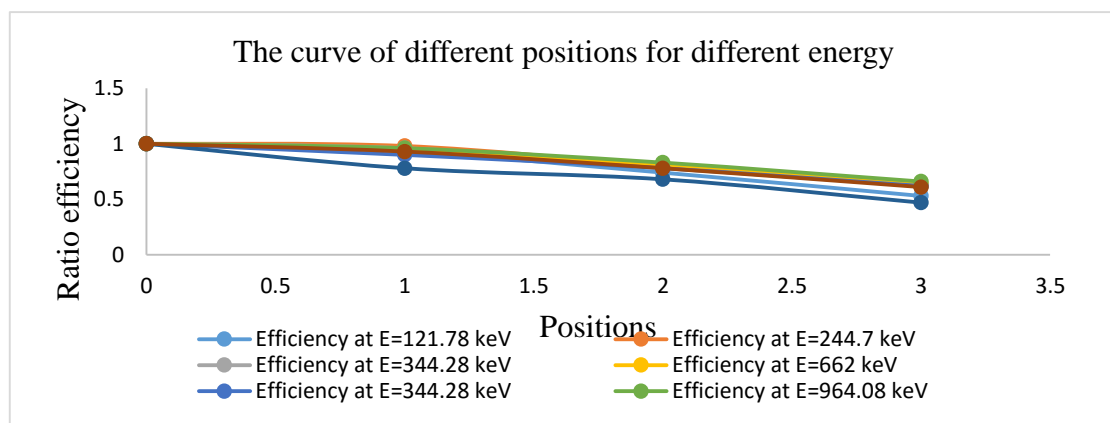
Figure 4. 10: The ratio efficiency curve of different position for different energy

The curve of counting rate related to position 0

$$Y = -0.0262X^2 - 0.057x + 1.0018$$
$$R^2 = 0.9131$$
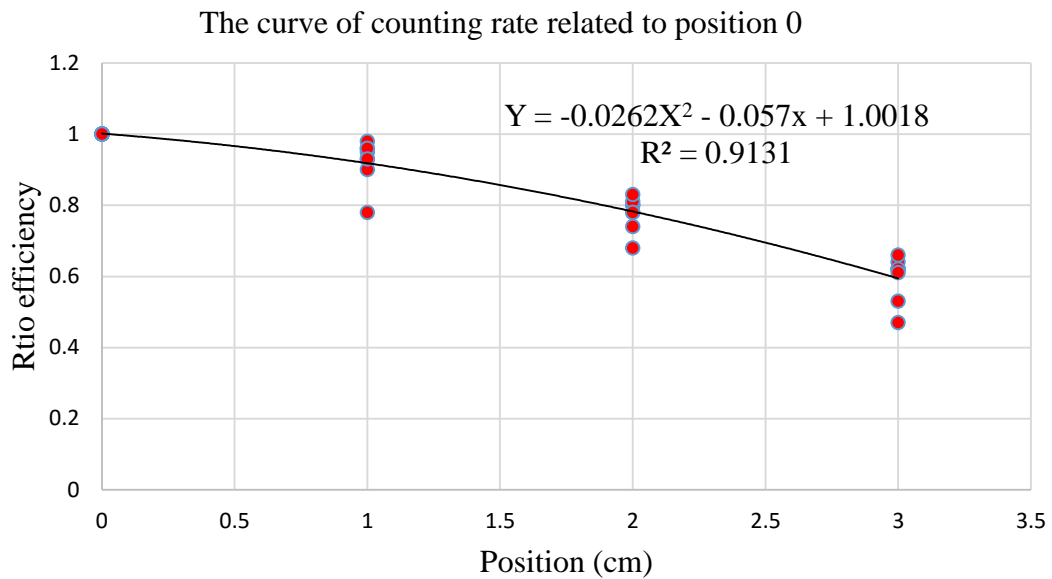
Figure 4. 11: The fitting curve for the ratio efficiency

According to the curve of counting rate related to position 0, the correction factor for the efficiency of this measurement is the average of the lowest (efficiency=0.47) and highest (efficiency=1). Therefore the correction factor for this efficiency of planar plywood with the surface of 10 cm × 10 cm is 0.74. The standard efficiency curve of the standard point sources, ^{152}Eu and ^{137}Cs at center.

Point sources efficiency curve

Energy (keV)

$$Y = 6.27X^{-1.036}$$
$$R^2 = 0.98$$
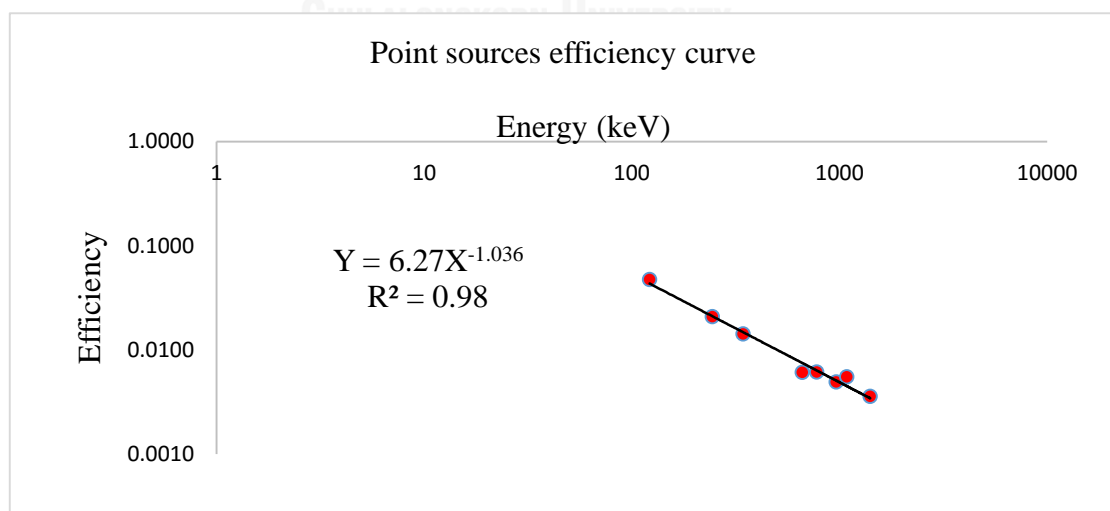
Figure 4. 12: The efficiency curve of point sources, ^{152}Eu and ^{137}Cs, at center
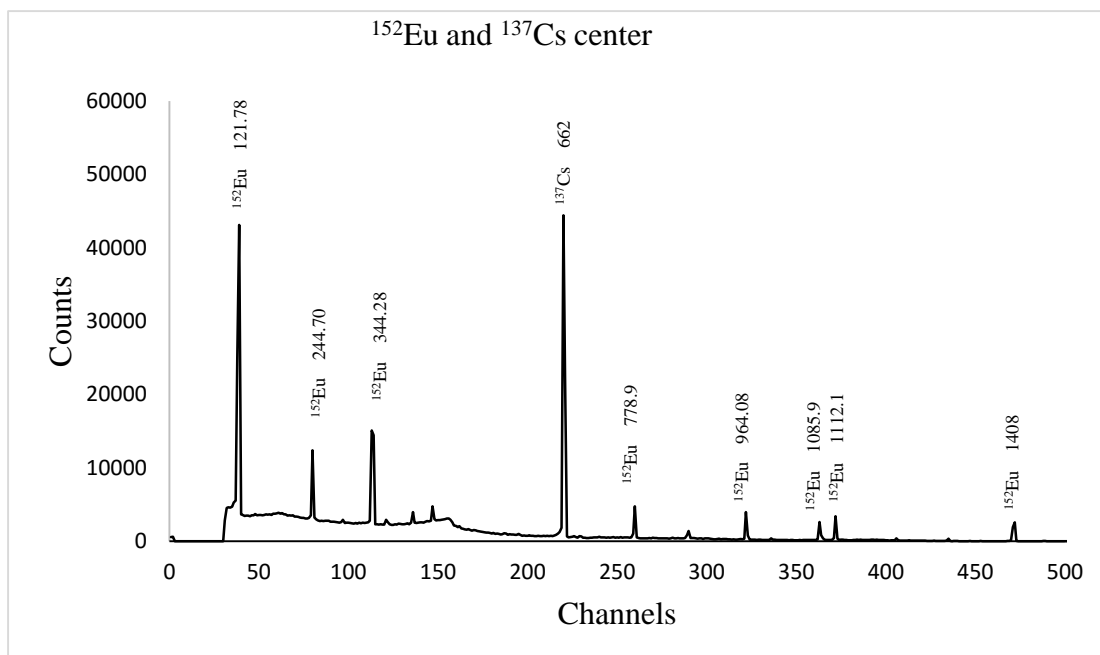
Figure 4. 13: The spectrum of ^{152}Eu and ^{137}Cs at center counting time 600 s

By using the linear equation of standard efficiency Vs energy at 2 cm away from the center of the detector, the efficiency of our measurement is calculated, and the correction factor which is equal to 0.74 is then taken into account.

Table 4.8: The energy and the efficiency of the radionuclides

Isotopes	Energy (keV)	Efficiency
^{212}Pb	238.7	0.0160
^{228}Ac	337.9	0.0111
^{214}Pb	352.2	0.0107
^{228}Ac	462.5	0.0080
^{208}Tl	510.9	0.0073
	583.1	0.0063
^{214}Bi	609.3	0.0060
^{212}Bi	726.7	0.0050
^{228}Ac	910.8	0.0040
	969	0.0037
^{208}Tl	2612.9	0.0013
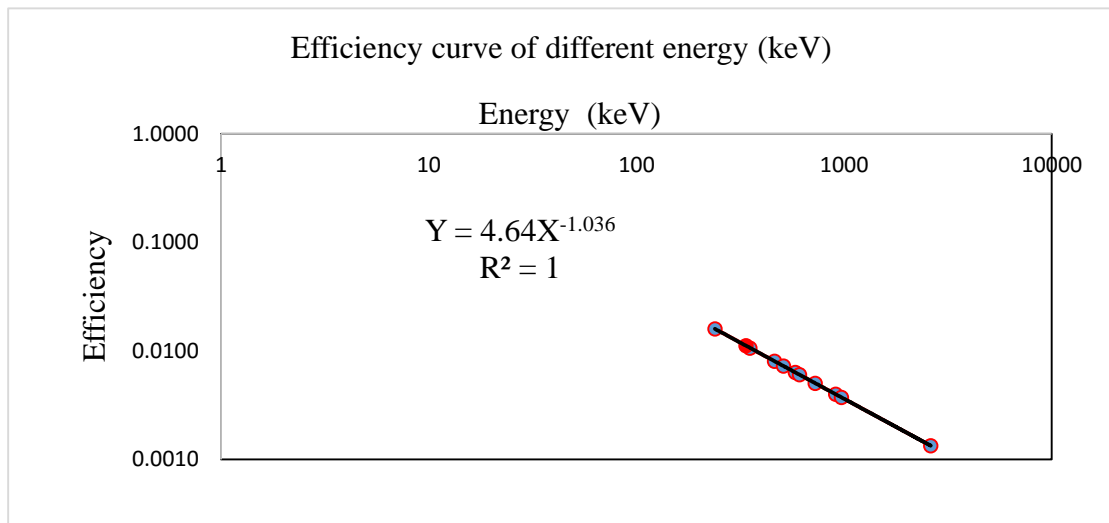
Figure 4. 14: The line of the efficiency and the energy of the radionuclides

4.2.3   In situ dose rate calculation

The gamma dose rate was calculated due to the gamma ray emission from radiation hazard of the radionuclides in ^{238}U series, and ^{232}Th series in the ceiling paint samples. The spectrum of samples W1a, W1b, W2a, W2b, G1a, G1b, G2a, G2b, M, and N below showed the emitting of different peak intensities from several radionuclides. The radionuclides in these spectrum are not in secular equilibrium
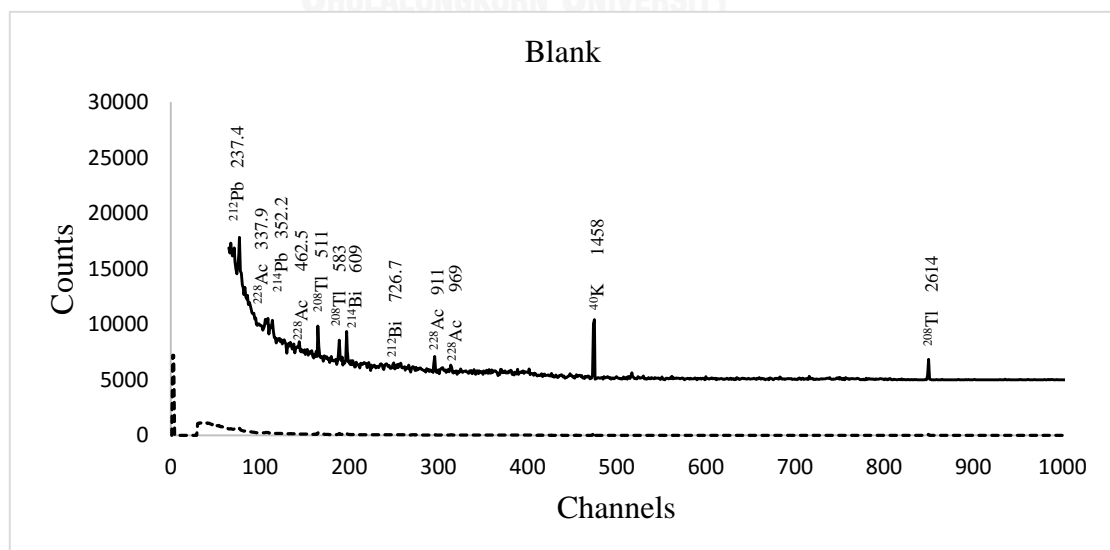
Figure 4. 15: The spectrum of blank, an interior paint sample, for in situ measurement with counting time of 7,200 s
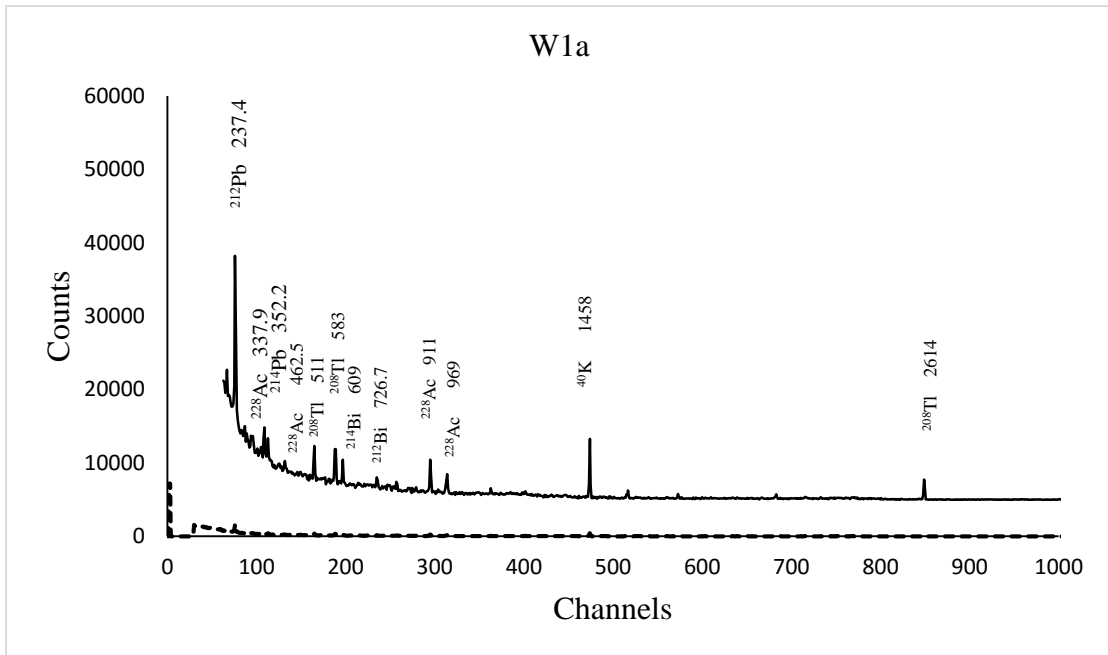
Figure 4. 16: The spectrum of sample W1a for in situ measurement with counting time of 7,200 s
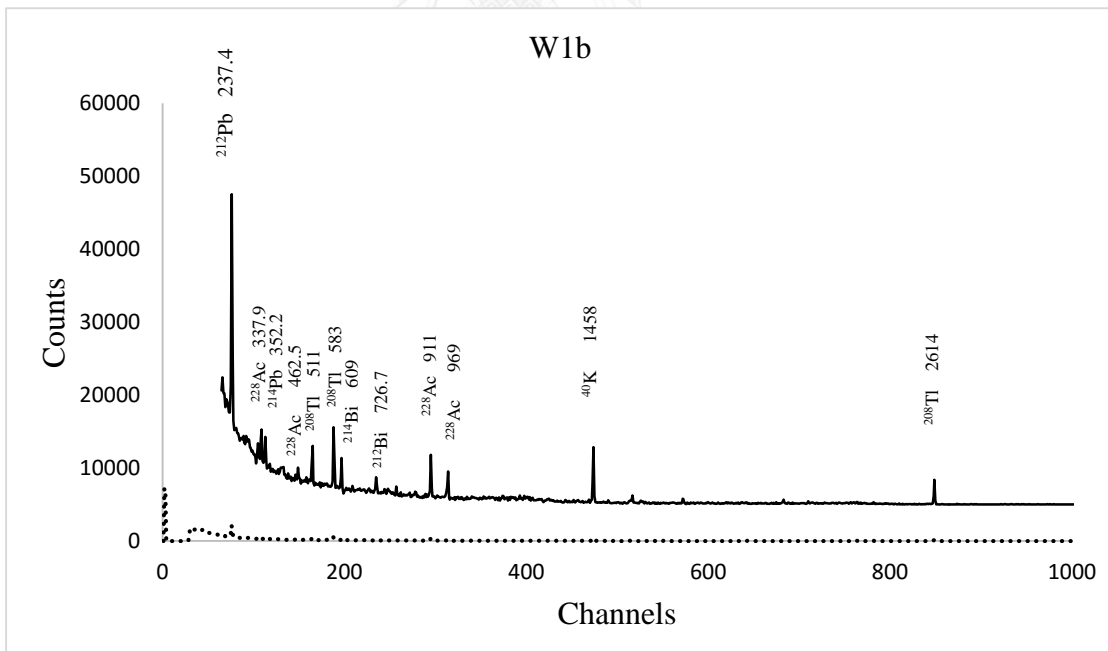
Figure 4. 17: The spectrum of sample W1b for in situ measurement with counting time of 7,200 s
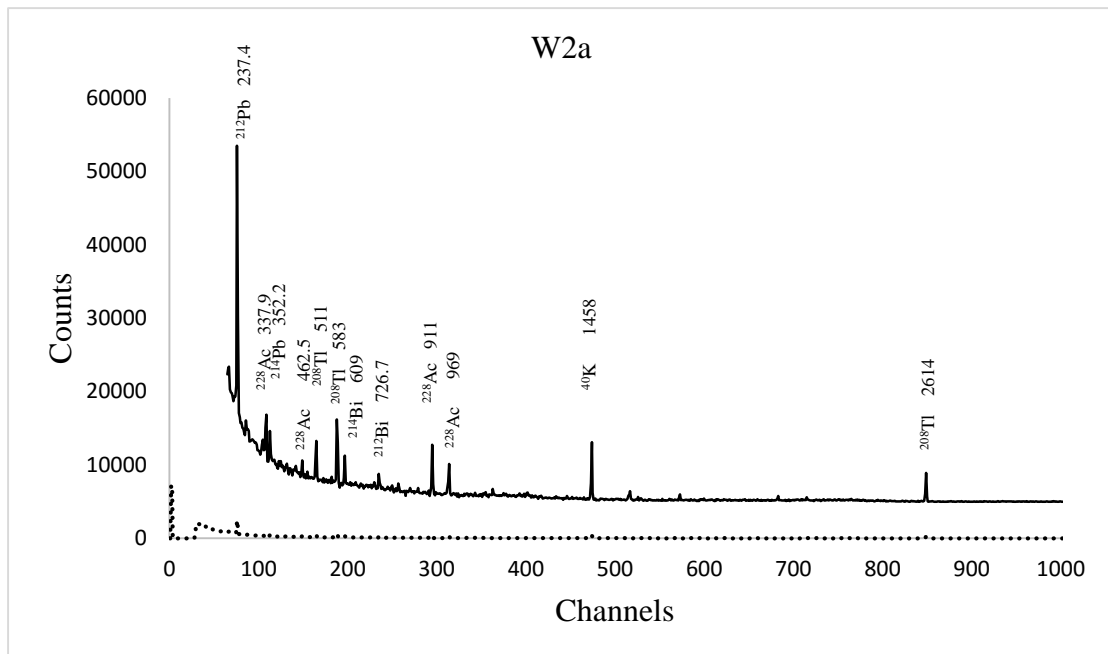
Figure 4. 18: The spectrum of sample W2a for in situ measurement with counting time of 7,200 s
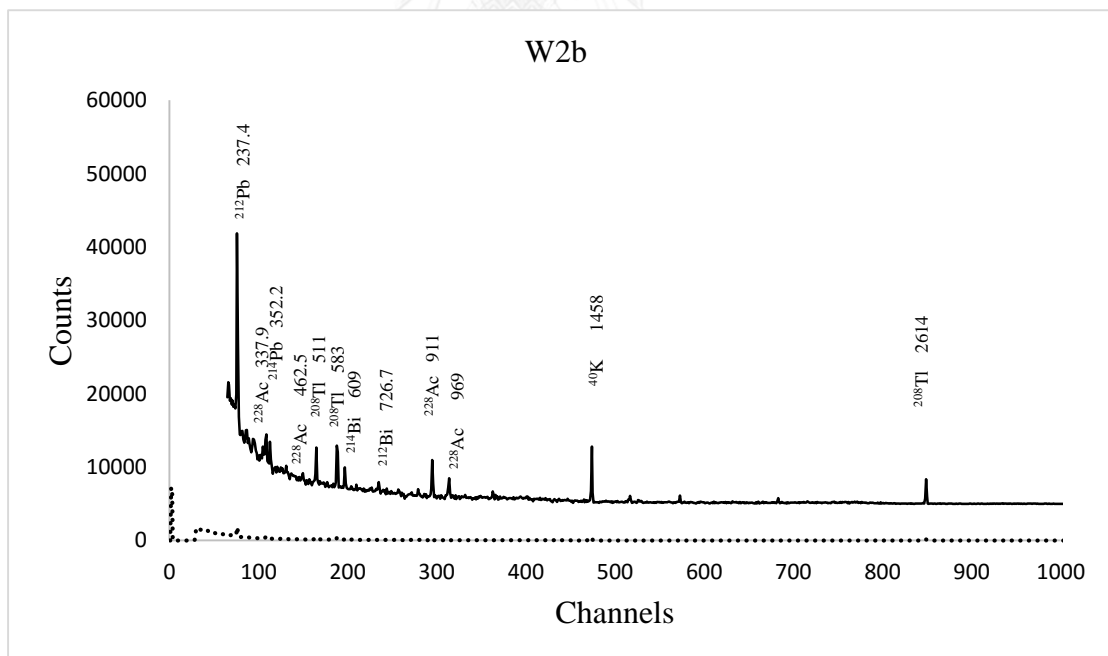
Figure 4. 19: The spectrum of sample W2b for in situ measurement with counting time of 7,200 s
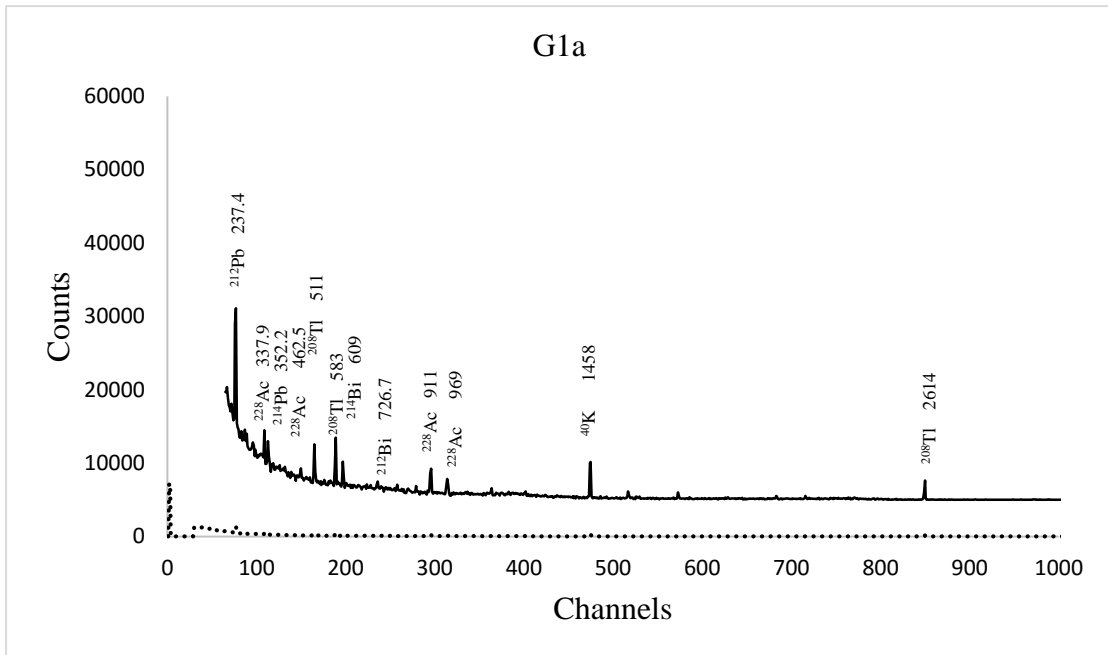
Figure 4. 20: The spectrum of sample G1a for in situ measurement with counting time of 7,200 s
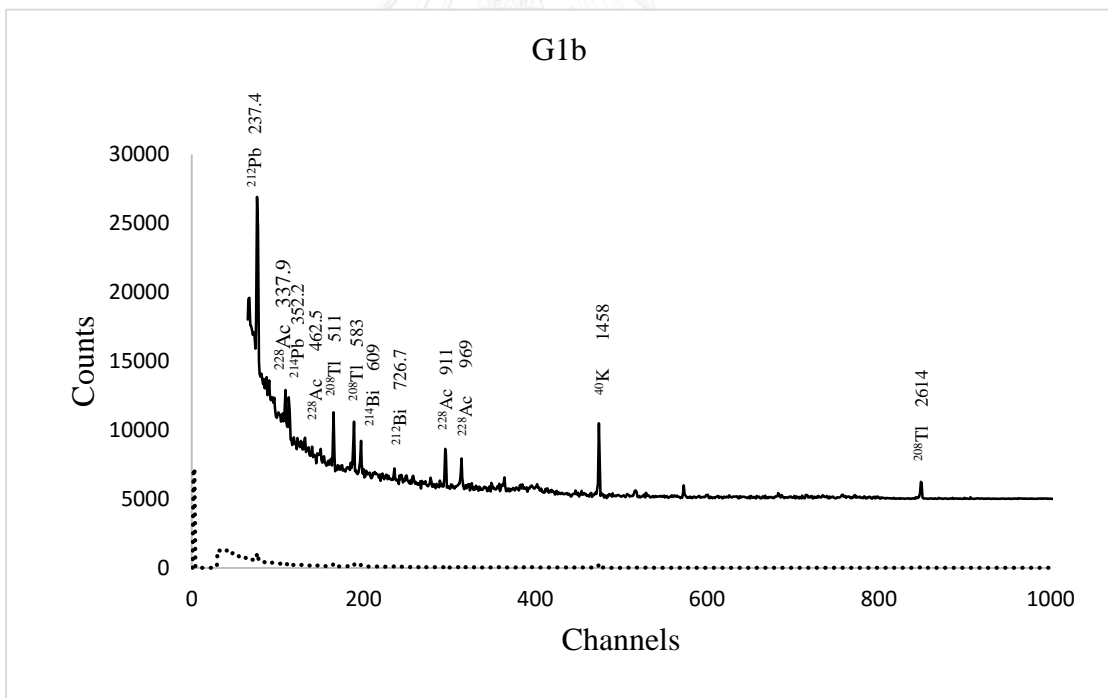
Figure 4. 21: The spectrum of sample G1b for in situ measurement with counting time of 7,200 s
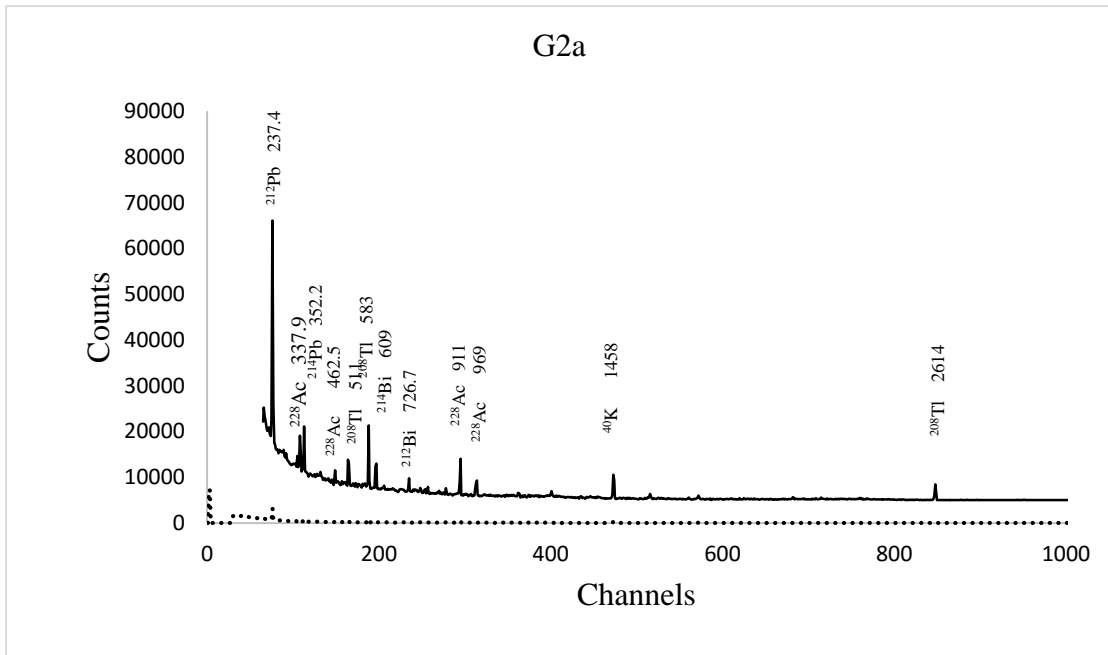
Figure 4. 22: The spectrum of sample G2a for in situ measurement with counting time of 7,200 s
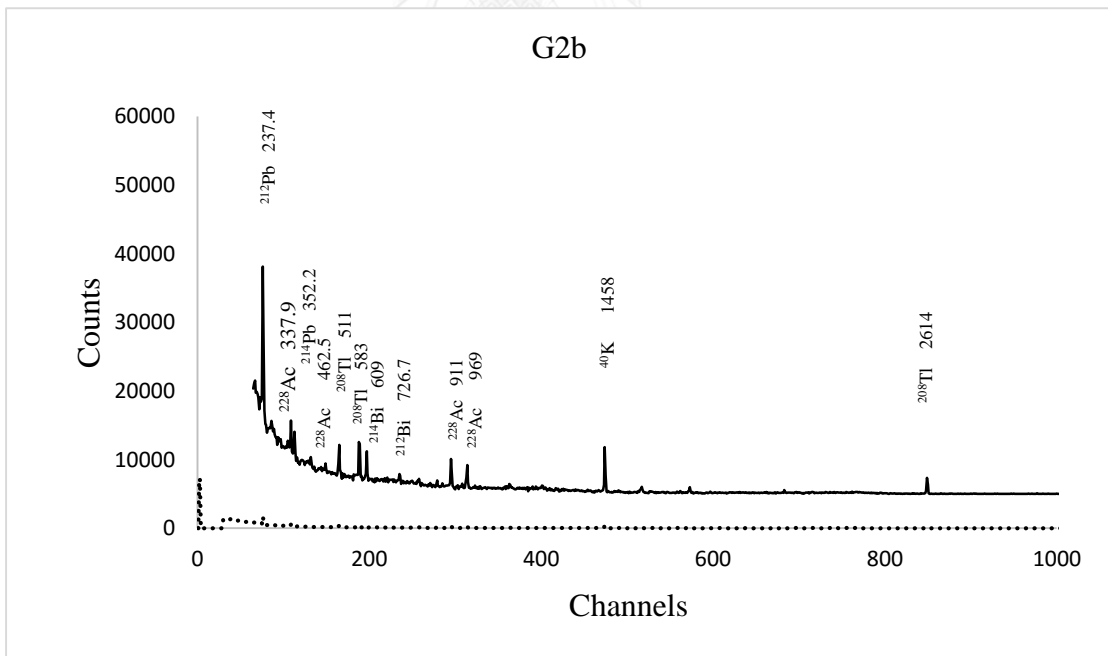
Figure 4. 23: The spectrum of sample G2b for in situ measurement with counting time of 7,200 s
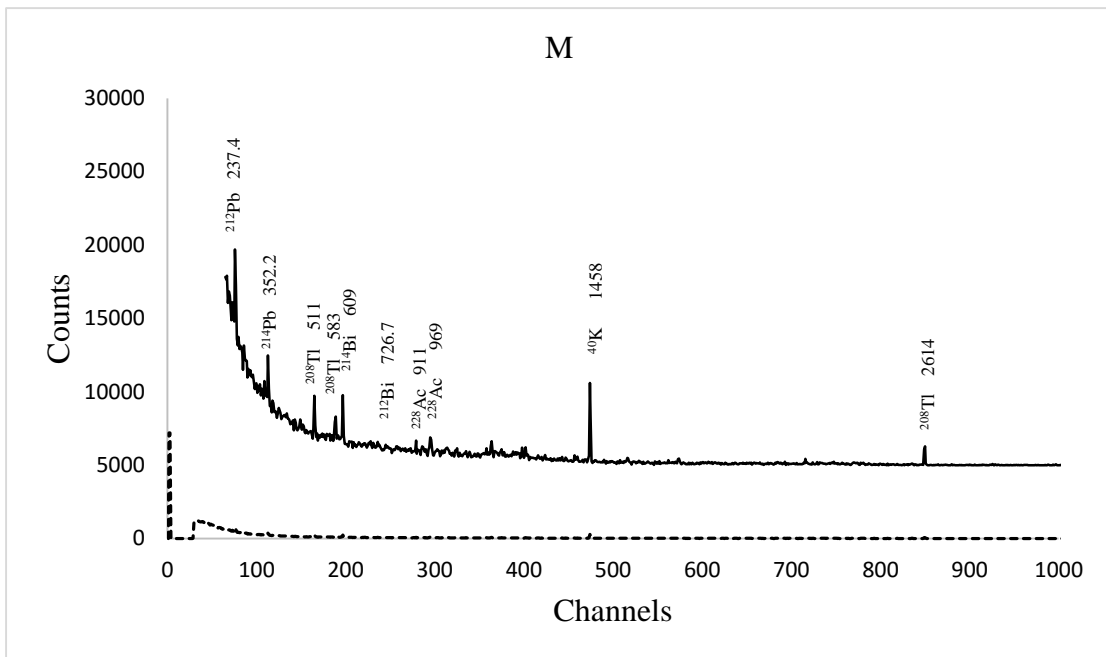
Figure 4. 24: The spectrum of the sample M for in situ measurement with counting time of 7200 s
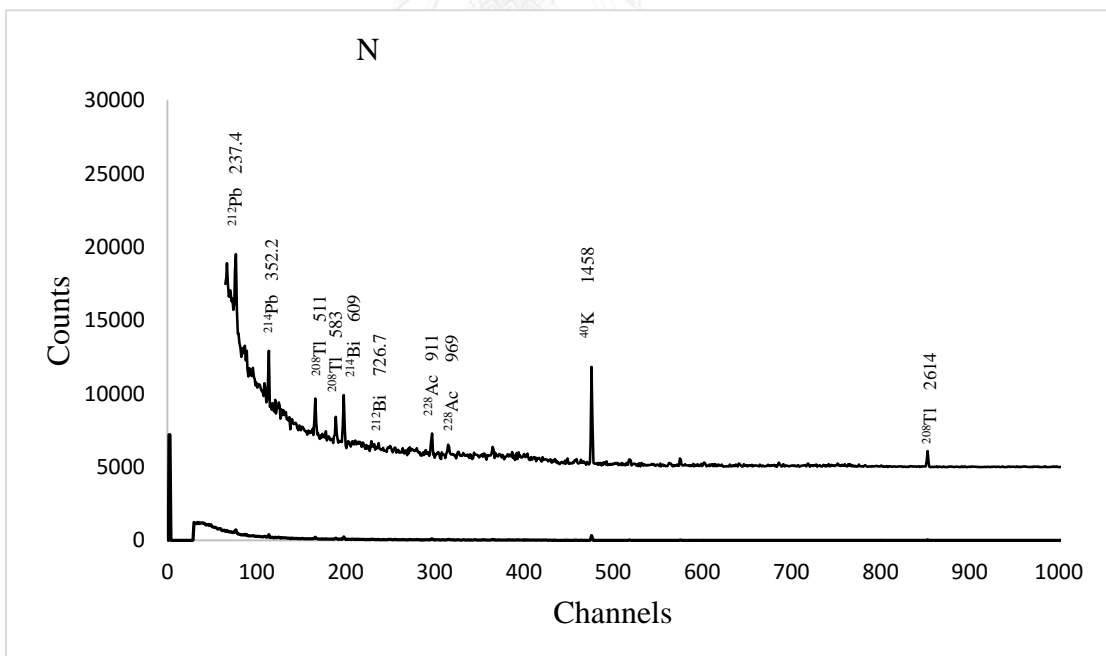
Figure 4. 25: The spectrum of the sample N for in situ measurement with counting time of 7200 s

Dose rate calculated from activity of known ^{238}U and ^{232}Th contents

The gamma dose rate was calculated due to the gamma ray emission from the radionuclides such as ^{238}U series and ^{232}Th series in the ceiling paint. The ceiling areas were 0.3m × 0.3 m = 0.09 m^2 (radius = 0.15 m) with the distance of 0.02 m between the ceiling paint samples and the people or the center of the detector. The list of mass absorption coefficient below are calculated by the interpolation from the figure. 9. Thus the flux and the dose rate were estimated.

Table 4.9: List of the gamma fraction and mass absorption coefficient of air $(\mu_A/\rho)^{air}$

Energy (MeV)	Gamma fraction	$(\mu_A/\rho)^{air}$ (cm^2/g)
0.3522	0.3710	0.0292
0.6093	0.4610	0.0296
0.2094	0.0388	0.0270
0.2387	0.4360	0.0276
0.2705	0.0343	0.0282
0.2776	0.0631	0.0284
0.3379	0.1130	0.0291
0.4625	0.0444	0.0297
0.5109	0.226	0.0297
0.5831	0.845	0.0296
0.7267	0.0665	0.0292
0.7942	0.0436	0.0289
0.8601	0.124	0.0286
0.9108	0.266	0.0284
0.969	0.162	0.0281
2.6129	0.99	0.0221

Table 4.10: The mass (g/cm^2) of all samples are shown below.

Samples	Mass (g/30cm^2)	Mass (g/cm^2)
W1a	132	0.1467
W1b	148	0.1644
W2a	220	0.2444
W2b	132	0.1467

Samples (cont.)	Mass (g/30cm^2) (cont.)	Mass (g/cm^2) (cont.)
G1a	146	0.1622
G1b	108	0.1200
G2a	208	0.2311
G2b	126	0.1400

By using the specific activity (Bq/g) and the mass in kilogram per square centimeter (g/cm2) in the analysis of uranium-238 and thorium-232 contents, the activity (Bq/cm^2) was calculated for the samples of our in situ measurement. Therefore, the activity (Bq/cm^2) for samples W1a, W1b, W2a, W2b, G1a, G1b, G2a, and G2b were be shown below.

Table 4.11: The specific activity (Bq/cm^2) of samples W1a, W1b, W2a, W2b, G1a, G1b, G2a, and G2b

Sample Activity	^{238}U	^{232}Th
W1a	0.0259	0.3116
W1b	0.0291	0.3494
W2a	0.0420	0.4935
W2b	0.0252	0.2961
G1a	0.0242	0.2908
G1b	0.0179	0.2151
G2a	0.0707	0.4893
G2b	0.0428	0.2964

Table 4.12: The specific activity (Bq/cm^2) of the samples M and N were be shown below.

Sample Activity	^{238}U	^{232}Th
M	0.0564	0.0429
N	0.0302	0.0273

Table 4.13: The list of flux or intensity with their energy

Energy (MeV)	Flux (photons/cm^2-sec)									
	W1a	W1b	W2a	W2b	G1a	G1b	G2a	G2b	M	N
0.3522	0.0097	0.0109	0.0158	0.0095	0.0091	0.0067	0.0265	0.0161	0.0113	0.0212
0.6093	0.0121	0.0136	0.0196	0.0118	0.0113	0.0083	0.0330	0.0200	0.0141	0.0263
0.2094	0.0122	0.0137	0.0194	0.0116	0.0114	0.0084	0.0192	0.0116	0.0011	0.0017
0.2387	0.1375	0.1541	0.2177	0.1306	0.1283	0.0949	0.2159	0.1308	0.0120	0.0190
0.2705	0.0108	0.0121	0.0171	0.0103	0.0101	0.0075	0.0170	0.0103	0.0009	0.0015
0.2776	0.0199	0.0223	0.0315	0.0189	0.0186	0.0137	0.0312	0.0189	0.0017	0.0027
0.3379	0.0356	0.0400	0.0564	0.0339	0.0333	0.0246	0.0559	0.0339	0.0031	0.0049
0.4625	0.0140	0.0157	0.0222	0.0133	0.0131	0.0097	0.0220	0.0133	0.0012	0.0019
0.5109	0.0713	0.0799	0.1129	0.0677	0.0665	0.0492	0.1119	0.0678	0.0062	0.0098
0.5831	0.2664	0.2987	0.4220	0.2532	0.2486	0.1839	0.4184	0.2534	0.0233	0.0368
0.7267	0.0210	0.0235	0.0332	0.0199	0.0196	0.0145	0.0329	0.0199	0.0018	0.0029
0.7942	0.0137	0.0154	0.0218	0.0131	0.0128	0.0095	0.0216	0.0131	0.0012	0.0019
0.8601	0.0391	0.0438	0.0619	0.0372	0.0365	0.0270	0.0614	0.0372	0.0034	0.0054
0.9108	0.0839	0.0940	0.1328	0.0797	0.0783	0.0579	0.1317	0.0798	0.0073	0.0116
0.9690	0.0511	0.0573	0.0809	0.0485	0.0477	0.0353	0.0802	0.0486	0.0045	0.0070
2.6129	0.3121	0.3500	0.4944	0.2966	0.2913	0.2155	0.4902	0.2969	0.0273	0.0431

Table 4.14: The list of total gamma dose rate with their energy calculated from known activity of ^{238}U and ^{232}Th contents of all samples

Energy (MeV)	Dose rate (mR/hr) 10^{-6} for each and summation energy (MeV)									
	W1a	W1b	W2a	W2b	G1a	G1b	G2a	G2b	M	N
0.3522	6.954	7.408	10.69	6.415	6.161	4.557	18.00	10.90	7.688	14.36
0.6093	15.13	16.12	23.26	13.96	13.40	9.913	39.15	23.70	16.72	31.23
0.2094	4.805	5.109	7.216	4.329	4.252	3.145	7.154	4.334	0.3992	0.6287
0.2387	62.88	66.86	94.43	56.66	55.65	41.16	93.63	56.72	5.224	8.228
0.2705	5.735	6.098	8.613	5.168	5.075	3.754	8.540	5.173	0.4765	0.7505
0.2776	10.88	11.57	16.34	9.806	9.630	7.123	16.20	9.816	0.9041	1.424
0.3379	24.35	25.89	36.57	21.94	21.55	15.94	36.26	21.96	2.023	3.186
0.4625	13.35	14.19	20.04	12.03	11.81	8.737	19.87	12.04	1.109	1.747
0.5109	75.12	79.87	112.8	67.68	66.47	49.17	111.8	67.75	6.240	9.829
0.5831	319.8	340.0	480.2	288.1	283.0	209.3	476.1	288.4	26.56	41.84
0.7267	30.88	32.83	46.37	27.82	27.32	20.21	45.97	27.85	2.565	4.040
0.7942	21.94	23.33	32.95	19.77	19.42	14.36	32.67	19.79	1.823	2.871
0.8601	66.91	71.14	100.5	60.29	59.21	43.80	99.62	60.35	5.558	8.755
0.9108	150.8	160.3	226.4	135.9	133.4	98.69	224.5	136.0	12.53	19.73
0.9690	96.80	102.9	145.4	87.22	85.66	63.36	144.1	87.30	8.041	12.67
2.6129	1255	1335	1885	1131	1111	821.6	1869	1132	104.3	164.3
Summation mR/hr	2162	2298	3247	1948	1913	1415	3243	1964	2021	325.5
Summation μSv/hr	**0.0189**	**0.0201**	**0.0284**	**0.0170**	**0.0167**	**0.0124**	**0.0284**	**0.0172**	**0.0018**	**0.0028**

The dose rate of these four samples ranged from 0.0018 to 0.0284 μSv/hr. The highest gamma dose rate was found in sample W2a and G2a (0.0284 μSv/hr for both samples), while the lowest gamma dose rate was found in sample M (0.0018 μSv/hr).

Dose rate calculated from measurement

The efficiency of each energy was calculated. Through this efficiency, the activity (Bq/cm^2) was also calculated. The ceiling areas were $0.3\ m \times 0.3\ m$ (radius 0.15 m) with the distance of 0.02 m between the ceiling paint samples and the people or the center of the detector. Therefore, the intensity and the dose rate were estimated.

Table 4.15: The list of the activity (Bq/cm^2) with their energy

Energy (MeV)	Activity (Bq/cm^2)									
	W1a	W1b	W2a	W2b	G1a	G1b	G2a	G2b	M	N
0.2387	0.3199	0.3622	0.4841	0.3513	0.2289	0.1803	0.4837	0.2432	0.0229	0.0597
0.3379	0.2504	0.2972	0.3751	0.2392	0.1192	0.1057	0.3863	0.1979	Not detectable	Not detectable
0.3522	0.0012	0.0349	0.0480	0.0278	0.0404	0.0232	0.1468	0.0301	0.0214	0.0340
0.4625	0.2022	0.4816	0.1232	0.4004	0.5096	0.2408	0.7196	0.1672	Not detectable	Not detectable
0.5109	0.1889	0.1618	0.1991	0.1398	0.1406	0.0881	0.2329	0.1584	Not detectable	0.0847
0.5831	0.0771	0.0976	0.1305	0.1074	0.0752	0.0317	0.0882	0.0994	Not detectable	Not detectable
0.6093	0.0259	0.0344	0.0463	0.0110	0.0140	0.0070	0.0982	0.0543	0.0110	0.0434
0.7267	0.4568	0.5733	0.3284	0.4031	0.0830	0.1463	0.4598	0.4299	0.0705	Not detectable
0.9108	0.4065	0.4227	0.4403	0.4497	0.3390	0.2539	0.5686	0.3957	0.0270	0.0608
0.9690	0.5126	0.5432	0.6184	0.5361	0.2610	0.2634	0.6913	0.4962	0.0917	0.1084
2.6129	0.1133	0.1342	0.1605	0.1374	0.0745	0.0252	0.2014	0.0912	Not detectable	Not detectable

Table 4.16: The list of flux or intensity with their energy

Energy (MeV)	Flux (photons/cm^2-sec)									
	W1a	W1b	W2a	W2b	G1a	G1b	G2a	G2b	M	N
0.2387	0.1128	0.1277	0.1708	0.1239	0.0807	0.0636	0.1706	0.0858	0.0100	0.0262
0.3379	0.0230	0.0274	0.0345	0.0220	0.0110	0.0097	0.0356	0.0182	Not detectable	Not detectable
0.3522	0.0004	0.0105	0.0145	0.0084	0.0122	0.0070	0.0444	0.0091	0.0080	0.0128
0.4625	0.0073	0.0174	0.0045	0.0145	0.0184	0.0087	0.0260	0.0060	Not detectable	Not detectable
0.5109	0.0348	0.0298	0.0366	0.0257	0.0259	0.0162	0.0429	0.0292	Not detectable	0.0194
0.5831	0.0531	0.0672	0.0899	0.0740	0.0519	0.0218	0.0608	0.0685	Not detectable	Not detectable
0.6093	0.0097	0.0129	0.0174	0.0041	0.0052	0.0026	0.0369	0.0204	0.0051	0.0202
0.7267	0.0247	0.0311	0.0178	0.0218	0.0045	0.0079	0.0249	0.0233	0.0047	Not detectable
0.9108	0.0854	0.0888	0.0925	0.0945	0.0712	0.0534	0.1195	0.0832	0.0071	0.0159
0.9690	0.0660	0.0699	0.0796	0.0690	0.0336	0.0339	0.0890	0.0639	0.0147	0.0173
2.6129	0.0913	0.1082	0.1294	0.1108	0.0600	0.0203	0.1624	0.0736	Not detectable	Not detectable

Table 4.17: The list of total gamma dose rate with their energy from the measurement of all samples

Energy (MeV)	Dose rate (mR/hr) 10^{-6} for each and summation energy (MeV)									
	W1a	W1b	W2a	W2b	G1a	G1b	G2a	G2b	M	N
0.2387	48.94	55.40	74.06	53.74	35.02	27.58	74.00	37.20	4.354	11.34
0.3379	14.93	17.73	22.38	14.27	7.111	6.305	23.04	11.80	Not detectable	Not detectable
0.3522	0.2537	7.146	9.839	5.696	8.285	4.764	30.09	6.162	5.449	8.665
0.4625	6.610	15.75	4.028	13.09	16.66	7.873	23.53	5.466	Not detectable	Not detectable
0.5109	34.76	29.77	36.63	25.72	25.87	16.21	42.86	29.15	Not detectable	19.36
0.5831	60.44	76.51	102.4	84.25	59.01	24.83	69.19	77.94	Not detectable	Not detectable
0.6093	11.55	15.33	20.66	4.888	6.221	3.110	43.77	24.22	6.072	24.01
0.7267	34.55	43.36	24.84	30.48	6.278	11.06	34.77	32.52	6.620	Not detectable
0.9108	145.6	151.4	157.7	161.1	121.4	90.96	203.7	141.8	12.02	27.05
0.9690	118.5	125.6	143.0	124.0	60.36	60.90	159.9	114.7	26.35	31.13
2.6129	348.3	412.8	493.4	422.4	229.0	77.39	619.2	280.6	Not detectable	Not detectable
Summation mR/hr	824.5	950.8	1089	939.7	5.75.2	331.0	1324	761.5	60.86	121.6
Summation µSr/hr	**0.0072**	**0.0083**	**0.0095**	**0.0082**	**0.0050**	**0.0029**	**0.0116**	**0.0067**	**0.0005**	**0.0011**

4.3   In situ dose rate measurement from the ISOC software

The ISOC software is required to have the proper collimator which fixes with the end cap of the detector. Due to this issue, our measurement could not conduct with the ISOC software. Another reason is that if The ISOCS is conducted the measurement without the collimator, it is required to have the large areas for the measurement, but the area of our samples is 30 cm × 30 cm. Therefore, the ISOCS is not practical in our measurement.

4.4   Recording of gamma-rays dose rate from survey meters

4.4.1   HDS-101-GN

The table showed the dose rate of samples W1a, W1b, W2a, W2b, G1a, G1b, G2a, and G2b which were obtained from the survey meter of HDS-101 GN and GM energy compensated. The dose rates of these samples were subtracted by the dose rate of blank, a non-radioactive paint sample.

Table 4.18: The dose rate of samples W1a, W1b, W2a, W2b, G1a, G1b, G2a, and G2b obtained from the HDS-101 GN

Samples	Dose rate (μSv/h)
W1a	0.003
W1b	0.003
W2a	0.005
W2b	0.004
G1a	0.002
G1b	0.001
G2a	0.005
G2b	0.003
M	Not detectable
N	Not detectable

The dose rate from these samples, Samples M and N, are lower than the dose rate obtained from our measurement and calculation above.

4.4.2 Gamma neutron survey meter, GM energy compensated

The dose rate from this survey meter is not stable, it means that it gives the different values. Therefore, the dose rate from this GM energy compensated needs to be recorded several times in order to find the average dose.

Table 4.19: The average dose rate from the GM energy compensated gamma survey meter

Number of measure ment	Dose rate (µSv/hr)										
	Blank	W1a	W1b	W2a	W2b	G1a	G1b	G2a	G2b	M	N
1	0.26	0.41	0.31	0.31	0.23	0.31	0.31	0.31	0.23	0.23	0.26
2	0.31	0.23	0.31	0.27	0.34	0.31	0.49	0.31	0.35	0.24	0.31
3	0.33	0.32	0.23	0.31	0.31	0.38	0.31	0.32	0.24	0.31	0.33
4	0.23	0.31	0.26	0.32	0.25	0.23	0.31	0.32	0.28	0.23	0.23
5	0.36	0.24	0.45	0.41	0.4	0.24	0.31	0.35	0.32	0.31	0.36
6	0.33	0.54	0.25	0.44	0.23	0.32	0.37	0.23	0.28	0.24	0.33
7	0.23	0.53	0.36	0.35	0.33	0.36	0.35	0.39	0.25	0.31	0.23
8	0.25	0.56	0.31	0.47	0.34	0.23	0.36	0.41	0.23	0.28	0.25
9	0.48	0.31	0.32	0.38	0.33	0.23	0.41	0.31	0.28	0.32	0.48
10	0.45	0.23	0.23	0.36	0.23	0.31	0.37	0.48	0.33	0.33	0.45
Summati on of dose rate µSv/hr	0.273	0.323	0.368	0.303	0.362	0.299	0.292	0.359	0.343	0.279	0.280
Summation dose rate (sample - blank)		0.050	0.095	0.030	0.089	0.026	0.019	0.086	0.070	0.006	0.007

4.5 Comparison the results of in situ dose rate measurement with the survey meters

Table 4.20: The dose rate (μSv/hr) measurement obtained from in situ dose rate measurement, dose rate calculated from known activity, and the survey meters of HDS-101 GN and GM energy compensated.

Name of measurement	Dose rate (μSv/hr)									
	W1a	W1b	W2a	W2b	G1a	G1b	G2a	G2b	M	N
Dose rate obtained from known activity	0.0189	0.0201	0.0284	0.0170	0.0167	0.0124	0.0284	0.0172	0.0018	0.0028
Dose rate obtained from in situ measurement	0.0072	0.0083	0.0095	0.0082	0.0050	0.0029	0.0116	0.0067	0.0005	0.0011
Survey meter of HDS-101 GN	0.0030	0.0030	0.0050	0.0040	0.0020	0.0010	0.0050	0.0030	Not detectable	Not detectable
Survey meter of GM energy compensated	0.050	0.095	0.030	0.089	0.026	0.019	0.086	0.070	0.006	0.007

The lowest dose rate of the measurements is from the survey meter of HdS-101 GN, while the highest dose rate is obtained from the survey meter of GM energy compensated. The dose rate obtained from the survey meter of GM energy compensated. The dose rate obtained from the in situ measurement is lower than the dose rate obtained from known activity.

Chapter 5

Conclusion and Recommendation

5.1   Conclusion

In these experiments, the lead shield was used, and the measurements were performed with an HPGe detector in order to acquire the gamma spectra for the measurement samples. The development of our simple technique for in situ measurement of the gamma-ray dose rate from planar sources using an HPGe detector for the desired coverage areas of 30 cm × 30 cm. Moreover, it is based on a collimator of lead shield of 5 cm thickness with the detector-to-source distance of 2 cm. As a result, the detectable areas of our sample are 10 cm × 10 cm. The worksheet to calibrate the energy and efficiency based on linear relations and to calculate the gamma-ray dose rate based on generally accepted formulas of this measurement can be used for the further research. These worksheets are prepared for the convenient of in situ dose rate calculation. It should be kept in mind that our method only measures the intensity of energy peaks, and it does not include the scattered peaks.

The ISOC software is not practical in our research because lacking of the proper collimator and having the small area. The lowest dose rate of the measurements is from the survey meter of HDS-101 GN, while the highest dose rate is obtained from the survey meter of GM energy compensated. The dose rate which was calculated from the activity of uranium-238 and thorium-238 contents is higher than the dose rate calculated from measurements. This is because the calculated dose rate from our measurement is not in secular equilibrium, while the calculated dose rate from the activity of uranium-238 and thorium-238 contents is in secular equilibrium. Furthermore, the dose rate of these two calculation is higher than the dose rate recording from the survey meter of HDS-101 GN but lower than the survey meter of GM energy compensated. Because of the very low dose rate of our samples, the survey meters which are used for this research are not suitable. Moreover, the survey meter is normally not used to analyze the

environmental samples, very low dose rate. In conclusion, the HPGe detector is the best choice for this in situ dose rate measurement. The in situ dose rate measurement using gamma-rays spectrometry of the HPGe detector of this research can use to determine the low dose rate gamma-ray. Therefore, it also can use this method to determine the high dose rate gamma-ray.

5.2 Recommendation

- The proper collimator is needed for the ISOC software. This is because the ISOC software needs the proper collimator which is fixed with the end cap of the detector for doing the measurement. If we want to compare, we need to procure from the manufacturer.

- It should be tested with the high activity samples. This is because the survey meters are not sensitive enough with the very low dose samples. Therefore, the high activity samples should be apply for further research.

- It should be measured with equilibrium samples. If the samples are in secular equilibrium, the dose rate can be determined by using the method of direct comparison with the equilibrium standards

REFERENCES

[1] Schmidt, K. (2011). Commercial radon survey report. Radon detection Sspecialists, Inc. Burr Ridge, Illinois. Searched on September 9, 2015, from

http://www.d107.org/media/Administration/FOIA/2014-
2015/Cooper/ES%20May%202006%20Radon%20Results.pdf

[2] EPA. (1993). Radon measurement inarch schools. United State environmental protection agency. Searched on August 10, 2015, from

http://www.epa.gov/radon/pdfs/radon_measurement_in_schools.pdf

[3] Kumar, A., Kumar, M., Singh, B., & Singh, S. (2003). Natural activity of ^{238}U, ^{232}Th, and ^{40}K in some Indian building materials. Elsevier science Ltd. Science direct. Paper no 36. Retrieved 3 August 2015 from http://www.sciencedirect.com

[4] Brune, D. 2001. Nuclear Technology. In: Brune. D, Hellborg et al. Radiation at home, outdoors and in the workplace. Scandinavian Science Publisher, Oslo, Norway, (pp. 166-186).

[5] Pattama. P. (2009). Preliminary Monitoring of the Change of Soil Gas Radon for Earthquake Pre-warning in the Khlong Marui Fault Zone. Prince of Songkla University.

[6] Smith. R. A. Thomas. J. K et al. 2014. Journal of Environmental Protection. Vol.5 No.3 (2014), Article ID: 43366, 15 pages

[7] The National Council on Radiation Protection and Measurements (NCRP). Report No. 93, Ionizing Radiation Exposure of the Population of the United States, 1987.

[8] Lamarsh, R. J., & Baratta, J. A. (2001). Introduction to nuclear engineering, (3rd ed). Radiation protection. New Jersey, USA: Prentice-Hall.

[9] Almgren. S. Isaksson. M. Journal of Environmental Radioactivity. Volume 91, Issues 1-2, 2006, Pages 90-102

[10] Lee. S. K. Wagiran. H et al. Journal of Environmental Radioactivity. Radiological monitoring. Volume 100. Issue 5, May 2009, pages 368-374

[11] Venkataraman. V. Bronson F et al. Nuclear Instruments and Methods in Physics Research. Volume 422, Issue 1-3, 11 February 1999, Pages 450-454

[12] Andrew N. Tyler. 2008. Radioactivity in the Environment. In situ and airborne gamma-ray spectrometry.

[13] Wikimedia.org. (2011). Diagram showing the different stages of thorium decay. Retrieved 10 November 2015, from:
https://commons.wikimedia.org/wiki/File:Decay_Chain_of_Thorium.svg

[14] Wikipedia.org. (2008). Decay chain 4n+2, Uranium series. Retrieved 10 November 2015, from:
https://en.wikipedia.org/wiki/File:Decay_chain%284n%2B2,_Uranium_series%29.PNG

[15] Knoll. G. F. (2000). Radiation detection and measurement, (3rd ed). Counting statistics and error prediction. John Wily and Sons. New York. USA: Quebecor Printing.

[16] Luca. C. Andrea. M et al. 2006. Gamma Spectroscopy.

[17] Edward. L Alphen. (1998). Radiation Biophysics (2nd). Academic Press Limited, London.

[18] Ahmad, N., Matiullah & Hussein, A. J. A. (1997). Natural radioactivity in Jordanian soil and building materials and the associated radiation hazards. Elsevier science Ltd. Science direct. 39. Paper no 1. Retrieved 10 August, 2015 from http://www.sciencedirect.com

[19] De Corte, F., Umans, H. De Wispelaere, A. D., & Van den haute. P. (2005). Direct gamma-spectrometric measurement of the ^{226}Ra 186.2 keV line for detecting ^{238}U/^{226}Ra disequilibrium in determining the environmental dose rate for the luminescence dating of sediment. Elsevier science Ltd. Science direct. Paper no 63. Retrieved 10 August, 2015 from http://www.sciencedirect.com

[20] Canberra Industries, Inc. 2002. Measurement Solution for Safety and Security. Model S573/S574. ISOCS/LabSOCS. Validation & Verification Maual. V4.0 9231205E.

[21] Canberra Industries, Inc. 2012. Measurement Solutions for Safety and Security. Model S573 ISOCS Calibration Software V4.3 9231013F. Technical Reference Manual

[22] MIRION TECHNOLOGIES. (2003). Hand-held gamma and Neutron Search Instrument HDS-101 GN. Operating Manual. Health Physics Division.

[23] MIRION TECHNOLOGIES. (2014). HDS-101 GN User's Training. Health Physics Division.

APPENDIXES

Appendix A

1. The work sheet for energy calibration by the point standard sources of ^{152}Eu, ^{137}Cs, and ^{60}Co
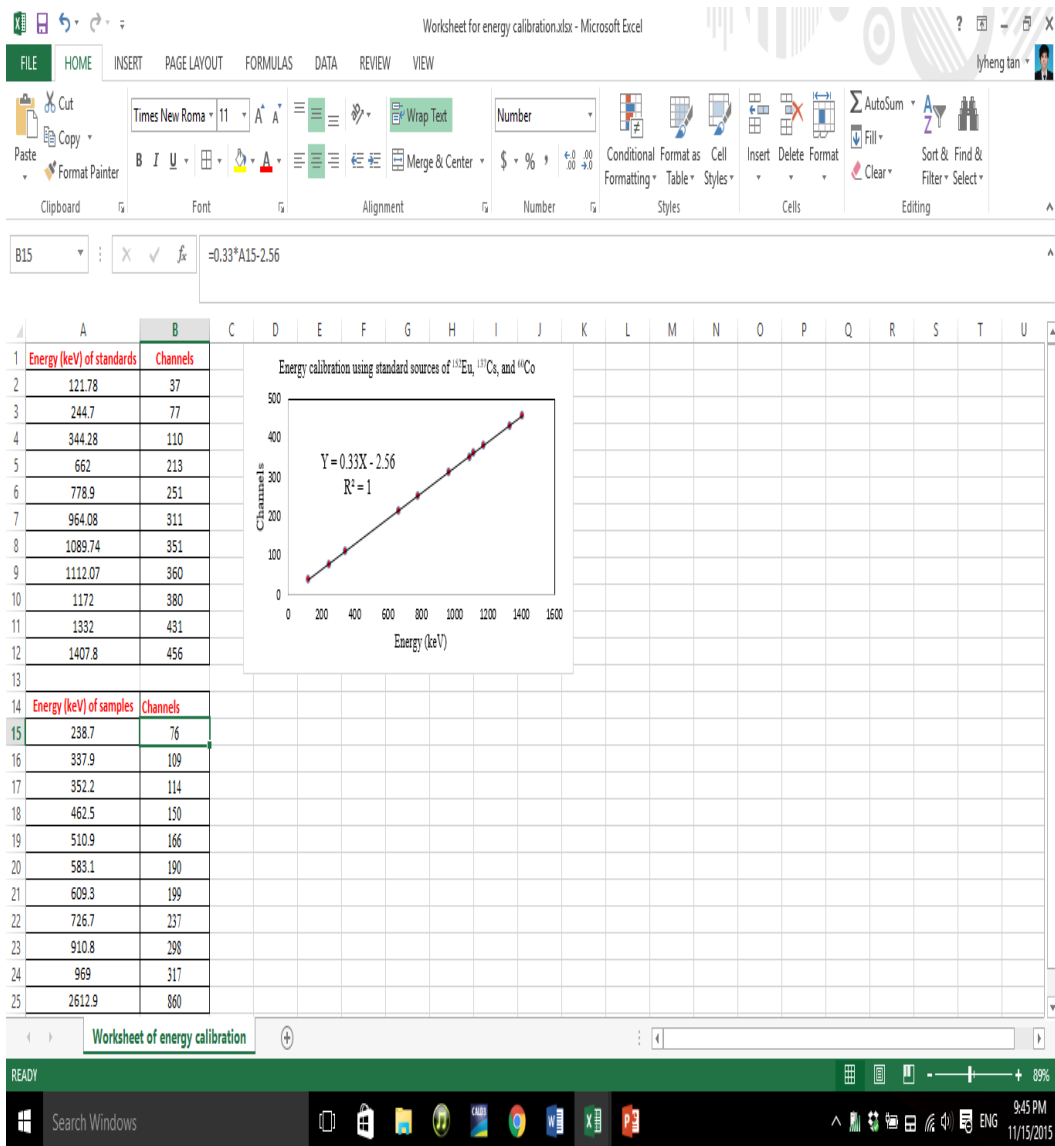
Appendix B

2. The worksheet for efficiency using the standard point sources of ^{152}Eu and ^{137}Cs
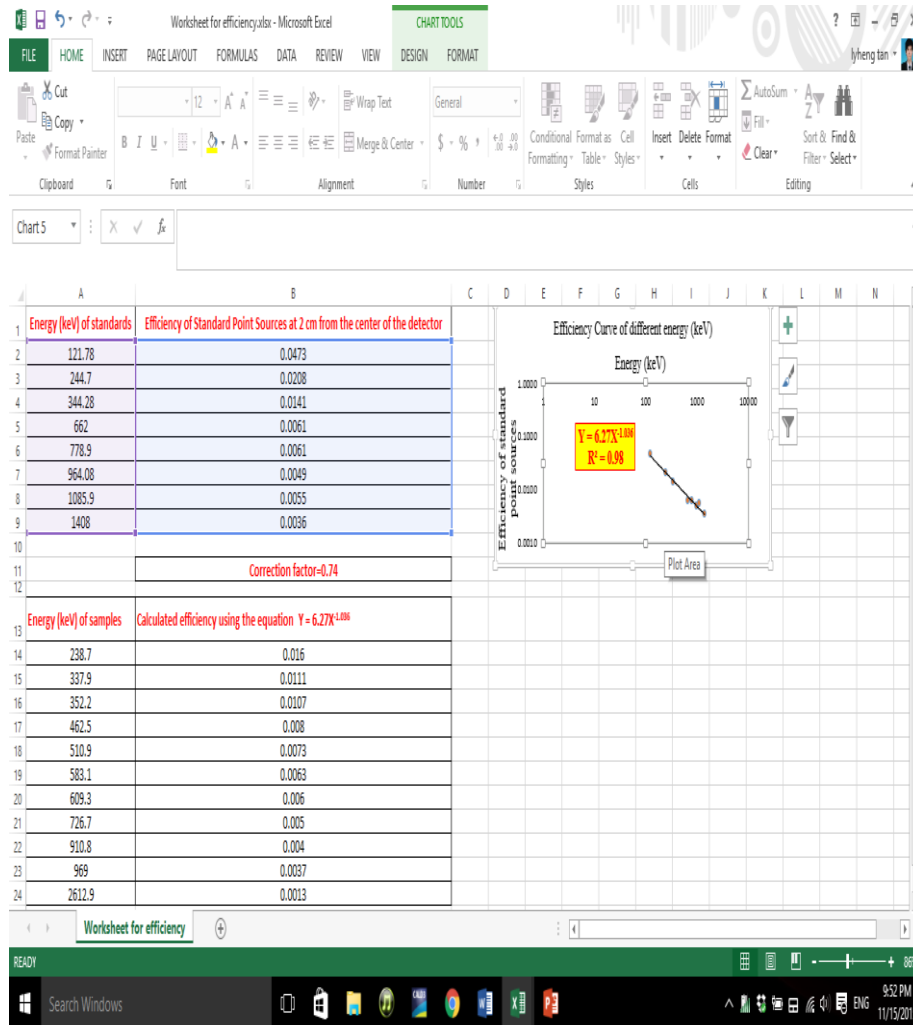
Appendix C

1. The worksheet for dose rate calculation from planar sources at 2 cm away from the center of the detector with the area of 30 cm × 30 cm

	A	B	C	D	E	F	G	H
1	Energy (MeV)	Efficiency	Net area W1a	(μ/ρ) air (cm^2/g)	Intensity I = (S/4)×ln[1+(R^2/X^2)]	Dose rate (mR/hr) W1a		
2	0.2387	0.0160	0.2211	0.0276	0.1128	4.89E-05		
3	0.3379	0.0111	0.0315	0.0291	0.0230	1.49E-05		
4	0.3522	0.0107	0.0005	0.0292	0.0004	2.54E-07		
5	0.4625	0.0080	0.0072	0.0297	0.0073	6.61E-06		
6	0.5109	0.0073	0.031	0.0297	0.0348	3.48E-05		
7	0.5831	0.0063	0.0413	0.0296	0.0531	6.04E-05		
8	0.6093	0.0060	0.0072	0.0296	0.0097	1.16E-05		
9	0.7267	0.0050	0.0153	0.0292	0.0247	3.45E-05		
10	0.9108	0.0040	0.0418	0.0284	0.0854	1.46E-04		
11	0.969	0.0037	0.0303	0.0281	0.0660	1.19E-04		
12	2.6129	0.0013	0.015	0.0221	0.0913	3.48E-04		
13					Summation dose rate (mR/hr)	8.24E-04		
14					Summation dose rate (µSv/hr)	0.0072		
15								
16								

Appendix D

2. Certificate of specifications for an HPGe detector with 10% relative efficiency

DETECTOR SPECIFICATIONS AND PERFORMANCE DATA

Specifications

Model _____ GC1020 _____   Serial Number ____ 5902318 _____

The purchase specifications and therefore the warranted performance of this detector are as follows:

Active volume _____ cc   Relative efficiency ___ 10 ___ %

Resolution ___ 2.0 ___ keV (FWHM) at 1.33 MeV

_____ keV (FWTM) at 1.33 MeV

___ 1.0 ___ keV (FWHM) at _ 122 keV _

_____ keV (FWTM) at _____

Peak/Compton __ 34 __ : 1   Cryostat well diameter _____ mm   Well depth _____ mm

Cryostat description or Drawing Number if special ____ 7935-7 (Big Mac) _____

Physical Characteristics

Geometry _____ Closed-end coaxial _____

Diameter _____ 43 _____ mm   Active volume ____ 56.9 ____ cc

Length _____ 41.5 _____ mm   Well depth _____ mm

Distance from window ____ 5 ____ mm   Well diameter _____ mm

Electrical Characteristics

Depletion voltage _(+) 4500_ V dc

Recommended bias voltage V dc _(+) 4500_ V dc

Leakage current at recommended bias ___ 0.07 ___ nA

Preamplifier test point voltage at recommended voltage ___ (−) 1.52 _ V dc

Capacitance at recommended bias ⌄ 16 ___ pF

Resolution and Efficiency

With amp time constant of ___ 4 ___ μs

Isotope	^{57}Co	^{60}Co			
Energy (keV)	122	1332			
FWHM (keV)	0.86	1.77			
FWTM (keV)	1.58	3.29			
Peak/Compton		43.0:1			
Rel. Efficiency		12.9			

Tested by: _Bill Soto_   Date: ____ June 1, 1990 ____

Approved by: _Denni Drzyrush._   Date: ____ June 1, 1990 ____

Appendix E

5. Certificate of specification for an HPGe detector with 30% relative efficiency

DETECTOR SPECIFICATIONS AND PERFORMANCE DATA

Specifications

Model   GC3021

Serial Number   8901825

The purchase specifications and therefore the warranted performance of this detector are as follows.

Active volume ____ cc   Relative efficiency   30 %

Resolution   2.1   keV (FWHM) at 1.33 MeV

____ keV (FWTM) at 1.33 MeV

1.1   keV (FWHM) at   122 keV

____ keV (FWTM) at ____

Peak/Compton   52 : 1   Cryostat well diameter ____ mm   Well depth ____ mm

Cryostat description or Drawing Number if special   7500

Physical Characteristics

Geometry	Closed-end coaxial	
Diameter	55 mm	Active volume 139.3 cc
Length	65 mm	Well depth ____ mm
Distance from window	5 mm	Well diameter ____ mm

Electrical Characteristics

Depletion voltage   (+)4000   V dc

Recommended bias voltage V dc   (+)4000   V dc

Leakage current at recommended bias   0.01   nA

Preamplifier test point voltage at recommended voltage   (-)1.62   V dc

Capacitance at recommended bias   ⌐28   pF

Resolution and Efficiency

With amp time constant of   4   μs

Isotope	^{57}Co	^{60}Co			
Energy (keV)	122	1332			
FWHM (keV)	1.10	1.98			
FWTM (keV)	2.05	3.70			
Peak/Compton		55.7:1			
Rel. Efficiency		31.7			

Tested by: _Ronald Ginkes Jr_   Date: August 27, 1990

Approved by: _Dennis Droponak_   Date: August 27, 1990

Appendix F

6. Certificate of testing some sources to measure dose rate using HDS-101 GN

Test sheet 133951D

PES #	133950 L
Operator name	Bombardier
Device #	13009125
Date-Time	9/10/2014 13:45:20
Comments	143993/F
Functional tests :	COMPLIANT
Final result :	COMPLIANT
Next Check. recommended Date	10/09/2016
Visa	BOF

Gamma answer

Source	Reference	Distance(cm)	Calculated dose rate(µSv/h)	HDS value(µSv/h)	Net response(ratio)	Acceptance range
Am 241	TP 816	10	2.100	1.897	0.882	0.7 - 1.3
Cs 137	OZ 820	10	2.967	2.646	0.877	0.7 - 1.3
Co 60	UT 117	10	11.441	10.754	0.936	0.7 - 1.3
Cs 137	OZ 819	4,1	191.312	174.682	0.913	0.7 - 1.3

Neutron sensitivity

Source	Reference	Distance(cm)	Calculated flux(n/s/cm2)	HDS value(cp/s)	Sensitivity((cp/s)/(n/s/cm2))	Acceptance range
Background	X	X	X	0.00	0.00	HDS value < 0.2cp/s
Cf 252	I9-170	8	37.97	0.00	0.00	Sensitivity > 0.072

Checking Settings

Discriminator threshold

Low fast (mV)	20
Low slow (mV)	104
Medium (mV)	120
High (mV)	200

OEM

| K1 P | 244.00 |
| S1 | 17 |

Gamma Rate

| Coeff. | 1.0000 |

HV (V)

| Preset Value | 834 |
| Reading | 833 |

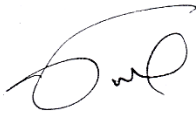Buttons: Initialize Cursor, Spectrum, Centroid, Print, Reset duration, Load, Read, Write, Save

Centroid
Channel (+/-5% 109.4   Resolution (<10%) 7.8

T°C 21.0   Acquisition time : (s)15

Curseur
Curs. 1   channel n° 80.0   Curs. 2   channel n°140.0

Gain (keV/channel) : 6.0622   Offset (keV) : 0

Appendix G

7. Certificate of ^{60}Co, gamma standard source, by British Calibration Service

Amersham International plc
Amersham UK

BRITISH CALIBRATION SERVICE
Approval No. 0146

Description	Principal radionuclide: Cobalt-60		Product code:	CKR.151
			Source number:	2U386

Measurement

Reference time: 1200 GMT on 1 December 1987

Total activity of cobalt-60: 11.28 microcuries

which is equivalent to: 417 kilobecquerels

Recommended half life: 5.27 years

Method of measurement:
The source was measured using equipment calibrated directly or indirectly with similar sources prepared from a series of absolutely standardized solutions.

Accuracy

The OVERALL UNCERTAINTY in the activity quoted above for the principal radionuclide was ± 1.9 %

The limits of uncertainty were taken as the arithmetic sum of the uncertainty due to random variations, calculated at the 99.7% confidence level, and the estimated systematic uncertainties in the measurement.

Radionuclidic Purity

The estimated activities of any radioactive impurities found by high resolution gamma spectrometry are listed below expressed as percentages of the principal radionuclide at the reference time.

Remarks

Tests for leakage and surface contamination have been carried out with satisfactory results.

Further information about this source including details of its construction is given in the data sheet accompanying the source.

This product meets the quality assurance requirements of NRC Regulatory Guide 4.15 for achieving implicit NBS traceability as defined in NCRP 58 (1985).

Approved Signatory

A.G.Tuck

Page 1 of 1

Amersham

Appendix H

8. Certificate of ^{137}Cs, gamma standard source, by British Calibration Service

Amersham International plc
Amersham UK

BRITISH CALIBRATION SERVICE
Approval No. 0146

Description	Principal radionuclide: Caesium-137		Product code:	CDR.121
			Source number:	7S690

Measurement

Reference time: 1200 GMT on 1 September 1987

Total activity of caesium-137:   1.136   microcuries

which is equivalent to: 42.0   kilobecquerels

Recommended half life: 30.17   years

Method of measurement:
The source was measured using equipment calibrated directly or indirectly with similar sources prepared from a series of absolutely standardized solutions.

Accuracy

The OVERALL UNCERTAINTY in the activity quoted above for the principal radionuclide was $\pm$ 6.0 %

The limits of uncertainty were taken as the arithmetic sum of the uncertainty due to random variations, calculated at the 99.7% confidence level, and the estimated systematic uncertainties in the measurement.

Radionuclidic Purity

The estimated activities of any radioactive impurities found by high resolution gamma spectrometry are listed below expressed as percentages of the principal radionuclide at the reference time.

Remarks

Tests for leakage and surface contamination have been carried out with satisfactory results.

Further information about this source including details of its construction is given in the data sheet accompanying the source.

This product meets the quality assurance requirements of NRC Regulatory Guide 4.15 for achieving implicit NBS traceability as defined in NCRP 58 (1985).

Approved Signatory

A.G.Tuck   Page 1 of 1   **Amersham**

Appendix I

9. Certificate of ^{152}Eu, gamma standard source, by Isotope Products Laboratories California

CERTIFICATE OF
GAMMA STANDARD SOURCE

Radionuclide: _____Eu-152_____ Half-life: ___13.33 ± 0.04 y___

Customer: Chulalongkorn Univer- P.O. No.: ___L/C 002IC33015400___
sity

Catalog No.: _GF-152_ Source No.: _239-30-6_ Reference Date: _Feb. 1, 1989_

Contained Radioactivity: _____1.156 uCi_____

Description of Source
    a. Capsule type: ___M___
    b. Nature of active deposit: _Evaporated Metallic Salts_
    c. Active diameter: _3 mm_
    d. Backing: _9.23 mg/cm^2 Kapton_
    e. Cover: _0.254 mm Aluminized Mylar_

Radioimpurities
    1.106% Eu-154 as of Aug. 1, 1988

Method of Calibration
    (X) The source was assayed by gamma spectrometry, integrating under the _0.122, 0.344_ Mev peak(s). The branching ratio(s) used was/were ___0.284, 0.266___ gamma rays per decay.
    ( ) The source was prepared from a weight aliquot of solution whose activity in uCi/gram was determined by the method above.

Uncertainty of Measurement
    a. Systematic uncertainty in instrument calibration: ± ___2.7___ %
    b. Random uncertainty
      1. In assay: ± ___0.8___ %
      2. In weighing(s): ± _____ %
    c. Total Uncertainty: ± ___3.5___ % at the 99% confidence level.

NBS Traceability
This calibration is implicitly traceable to the National Bureau of Standards.

Notes
    1. Nuclear data were taken from "Table of Isotopes", Seventh Edition, edited by C. Michael Lederer et al.
    2. IPL participates in an NBS measurement assurance program to establish and maintain implicit traceability for a number of nuclides, based on the blind assay (and later NBS certification) of Standard Reference Materials. (As in NRC Regulatory Guide 4.15)

Quality Control

ISOTOPE PRODUCTS LABORATORIES
1800 No. Keystone St., Burbank, California 91504
(818) 843-7000

Appendix J

10. Certificate of IAEA RGK-1, Potassium Sulfate

Reference Products

About IAEA Reference Materials

Reference Material Online Catalog

Radionuclides

Trace Elements & Methyl Mercury

Organic Contaminants

Stable Isotopes

Ordering Information

Miscellaneous Documents

How to contact us

News and Announcements

Publications

Links

Events

ALMERA

40+ Years Delivering Quality to abs Worldwide

Nuclear Instrumentation

Analytical Methods

Interlaboratory Studies

IAEA-RGK-1 , Potassium Sulfate

Inorganic , Ores

- Unit Size: 500g
- Price per Unit: 60 EUR
- Report: IAEA/AL/148
- Date of Release: 1987-01-01
- Producing Laboratory: email

- Certificate of Irradiation: Certificate_of_Irradiation_IAEA-RGK-1

The IAEA-RGK-1 material is produced from high purity (99.8%) potassium sulphate supplied by the Merck Company. The potassium property value and its uncertainty were obtained from repeated measurements performed at the IAEA Laboratories Seibersdorf and the results confirmed the value certified by Merck. The upper limits for the uranium and thorium property values were estimated by the IAEA Laboratories Seibersdorf using fluorimetry and activation analysis, respectively.

Analyte	Value	Unit	95% C.I.	N	R/I/C
40K	14000?	Bq/kg	13600 - 14400	20	R
K	448000	mg/kg	445000 - 451000	20	R
Th	< 0.01	mg/kg	-	20	I
U	< 0.001	mg/kg	-	20	I

(Value) Concentration calculated as a mean of the accepted laboratory means
(N) Number of accepted laboratory means which are used to calculate the recommended or information values and their respective confidence intervals
(R/I/C) Classification assigned to the property value for analyte (Recommended/Information/Certified)
(?) Natural radionuclide activity concentrations derived from the elemental concentrations on basis of isotopic abundance and half-life data

The values listed above were established on the basis of a gravimetric dilution of materials with known uranium, thorium and potassium composition. The details concerning the criteria for qualification as a recommended or information value can be found in the respective report (attached).

My Shopping Cart

Total   €0

Go to Shopping Cart

Your Account

Edit My Profile

View My Orders

Help and Service

Terms of Service

Contact Us

Appendix K

11. Certificate of analysis for IAEA RGK-1

– 48 –

INTERNATIONAL ATOMIC ENERGY AGENCY

REFERENCE MATERIAL
FOR
GAMMA-RAY SPECTROMETRIC ANALYSIS
OF
GEOLOGICAL MATERIALS

IAEA/RGK-1

CERTIFICATE OF ANALYSIS

COMPONENT	CONCENTRATION*	CONFIDENCE INTERVAL**
Potassium	44.8 %	± 0.3 %
Uranium	less than 0.001 µg/g	
Thorium	less than 0.01 µg/g	

*Expressed on dry-weight basis (constant weight at 130°C)
**At a significance level of 0.05

DESCRIPTION OF MATERIAL

RGU-1, RGTh-1 and RGK-1 are intended for use in calibrating laboratory gamma-ray spectrometers for the determination of U, Th and K in geological materials. RGK-1 is intended for use in calibrating laboratory gamma-ray spectrometers for the determination of U, Th and K in geological materials. The material is extra pure (99.8%) potassium sulphate supplied by Merck Company. The potassium value and its uncertainty were obtained from repeated measurements by atomic absorption spectrometry in the IAEA Laboratory which confirmed the potassium sulphate value certified by Merck. The upper limits of the uranium and thorium values were estimated by the IAEA Laboratory using fluorimetry and activation analysis, respectively. A complete description of RGK-1 may be found in the reference.

REFERENCE

Preparation of Gamma-ray Spectrometry Reference Materials
RGU-1, RGTh-1 and RGK-1 Report - IAEA/RL/148, Vienna, 1987

This report may be obtained from:
INTERNATIONAL ATOMIC ENERGY AGENCY
Agency's Laboratories
Analytical Quality Control Services
P.O.Box 100
A-1400 Vienna, AUSTRIA

Appendix L

12. Certificate of IAEA RGU-1, Uranium Ore

Reference Products

About IAEA Reference Materials

Reference Material Online Catalog

Radionuclides

Trace Elements & Methyl Mercury

Organic Contaminants

Stable Isotopes

Ordering Information

Miscellaneous Documents

How to contact us

News and Announcements

Publications

Links

Events

ALMERA

40+ Years Delivering Quality to abs Worldwide

Nuclear Instrumentation

Analytical Methods

Interlaboratory Studies

IAEA-RGU-1 , Uranium Ore

Inorganic , Ores

- Unit Size: 500g
- Price per Unit: 60 EUR
- Report: IAEA/RL/148
- Date of Release: 1987-01-01
- Producing Laboratory: email

- Certificate of Irradiation: Certificate_of_Irradiation_IAEA-RGU-1

Both, IAEA-RGU-1 and IAEA-RGTh-1 reference materials were prepared on behalf of the International Atomic Energy Agency by the Canada Centre for Mineral and Energy Technology by dilution of a uranium ore BL-5 (7.09% U) and a thorium ore OKA-2 (2.89% Th, 219 µg U/g) with floated silica powder of similar grain size distribution, respectively. No evidence for between-bottles inhomogeneity was detected after mixing and bottling. BL-5 has been certified for uranium, ^{226}Ra and ^{210}Pb confirming that it is in radioactive equilibrium. The agreement between radiometric and chemical measurements of thorium and uranium in OKA-2 shows both series to be in radioactive equilibrium.

Analyte	Value	Unit	95% C.I.	N	R/I/C
232Th	< 4?	Bq/kg	-	None	I
235U	228?	Bq/kg	226 - 230	None	R
238U	4940?	Bq/kg	4910 - 4970	None	R
40K	< 0.63?	Bq/kg	-	None	I
K	< 20	mg/kg	-	None	I
Th	< 1	mg/kg	-	None	I
U	400	mg/kg	398 - 402	None	R

(Value) Concentration calculated as a mean of the accepted laboratory means
(N) Number of accepted laboratory means which are used to calculate the recommended or information values and their respective confidence intervals
(R/I/C) Classification assigned to the property value for analyte (Recommended/Information/Certified)
(?) Natural radionuclide activity concentrations derived from the elemental concentrations on basis of isotopic abundance and half-life data
The values listed above were established on the basis of a gravimetric dilution of materials with known uranium, thorium and potassium composition. The details concerning the criteria for qualification as a recommended or information value can be found in the respective report (attached).

IAEA-RGU-1 Uranium Ore diluted, 500g

€60/Unit

Quantity:

Add to Basket

My Shopping Cart

Total   €0

Go to Shopping Cart

Your Account

Edit My Profile
View My Orders

Help and Service

Terms of Service
Contact Us

Appendix M

13. Certificate of analysis for IAEA RGU-1

INTERNATIONAL ATOMIC ENERGY AGENCY

REFERENCE MATERIAL
FOR
GAMMA-RAY SPECTROMETRIC ANALYSIS
OF
GEOLOGICAL MATERIALS

IAEA/RGU-1

CERTIFICATE OF ANALYSIS

COMPONENT	CONCENTRATION*	CONFIDENCE INTERVAL**
Uranium	400 µg/g	± 2 µg/g
Thorium	less than 1 µg/g	---
Potassium	less than 20 µg/g	---

*Expressed on dry weight basis (constant weight at 130°C)
**At a significance level of 0.05

DESCRIPTION OF MATERIAL

RGU-1, RGTh-1 and RGK-1 are intended for use in calibrating laboratory gamma-ray spectrometers for the determination of U, Th and K in geological materials. RGU-1 was prepared by the Canada Centre for Mineral and Energy Technology (CANMET) under a contract with the International Atomic Energy Agency. The material was prepared by dilution of Canada Certified Reference Material Project (CCRMP) uranium ore BL-5 (7.09% U) with a floated silica powder of similar grain size distribution. BL-5 has been certified for uranium, ^{226}Ra and ^{210}Pb confirming that it is in radioactive equilibrium. The complete description of the preparation and certification of RGU-1 may be found in the reference.

REFERENCE

Preparation of Gamma-ray Spectrometry Reference Materials RGU-1, RGTh-1 and RGK-1 Report - IAEA/RL/148, Vienna, 1987

This report may be obtained from:
INTERNATIONAL ATOMIC ENERGY AGENCY
Agency's Laboratories
Analytical Quality Control Services
P.O.Box 100
A-1400 Vienna, AUSTRIA

Appendix N

14. Certificate of IAEA RGTh-1, Thorium Ore

IAEA-RGTh-1 , Thorium Ore

Inorganic , Ores

**IAEA-RGTh-1
Thorium Ore diluted,
500g**

€60/Unit

- Unit Size: 500g
- Price per Unit: 60 EUR
- Report: IAEA/RL/148
- Date of Release: 1987-01-01
- Producing Laboratory: email

Quantity:

Add to Basket

- Certificate of Irradiation: Certificate_of_Irradiation_IAEA-RGTh-1

Both, IAEA-RGU-1 and IAEA-RGTh-1 reference materials were prepared on behalf of the International Atomic Energy Agency by the Canada Centre for Mineral and Energy Technology by dilution of a uranium ore BL-5 (7.09% U) and a thorium ore OKA-2 (2.89% Th, 219 µg U/g) with floated silica powder of similar grain size distribution, respectively. No evidence for between-bottles inhomogeneity was detected after mixing and bottling. BL-5 has been certified for uranium, ^{226}Ra and ^{210}Pb confirming that it is in radioactive equilibrium. The agreement between radiometric and chemical measurements of thorium and uranium in OKA-2 shows both series to be in radioactive equilibrium.

My Shopping Cart

Total   €0

Go to Shopping Cart

Your Account

Edit My Profile
View My Orders

Help and Service

Terms of Service
Contact Us

Analyte	Value	Unit	95% C.I.	N	R/I/C
232Th	3250?	Bq/kg	3160 - 3340	155	R
235U	3.6?	Bq/kg	3.3 - 3.9	145	R
238U	78?	Bq/kg	72 - 84	145	R
40K	6.3?	Bq/kg	3.1 - 9.5	45	I
K	200	mg/kg	100 - 300	45	I
Th	800	mg/kg	784 - 816	155	R
U	6.3	mg/kg	5.9 - 6.7	145	R

(Value) Concentration calculated as a mean of the accepted laboratory means
(N) Number of accepted laboratory means which are used to calculate the recommended or
    information values and their respective confidence intervals
(R/I/C) Classification assigned to the property value for analyte (Recommended/Information/Certified)
(?) Natural radionuclide activity concentrations derived from the elemental concentrations on basis of isotopic abundance and half-life data

The values listed above were established on the basis of a gravimetric dilution of materials with known uranium, thorium and potassium composition. The details concerning the criteria for qualification as a recommended or information value can be found in the respective report (attached).

Appendix O

15. Certificate of analysis IAEA RGTh-1

- 47 -

INTERNATIONAL ATOMIC ENERGY AGENCY

REFERENCE MATERIAL
FOR
GAMMA-RAY SPECTROMETRIC ANALYSIS
OF
GEOLOGICAL MATERIALS

IAEA/RGTh-1

CERTIFICATE OF ANALYSIS

COMPONENT	CONCENTRATION*	CONFIDENCE INTERVAL**
Thorium	800 µg/g	± 16 µg/g
Uranium	6.3 µg/g	± 0.4 µg/g
Potassium	0.02%	± 0.01%

*Expressed on dry weight basis (constant weight at 130°C)
**At a significance level of 0.05

DESCRIPTION OF MATERIAL

RGU-1, RGTh-1 and RGK-1 are intended for use in calibrating laboratory gamma-ray spectrometers for the determination of U, Th and K in geological materials. RGTh-1 was prepared by the Canada Centre for Mineral and Energy Technology (CANMET) under a contract with the International Atomic Energy Agency. The material was prepared by dilution of Canada Certified Reference Material Project (CCRMP) thorium ore OKA-2 (2.89% Th, 219 µg/g U) with a floated silica powder of similar grain size distribution. The agreement between radiometric and chemical measurements of thorium and uranium in OKA-2 shows both series to be in radioactive equilibrium. The complete description of the preparation and certification of RGTh-1 may be found in the reference.

REFERENCE

Preparation of Gamma-ray Spectrometry Reference Materials RGU-1, RGTh-1 and RGK-1 Report - IAEA/RL/148, Vienna, 1987

This report may be obtained from:
INTERNATIONAL ATOMIC ENERGY AGENCY
Agency's Laboratories
Analytical Quality Control Services
P.O.Box 100
A-1400 Vienna, AUSTRIA

Appendix P

16. Gamma and neutron survey meter, GM energy compensated

Specifications

Ranges: four linear range multiples of ×0.1, ×1, ×10, and ×100; used in combination with the 0-10 mrem/hr meter dial, providing an overall range of 0-1000 mrem/hr

Gamma Energy Range: 60 keV to 3 MeV

Gamma Energy Response: ≤ 15%

Sensitivity: Gamma is approximately 1000 cpm/mR/hr (internal detector. Neutron is approximately 350 cpm/mrem/hr (with Model 42-41L).

Thresholds: Gamma threshold is fixed at 50 millivolts (mV). Neutron threshold is adjustable from 5 to 100 mV.

Neutron High Voltage: internally adjustable from 500 to 1500 Vdc

Gamma High Voltage: fixed at 550 Vdc

Linearity: within 10% of true value for the analog rate meter; 2% for the LCD

Response Time: ×0.1 range multiplier = 7 seconds, ×1 = 7 seconds, ×10 = 2 seconds, ×100 = 2 seconds; all response times measured from 10-90% of full scale

Audio: dual- or single-tone click-per-event through a built-in speaker with an adjustable volume control located on the front panel; headset jack located on the instrument can

VITA

Mr. Lyheng Tan is from Siem Reap province, Cambodia. He was born in 1991. From 2009-2103, He went to study the Bachelor of Science in Chemistry at Royal University of Phnom Penh, Phnom Penh, Cambodia. From 2013-2015, He continued his study for the Master of Science and Technology in Nuclear Security and Safeguards (NSS) at Chulalongkorn University, Bangkok, Thailand.